UNIVERSIDADE DA BEIRA INTERIOR
Ciências da Saúde

Biosynthesis, Isolation and Magnetization of gellan spheres for biorecognition of therapeutic His-tag proteins

Joana Filipa Silva Coelho

Dissertação para obtenção do Grau de Mestre em
Ciências Biomédicas
(2º ciclo de estudos)

Orientador: Prof. Doutor Luís António Paulino Passarinha
Co-orientador: Prof. Doutora Ângela Maria Almeida de Sousa

Covilhã, junho de 2017

Acknowledgements

Firstly, I would like to express my sincere gratitude to my supervisors Professor Luís Passarinha and Professor Ângela Sousa for all their patience and support, for the scientific learning that you gave me and for all the interest demonstrated in this work to make it better each day. You always have been helpful, concerned, good advisors and good "psychologists". I would like to express my admiration and satisfaction in having worked with you.

I would also like to acknowledge to Health Sciences Research Centre and University of Beira Interior, which allowed me to develop this work.

To my dear family, especially to my parents that always support me unconditionally, for the sacrifices, for the patience, for all the times that they told me to not give up and for the immense love that they always gave me. Without them, I would not have gotten here.

Also, I would like to thank Professor Renato Boto for all the help that he gave me during this work with the NMR analysis.

I am also thankful to Margarida Grilo, Fátima Santos and Margarida Almeida for helping me in the lab and for the advice and encouragement they gave me to continue this work.

Also, my acknowledgments to my lab friends for the help, support and friendship in this long journey.

A special thanks to all my friends, in particularly to Inês, Gonçalo, Joana, Ivo, Rita S., Ana Manuela, Carla Cristina, Rita A., Liliana and Adriana, for all the encouragement, support and motivation; for their company during long nights at the laboratory and for all the laughs. You know that our short friendship has become gigantic, and made me shed tears of happiness even during the most troubled of times. I am very thankful to have friends like you.

At last, but not least, to my dear boyfriend, my genuine appreciation for all the support, patient and motivation. Since the beginning of this journey, he has always been there to listen, help and encourage me to overcome all the obstacles. I do not need to say anything else because you already know how important you were to finish this voyage, once again thank you very much.

Resumo

A bactéria *Sphingomonas paucimobilis* ATCC 31461 tem a capacidade de produzir um polissacarídeo aniónico de baixo custo, a goma de gelana, constituído por um tetrassacarídeo composto por unidades de glucose, ácido glucurónico e ramnose. Este biopolímero possui diversas aplicações na alimentação e na indústria farmacêutica e cosmética.

Tipicamente, a presença de iões divalentes é necessária para diminuir a repulsão electroestática entre as hélices de gelana, permitindo a ligação entre cadeias e comsequente agregação. Curiosamente, a interação por afinidade que se promove entre os iões metálicos de transição e os aminoácidos de histidina tem explorada como um método não covalente de purificação e imobilização de proteínas recombinantes, contendo três a dez unidades consecutivas de histidina no seu terminal amino ou carboxil.

Assim, o presente trabalho pretende formular e magnetizar esferas de gelana biossintética para extrair a proteína COMT de uma amostra de lisado. A produção de goma de gelana pela bactéria *Sphingomonas paucimobilis* ATCC 31561 foi otimizada usando dois meios de cultura diferentes, o meio N e o meio S. A fermentação foi realizada com uma agitação de 250 rpm, a 30 ºC durante 48 horas, e uma maior produção de gelana foi conseguida através do meio S. De seguida, de forma a recuperar a goma de gelana produzida por fermentação, foram testados diferentes processos, como a filtração, a diálise, lavagens com acetona e éter e dissolução em água destilada. O melhor método para recuperar a goma de gelana com um maior grau de pureza, comparativamente à goma de gelana comercial, foi a filtração com acetona e éter e dissolução em água destilada. Todas as amostras obtidas através dos diferentes procedimentos de recuperação foram analisadas por ressonância magnética nuclear e por espetroscopia de infravermelho da transformada de Fourier.

As esferas de gelana foram preparadas pela técnica de emulsão de água-em-óleo. Para isso, a goma de gelana foi dissolvida em água destilada com uma agitação de 300 rpm, a 90 ºC durante 30 minutos, e esta solução foi transferida para uma seringa e libertada gota a gota para uma solução de óleo de cozinha 100% vegetal com uma agitação de 750 rpm, a 100 ºC. A mistura foi transferida para diferentes soluções de 200 mM de $BaCl_2$, $CaCl_2$, $CoCl_2$, $CuCl_2$ e $NiCl_2$ com uma agitação de 750rpm, durante 30 minutos à temperatura ambiente. As esferas com níquel como ligando foram magnetizadas pelo método químico de co-precipitação. Todas as esferas com diferentes ligandos assim como as esferas magnetizadas foram caracterizadas morfologicamente e quimicamente por microscopia eletrónica de varrimento e por espetroscopia de energia dispersiva de raios-X.

Finalmente, as esferas de gelana foram usadas para capturar proteínas modelo, BSA e lisozima, e uma proteína mais complexa, SCOMT, através do método de batch. Assim, foram estudadas

diferentes condições para ligar e eluir a proteína, através da variação da quantidade de esferas, da presença de ureia no lisado, do pH e da força iónica das soluções de ligação e eluição. Deste modo, as melhores condições para a captura de proteína total de um lisado complexo são o equilíbrio de 10 mL de esferas (com ou sem magnetização) a pH ácido, o passo de ligação com ureia no lisado de SCOMT e o passo de eluição com um aumento de pH e, de seguida, da força iónica. Contudo, de forma a isolar seletivamente a SCOMT, poderia ser mais adequado explorar as condições de equilíbrio e de ligação com um pH de cerca de 7.5 e a condição de eluição pela diminuição do pH para o ponto isoelétrico com esferas magnetizadas.

Palavras-chave

Biossíntese; *Sphingomonas paucimobilis; Goma de gelana; Ca*techol-*O*-methyltransferase; Magnetização.

Abstract

The bacterium *Sphingomonas paucimobilis* ATCC 31461 has the ability to produce a low cost anionic polysaccharide gellan gum, composed of a tetrasaccharide structure of glucose, glucuronic acid and rhamnose units. This biopolymer has many applications in the food, pharmaceutical and cosmetic industries.

Typically, for gellan aggregation, the presence of divalent ions is required to decrease the electrostatic repulsion between helices, allowing the cross-link. Curiously, the affinity interaction between transition metal ions and histidine has been used as a site-specific, noncovalent method for the purification and immobilization of recombinant proteins bearing three to ten consecutive histidine amino acids at their amino- or carboxyl-terminus.

Thus, the present project intends to formulate and magnetize biosynthetic gellan spheres to extract COMT protein from a lysate sample. Gellan gum production was improved by using two different media, N medium and S medium. The fermentation procedure was performed with a stirring of 250 rpm at 30 ºC for 48 hours, and a higher production of gellan gum was achieved through the S medium. Then, in order to recover the gellan gum produced by fermentation, different processes, like filtration, dialysis, washes with acetone and ether and dissolution in distilled water, were tested. The best method to recover gellan gum with a high degree of purity, comparatively with the commercial gellan gum was the filtration with acetone and ether and dissolution with distilled water. All the samples obtained from the different procedures of recovery were analyzed by nuclear magnetic resonance and Fourier transform infrared spectroscopy.

The gellan spheres were prepared by water-in-oil emulsion technique. For that, the gellan gum was dissolved in distilled water with a stirring of 300 rpm at 90 ºC during 30 minutes and this solution was transferred to a syringe and trickled in individual drops into a 100 % vegetable cooking oil solution with a 750 rpm stirring, at 100 ºC. The mixture was transferred to different solutions of 200 mM $BaCl_2$, $CaCl_2$, $CoCl_2$, $CuCl_2$ and $NiCl_2$ with a stirring of 750 rpm for 30 minutes, at room temperature. The spheres with nickel as a cross-linker were magnetized by the chemical co-precipitation method. All the spheres with different cross-linkers and magnetized spheres were characterized morphologically and chemically by scanning electron microscopy and energy-dispersive X-Ray spectroscopy.

Finally, the gellan spheres were used to capture model proteins, BSA and lysozyme, and a more complex protein, SCOMT, through the batch method. Thus, different conditions to bind and elute the protein were study, through the variation of the amount of spheres, the presence of urea in the lysate, the pH and ionic strength of the binding and elution solutions. So, the best conditions for the capture of the total protein from the complex lysate are the equilibrium of

10 mL of spheres (with or without magnetization) at acidic pH, binding step with urea in the SCOMT lysate and elution step with the increase of pH and then the ionic strength. However, to selectively isolate the SCOMT, it could be more adequate to explore the equilibrium and binding conditions with a pH around 7.5 and the elution condition by decreasing the pH to the protein isoelectric point with magnetic spheres.

Keywords

Biosynthesis; *Sphingomonas paucimobilis;* Gellan gum; catechol-*O*-methyltransferase; Magnetization.

Index

Chapter I – Introduction

1.1. Microbial Exopolysaccharides 1

1.2. The exopolysaccharide: Gellan gum 2

1.2.1. Physical and chemical properties 3

1.2.2. Functional properties 4

1.2.3. The pathway of gellan biosynthesis 5

1.2.4. Gellan production 7

1.2.5. Recovery of gellan gum 8

1.2.6. Applications 9

1.3. Magnetization 12

1.4. Chromatography 13

1.4.1. Ion-exchange chromatography 15

1.4.2. Size exclusion chromatography 15

1.4.3. Reverse phase chromatography 16

1.4.4. Hydrophobic interaction chromatography 17

1.4.5. Affinity chromatography 17

1.4.5.1. Immobilized Metal Ion Affinity Chromatography 18

1.4.6. Batch method 18

1.5. Catechol-*O*-methyltransferase (COMT) 19

1.5.1. COMT structure 20

1.5.2. The two isoforms of COMT: SCOMT and MBCOMT 21

1.5.3. Inhibitors of COMT in Parkinson´s disease 22

Chapter II – Objectives 23

Chapter III – Materials and methods

3.1. Materials 25

3.2. Gellan gum biosynthesis 26

3.2.1. N medium 26

3.2.3. S medium 26

3.2.3. Quantification of growth bacteria and gellan gum 27

3.3. Recovery of gellan gum 27

3.3.1. Precipitation, washing, dissolution and precipitation 27

3.3.2. Precipitation, washing, dissolution, dialysis and precipitation 28

3.3.3. Dialysis and precipitation 28

3.3.4. Filtration and precipitation 28

3.3.5. Filtration, washing and precipitation 28

3.3.6. Filtration, washing, dissolution and precipitation 28

3.3.7 FTIR and NMR analysis 29

3.4. Gellan spheres formation with water-in-oil emulsion 29
3.4.1. Zeta-potential analysis 29
3.4.2. Magnetization of gellan spheres 30
3.4.3. Semi-optical and SEM analysis of gellan spheres 30
3.4.4. EDX analysis of gellan spheres 30
3.5. SCOMT production and extraction 31
3.6. Batch method to capture model and SCOMT proteins 31
3.6.1. Total protein quantification 34
3.6.2. DOT-BLOT and SDS-PAGE electrophoresis analysis 35
Chapter IV – Results and discussion 37
4.1. Gellan gum biosynthesis 37
4.2. Recovery of gellan gum 39
4.2.1. Precipitation, washing, dissolution and precipitation 40
4.2.2. Precipitation, washing, dissolution, dialysis and precipitation 42
4.2.3. Dialysis and precipitation 43
4.2.4. Filtration and precipitation 45
4.2.5. Filtration, washing and precipitation 46
4.2.6. Filtration, washing, dissolution and precipitation 47
4.3. Gellan spheres formulation with water-in-oil emulsion 49
4.3.1. Zeta-Potential 49
4.3.2. Semi-optical microscopy analysis 50
4.3.3. SEM and EDX analysis 51
4.4. Magnetic spheres formulation 59
4.5. Batch method assays to capture model proteins 61
4.6. Batch method assays to capture SCOMT protein 64
Chapter V – Conclusions 79
Chapter VI – Future perspectives 81
Chapter VII – References 83
Chapter VIII – Annex 93

List of figures

Figure 1 - Tetrasaccharide repeating units of chemical structure of native gellan gum.....3

Figure 2 - Schematic representation of the aggregation helices into the "junction zones".....4

Figure 3 - Structure of modified gellan gum (A) High acetyl gellan gum; (B) Low acetyl gellan gum.....5

Figure 4 - Proposed pathway for nucleotide-sugar precursors and glucose catabolism in *Sphingomonas paucimobilis*.....6

Figure 5 - Schematic model of production and recovery of gellan gum.....9

Figure 6 - Magnetic spheres.....13

Figure 7 - Schematic chromatography stages: the equilibrium phase, binding, washing and, finally, elution and regeneration.....14

Figure 8 - Ion-exchange chromatographic matrix.....15

Figure 9 - Size exclusion chromatography.....16

Figure 10 - Reverse phase chromatography.....16

Figure 11 - Hydrophobic interaction chromatography.....17

Figure 12 - Affinity chromatography.....18

Figure 13 - Schematization of a batch method.....19

Figure 14 - Reaction catalysed by COMT. COMT in the presence of magnesium (Mg^{2+}) transfers a methyl group from S-adenosyl-L-methionine (SAM) to a hydroxyl group of the substrate.....19

Figure 15 - Schematic representation of the three-dimensional structure of COMT. It is illustrated the S-adenosyl-L-methionine co substrate (SAM), the inhibitor 3,5-dinitrocatechol (3,5-DNC), the Mg^{2+} and coordinated water molecules.....20

Figure 16 - Standard curve for MES buffer, using BCA protein assay kit.....34

Figure 17 - Standard curve for citrate buffer, using BCA protein assay kit.....34

Figure 18 - Standard curve for Tris buffer, using BCA protein assay kit.....35

Figure 19 - Bacteria growth for 48 hours in relation with the optical density (640 nm).....38

Figure 20 - Gellan gum production by *Sphingomonas paucimobilis* ATCC 31461, for 48 hours.....38

Figure 21 - FTIR spectra of commercial gellan gum.....39

Figure 22 - ^{1}H-NMR spectrum of commercial gellan gum.....40

Figure 23 - FTIR spectra of commercial gellan gum and recovered gellan gum.....41

Figure 24 - ^{1}H-NMR spectrum of gellan gum recovered.....41

Figure 25 - FTIR spectra of commercial gellan gum and gellan gum precipitated and dialysed.....42

Figure 26 - ^{1}H-NMR spectrum of gellan gum precipitated and dialysed.....43

Figure 27 - FTIR spectra of commercial gellan gum and dialysed gellan gum.....44

Figure 28 - ^{1}H-NMR spectrum of gellan gum recovered by dialysis.....44

Figure 29 - FTIR spectra of commercial gellan gum and gellan gum filtered.....45

Figure 30 - ^{1}H-NMR spectrum of gellan gum recovered by filtration.....45

Figure 31 - FTIR spectra of commercial gellan gum and gellan gum filtered with acetone, ether and distilled water.....46

Figure 32 - ^{1}H-NMR spectrum of gellan gum filtered with acetone, ether and distilled water.....47

Figure 33 - FTIR spectra of commercial gellan gum and gellan gum filtered, washed and dissolved with distilled water.....48

Figure 34 - ^{1}H-NMR spectrum of gellan gum filtered and washed with distilled water.....48

Figure 35 - Gellan gum spheres visualized at semi-optical microscope. A – Biosynthetic gellan gum spheres. B – Commercial gellan gum spheres.....50

Figure 36 - Schematic representation of gellan gum spheres with barium as a cross-linker, visualized at SEM.....52

Figure 37 - Schematic representation of gellan gum spheres with calcium as a cross-linker, visualized at SEM.....52

Figure 38 - Schematic representation of gellan gum spheres with cobalt as a cross-linker, visualized at SEM.....53

Figure 39 - Schematic representation of gellan gum spheres with copper as a cross-linker, visualized at SEM.....53

Figure 40 - Schematic representation of gellan gum spheres with nickel as a cross-linker, visualized at SEM.....54

Figure 41 - Schematic representation of magnetized gellan gum spheres, visualized at SEM.....60

Figure 42 - SDS-PAGE electrophoretic analysis of the recovered supernatant from spheres with nickel as a cross-linker, through batch method using model proteins.....62

Figure 43 - SDS-PAGE electrophoretic analysis of the recovered supernatant from magnetic spheres, through batch method using model proteins.....63

Figure 44 - DOT-BLOT analysis of the recovered supernatant from 500 µL of spheres with nickel as a cross-linker, through the batch method.....64

Figure 45 - SDS-PAGE electrophoretic analysis of the recovered supernatant from spheres with nickel as a cross-linker, through batch method in SCOMT lysate.....65

Figure 46 - DOT-BLOT analysis of the recovered supernatant from 10 mL of spheres with nickel as a cross-linker, through the batch method.....66

Figure 47 - SDS-PAGE electrophoretic analysis of the recovered supernatant from 10 mL of spheres with nickel as a cross-linker, through batch method in SCOMT lysate.....67

Figure 48 - DOT-BLOT analysis of the recovered supernatant from 10 mL of spheres with nickel as a cross-linker and from magnetic spheres, through the batch method.....68

Figure 49 - SDS-PAGE electrophoretic analysis of the recovered supernatant from 10 mL of spheres with nickel as a cross-linker and from magnetic spheres, through batch method in SCOMT lysate.....68

Figure 50 - DOT-BLOT analysis of the recovered supernatant from 10 ml of spheres with nickel as a cross-linker and from magnetic spheres, through the batch method.....70

Figure 51 - SDS-PAGE electrophoretic analysis of the recovered supernatant from 10 mL of spheres with nickel as a cross-linker and from magnetic spheres, through batch method in SCOMT lysate.....70

Figure 52 - DOT-BLOT analysis of the recovered supernatant from 10 mL of spheres with nickel as a cross-linker and from magnetic spheres, through the batch method.....71

Figure 53 - SDS-PAGE electrophoretic analysis of the recovered supernatant from 10 mL of spheres with nickel as a cross-linker and from magnetic spheres, through batch method in SCOMT lysate.....72

Figure 54 - DOT-BLOT analysis of the recovered supernatant from 10 mL of spheres with nickel as a cross-linker and from magnetic spheres, through the batch method.....74

Figure 55 - SDS-PAGE electrophoretic analysis of the recovered supernatant from 10 mL of spheres with nickel as a cross-linker and from magnetic spheres, through batch method in SCOMT lysate.....74

Figure 56 - DOT-BLOT analysis of the recovered supernatant from 10 mL of spheres with nickel as a cross-linker and from magnetic spheres, through the batch method.....76

Figure 57 - SDS-PAGE electrophoretic analysis of the recovered supernatant from 10 mL of spheres with nickel as a cross-linker and from magnetic spheres, through batch method in SCOMT lysate.....77

Figure 18 - FTIR spectrum of casein.....93

Figure 59 - FTIR spectrum of glucose.....93

Figure 60 - ^{1}H-NMR spectrum of casein.....94

Figure 61 - ^{1}H-NMR spectrum of yeast extract.....94

List of tables

Table 1 - The source, physical properties and applications of some microbial exopolysaccharides.....2

Table 2 - Food applications of gellan gum.....10

Table 3 - Application of gellan in pharmaceutical products.....11

Table 4 - Different types of chromatography and heir principle of action and separation.....14

Table 5 - Mean value of zeta-potential measurements for commercial and biosynthetic gellan spheres.....49

Table 6 - Mean diameter of commercial and biosynthetic gellan gum spheres take into account the counter ion.....51

Table 7 - Elementary analysis of commercial gellan spheres with barium as a cross-linker, through EDX.....55

Table 8 - Elementary analysis of commercial gellan spheres with calcium as a cross-linker, through EDX.....55

Table 9 - Elementary analysis of commercial gellan spheres with cobalt as a cross-linker, through EDX.....55

Table 10 - Elementary analysis of commercial gellan spheres with copper as a cross-linker, through EDX.....56

Table 11 - Elementary analysis of commercial gellan spheres with nickel as a cross-linker, through EDX.....57

Table 12 - Elementary analysis of biosynthetic gellan spheres with barium as a cross-linker, through EDX.....57

Table 13 - Elementary analysis of biosynthetic gellan spheres with calcium as a cross-linker, through EDX.....57

Table 14 - Elementary analysis of biosynthetic gellan spheres with cobalt as a cross-linker, through EDX.....58

Table 15 - Elementary analysis of biosynthetic gellan spheres with copper as a cross-linker, through EDX.....58

Table 16 - Elementary analysis of biosynthetic gellan spheres with nickel as a cross-linker, through EDX.....58

Table 17 - Elementary analysis of commercial magnetic gellan spheres, through EDX.....60

Table 18 - Elementary analysis of biosynthetic magnetic gellan spheres, through EDX.....61

Table 19 - Absorbance obtained from the recovered supernatant, at 280 nm, with 1 mL of 5 mg/mL BSA and 10 mg/mL lysozyme, in 10 mM MES buffer, pH 6.2, added to 500 µL of spheres.....62

Table 20 - Absorbance obtained from the recovered supernatant, at 280 nm, with 1 mL of SCOMT lysate solution, in 10 mM MES buffer, pH 6.2, added to 500 µL of spheres with nickel as a cross-linker.....64

Table 21 - Absorbance obtained from the recovered supernatant, at 280 nm, with 1 mL of SCOMT lysate solution, containing urea, in 10 mM MES buffer, pH 6.2, added to 500 µL of spheres with nickel as a cross-linker.....65

Table 22 - Absorbance obtained from the recovered supernatant, at 280 nm, with 4 mL of SCOMT lysate solution, containing urea, in 10 mM MES buffer, pH 6.2, added to 10 mL of spheres with nickel as a cross-linker.....66

Table 23 - Absorbance obtained from the recovered supernatant, at 280 nm, with 4 mL of SCOMT lysate solution, containing urea, in 10 mM MES buffer, pH 6.2, added to 10 mL of spheres.....68

Table 24 - Absorbance obtained from the recovered supernatant, at 280 nm, with 4 mL of SCOMT lysate solution, containing urea, in 10 mM MES buffer, pH 6.2, added to 10 mL of spheres.....69

Table 25 - Absorbance obtained from the recovered supernatant, at 280 nm, with 4 mL of SCOMT lysate solution, containing urea, in 10 mM MES buffer, pH 6.2, added to 10 mL of spheres.....71

Table 26 - Absorbance obtained from the recovered supernatant, at 280 nm, with 4 mL of SCOMT lysate solution, containing urea, in 10 mM Tris buffer, pH 7.5, added to 10 mL of spheres.....73

Table 27 - Absorbance obtained from the recovered supernatant, at 280 nm, with 4 mL of SCOMT lysate solution, containing urea, in 10 mM citrate buffer, pH 4.0, added to 10 mL of spheres.....76

List of acronyms

3-OMD	3-*O*-methyldopa
AADC	Aromatic Amino acid Decarboxylase
AC	Affinity Chromatography
$BaCl_2$	Barium Chloride
$CaCl_2$	Calcium Chloride
$CoCl_2$	Cobalt Chloride
COMT	Catechol-*O*-Methyltransferase
$CuCl_2$	Copper Chloride
D_2O	Deuterated Water
EDX	Energy-Dispersive X-ray Spectroscopy
EPS	Exopolysaccharide
FDA	Food and Drug Administration
$FeCl_3.6H_2O$	Iron (III) Chloride Hexahydrate
FeO_4	Ferrate
$FeSO_4.7H_2O$	Iron (II) Sulphate Heptahydrate
FTIR	Fourier Transform Infrared Spectroscopy
H_2SO_4	Sulfuric Acid
HCl	Hydroclorich Acid
HIC	Hydrophobic Interaction Chromatography
His-tag	Polyhistidine-tag
IMAC	Immobilized Metal Ion Affinity Chromatography
IEC	Ion-Exchange Chromatography
KH_2PO_4	Potassium Phosphate Monobasic
KOH	Potassium Hydroxide
MES	4-Morpholineethanesulfonic Acid
$MgSO_4$	Magnesium Sulphate
$MgSO_4.7H_2O$	Magnesium Sulphate Heptahydrate
$MnCl_2.4H_2O$	Manganese (II) Chloride Tetrahydrate
$MnFe_2O_4$	Manganese Ferrite
MBCOMT	Membrane Catechol-*O*-Methyltransferase
MWCO	Molecular Weight Cut Off
Na_2HPO_4	Sodium Phosphate Dibasic
Na_2SO_4	Sodium Sulphate
NaCl	Polyvinylidene
NaOH	Sodium chloride
$NiCl_2$	Nickel Chloride

NMR	Nuclear Magnetic Resonance
NSAID	Nonsteroidal Anti-Inflammatory Drugs
OD	Optical Density
PD	Parkinson´s Disease
pgmG	Phosphoglucomutase
PSA	Ammonium Persulfate
PVDF	Polyvinylidene
rmlA	TDP-glucose pyrophosphorylase
RPC	Reverse Phase Chromatography
SAH	S-Adenosyl-L-Homocysteine
SAM	S-Adenosyl-L-Methionine
SEM	Scanning Electron Microscopy
SCOMT	Soluble Catechol-*O*-Methyltransferase
SDS-PAGE	Sodium Dodecyl Sulphate
SDS	Sodium Dodecyl Sulphate-Polyacrylamide Gel Electrophoresis
SEC	Size-Exclusion Chromatography
TBS	Tris-Buffered Saline
TDP-G	Thymidine 5-Diphosphate Glucose
Tris	Tris(hydroxymethyl)aminomethane
UDP-G	Uridine 5-Diphosphate D-Glucose
UDP-GA	Uridine 5-Diphosphate D-Glucuronic Acid
ugpG	Glucose-1-phosphate uridyltransferase
UTP	Uridine 5-Triphosphate
TEMED	N,N,N',N'-tetramethylethylenediamine
TDP-R	Thymidine 5-Diphosphate L-rhamnose

Chapter I - Introduction

1.1. Microbial Exopolysaccharides

Microbial polysaccharides are long-chain, natural and/or semisynthetic polymers with different molecular weight and structure [1]. Their extensive diversity allows them to be categorized based on chemical structure, functionality, molecular weight and linkage bonds. Thus, they can be classified as intracellular polysaccharides, cell polysaccharides and extracellular polysaccharides, which are the most abundant. These polysaccharides confer structural and protective functions at the cell wall. In the external cell, the polysaccharides can acquire the form of a covalently bound cohesive layer, a morphologic entry termed capsule [2] or be totally excreted into the extracellular environment [3].

In the middle of 19th century, bacterial exopolysaccharides (EPS) started appearing with the discovery of dextran, an exopolysaccharide in wine. The microorganism responsible for its production was identified as *Leuconostoc mesenteriodes* [4].

Exopolysaccharides are a heterogeneous matrix of polymers comprised by polysaccharides, proteins, nucleic acids and (phospho) lipids [5]. They are regarded as substitutes for natural or synthetic water-soluble polymers or as original polymers [6], and they have an inherent biocompatibility and apparent non-toxic nature which allows their use in many medical applications such as scaffolds or matrices in tissue engineering, drug delivery methods and as wound dressings. These features make them more attractive when compared to polysaccharides obtained from microalgae or plants [1, 6]. The composition of these polysaccharides includes repeated units of D-glucose, D-galactose, L-rhamnose and, in some cases, *N*-acetylglucosamine (GlcNAc), *N*-acetylgalactosamine (GalNAc) or glucuronic acid (GlcA) [2].

Bacterial exopolysaccharides have becoming promising and economically competitive and they can be biosynthesised by microorganisms such as *Xanthomonas campestris, Sphingomonas paucimobilis and Leuconostoc mesentroides* [1, 7, 8], represented in table 1. In particular, gellan gum is an extracellular polysaccharide synthetized aerobically by the non-pathogenic *Sphingomonas Paucimobilis* ATCC 31561 [9], with good rheological characteristic and commercial potential.

Table 1 – The source, physical properties and applications of some microbial exopolysaccharides (adapted by [7, 8]).

Source	EPS	Molecular weight (Da)	Possible applications
Acetobacter xylinum	Acetan	2.5×10^6	Thickener and gelling agent
Acinetobacter calcoaceticus	Curdlan	500 – 240 000	Gelling agent
Alcaligenes viscosus	Levan	$< 10^8$	Thickener and stabilizer agent
Leuconostoc mesenteroides	Dextran	1×10^6	Blood plasma extender or blood flow improving agent, cholesterol lower agent and microcarrier in tissue
Sphingomonas Paucimobilis	Gellan	5×10^6	Stabilizer, solidifier and gelling agent
Xanthomonas campestris	Xanthan	6×10^6	Emulsifier and gelatinate

The bacterium *Sphingomonas Paucimobilis* is a non-fermentative, nonspore-forming and strictly aerobic Gram-negative bacillus which can be characterized by catalase and oxidase activity, slow motility with single polar flagellum and yellow pigment production [10]. This microorganism is abundant in natural environments, particularly in water and soil, and is used in the bioremediation of the ambience due to its capacity to decompose aromatic compounds [11].

1.2. The exopolysaccharide: Gellan gum

Gellan gum is a exopolysaccharide with a high molecular weight of 5×10^6 Da, discovered in 1978 and approved for use as a food additive in 1992, by the Food and Drug Administration (FDA) [12].

This polysaccharide has wide applications in food, cosmetic and pharmaceutical industries as thickening, binding and emulsifying agent. Also, it is used to solidify tissue culture media [13], as a vehicle for ophthalmic preparations [14], in implants for insulin delivery [15], as cross-linked hydrogels for tissue engineering scaffolds [16], as an agar substitute for microbiological

applications [17], as a film for the controlled release of pharmaceuticals [18] and more recently in microspheres for drug delivery [19].

1.2.1. Physical and chemical properties

Native gellan gum consists in a tetrasaccharide backbone with repeated units of one molecule of L-rhamnose [α-1,4-L-rhamnose], one of D-glucuronic acid [β-1,4-D-glucuronic acid], two of D-glucose [β-1,3-D-glucose; β-1,3-D-glucose] and two acyl groups, glycerate and acetate bounds to the glucose residue adjacent to glucuronic acid, represented in figure 1. The three fundamental compounds are present in a percentage of 60% glucose, 20% rhamnose and 20% glucuronic acid [20, 21].

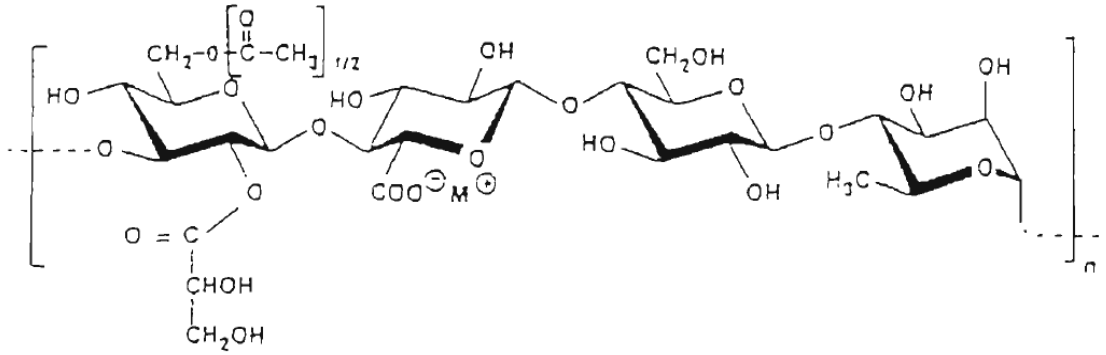

Figure 2 - Tetrasaccharide repeating units of chemical structure of native gellan gum [18].

Gellan gum presents a different conformation and structure depending on the polymer concentration, aqueous environment, temperature and in the presence of divalent or monovalent cations in solution. At low temperatures, these exopolysaccharide form an arrangement in double stranded helices and at high temperatures a single-stranded polysaccharide occurs, which reduces the viscosity of the solution [22].

Besides, gellan dissolved in water tends to ramify and/or cyclize enhancing the volume of the molecule. Thus, the double-stranded helices aggregate and bind to one another at the "junction zones" via salt bridges. Furthermore, secondary interactions, including hydrogen bonds, link the chains to the junction zones [22, 23], represented in figure 2.

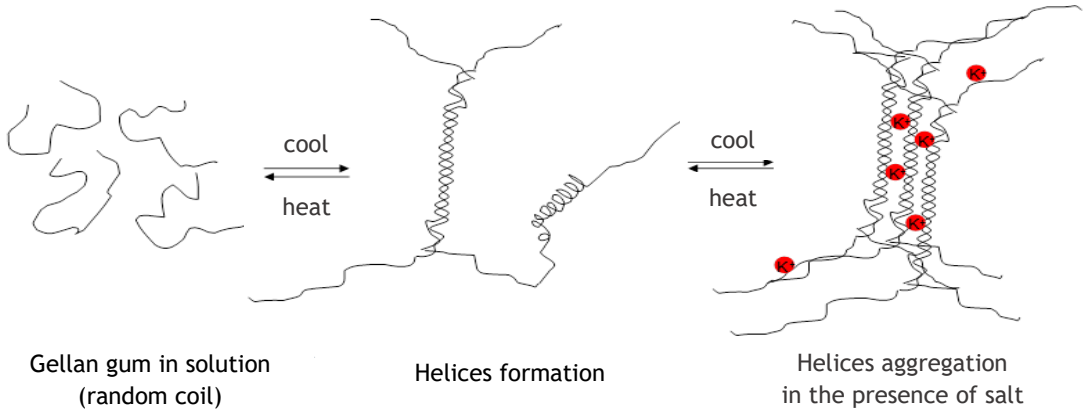

Figure 3 - Schematic representation of the aggregation helices into the "junction zones" (adapted by [23]).

A higher concentration of chains at the junction zones occurs with the decreasing of the temperature below the setting point, while some chains are released with the temperature increase. Additionally, the increment of junction zones, due to divalent and monovalent cations, make them more resistant to heating, improving the gelling potential of gellan gum [22].

1.2.2. Functional properties

Gellan gum possesses many different properties due to its versatile texture, stability, compatibility and dispersibility [12, 24, 25]. One of the most important properties of gellan gum is the versatile texture, frequently defined as *modulus*, which measures the stability of the gel, its *hardness*, quantifying the rupture strength, *elasticity*, which measures the robberies, and *brittleness*, which is the strain necessary to break the gel. The stability of this anionic polysaccharide can be affected by pH variations or by heating. Also, the dispersibility is one of the most important characteristic of gellan, which facilitates the full dissolution in water without any preliminary steps.

Gellan gels present high clarity due to their 15% sugar content are crystal clear. Their setting temperature and melting point flexibilities, where the gels can be formulated to set with or without heating, are also very important benefits.

This polysaccharide can be combined with other polymers allowing a bigger range of functional properties and applications. Low concentrations of this exopolysaccharide are usually required, with the gels being prepared with 0.04 to 0.05% (w/v).

Its ability to quickly release flavour is another of its benefits, which is possible due the water binding properties of gellan gum molecules. For example, in fruit fillings it allows a fast release

of their natural flavours [12] and in cheese it contributes to its characteristic taste [26]. Besides the basic native gellan, there are three types of modified gellan gum. The high acetyl gellan gum, partially deacetylated, provides a soft, elastic and non-brittle thermoreversible gel. The low acetyl gellan, highly deacetylated, is ideal for the major applications, like brittle gels and firmer forms. Lastly, the high clarity gellan, highly deacetylated and clarified, is appropriate for some confectionary products where clarity is a crucial quality issue, and it additionally can be used as a gelling agent for microbial growth media [27, 28].

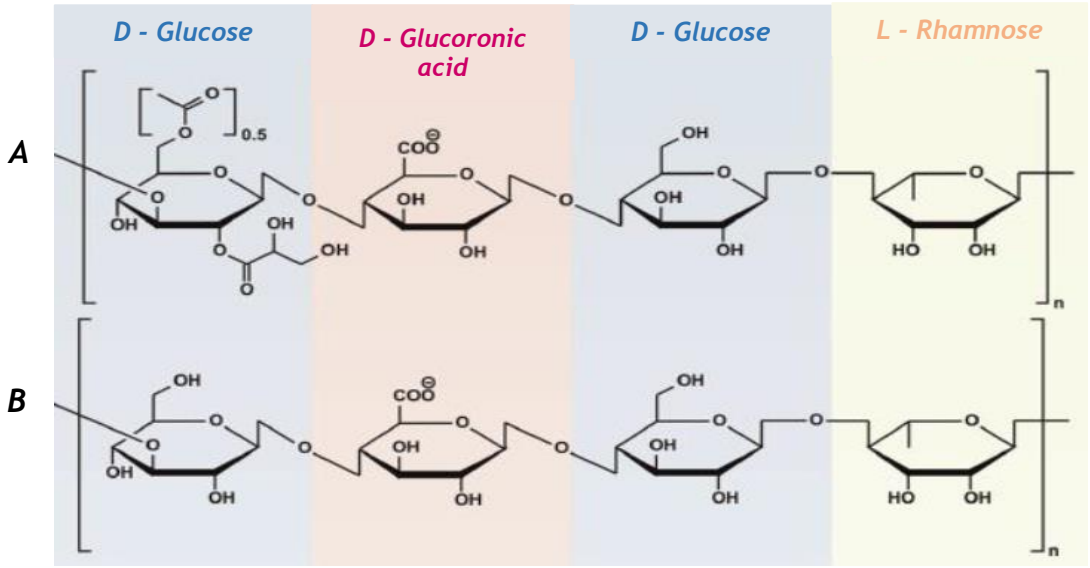

Figure 4 - Structure of modified gellan gum **(A)** High acetyl gellan gum; **(B)** Low acetyl gellan gum [28].

1.2.3. The pathway of gellan biosynthesis

The pathway to the synthesis of the repeating units of gellan gum by *Sphingomonas paucimobilis* has been studied and this bacterium appears to catabolize glucose in two different ways, through Entner-Doudoroff pathway and via pentose phosphate pathway. Entner-Doudoroff pathway apparently does not have a function in degradation of glucose since phosphofructokinase activity, an enzyme essential to glycolysis, has not been detected [29]. Moreover, gellan biosynthesis can be divided in three successive steps. The pathway starts by synthesising the sugar-activated precursors in the intracellular cell, then the assembly of the tetrasaccharide repeat unit linked to the inner membrane occurs and finally the repeat unit moves to the periplasmic space, which is polymerized and exported from the polymer through the external membrane [30].

Glucose catabolism in *Sphingomonas paucimobilis* is represented in figure 4. The glucose molecule enters the cell before to be degraded, following these steps [29, 31].

$$\text{Glucose}_{out} \longrightarrow \text{Glucose}_{in} \longrightarrow \text{Gluconate} \longrightarrow \text{Gluconate-6-phosphate} \quad (1)$$

$$\text{Glucose}_{out} \longrightarrow \text{Gluconate-6-phosphate}_{in} \longrightarrow \text{Gluconate-6-phosphate} \quad (2)$$

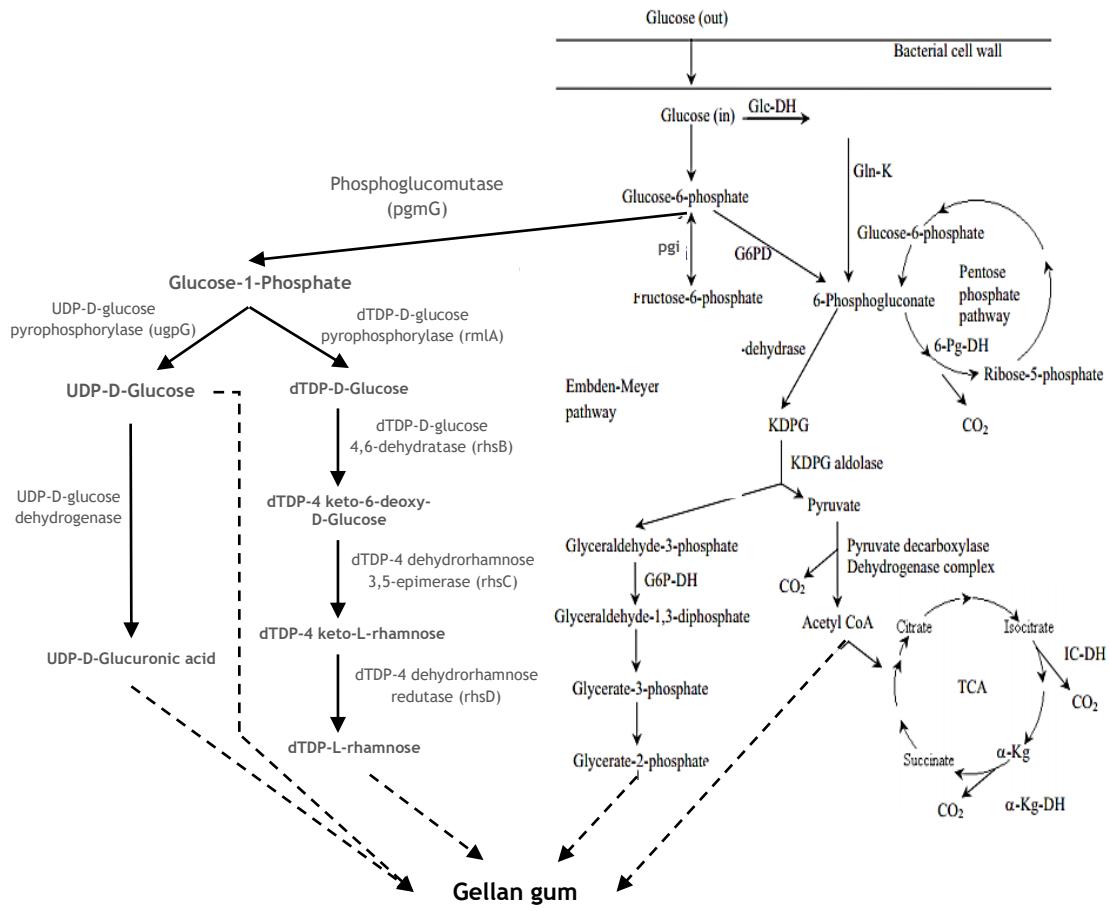

Figure 5 - Proposed pathway for nucleotide-sugar precursors and glucose catabolism in *Sphingomonas paucimobilis*. **Abbreviations: a-kg**, a-ketoglutarate; **a-kg-DH**, a-kg-dehydrogenase; **G3P-DH,** glyceraldehyde-triphosphate-dehydrogenase; **Glc-DH,** Glucose dehydrogenase; **Glc-K,** Glucosekinase; **Gln-K,** gluconate kinase; **IC-DH,** isocitrate dehydrogenase; **KDPG,** 2-keto-3-deoxy-6-phospho-gluconate; **6-Pg-DH,** 6-phosphogluconate dehydrogenase; **Pgi,** phosphoglucoisomerase; **Zwf,** glucose-6-phosphate-dehydrogenase; **TCA,** tricarboxylic acid cycle (adapted by [29, 31]).

Before to begin the intracellular catabolism, glucose is externally converted in gluconate and then to 2-keno-gluconate (KDP-G) [29]. The gellan synthesis needs to activate precursors before the repeating units aggregate, similarly to other exopolysaccharides, which were detected by enzyme assays and found to be nucleotide diphosphate sugars [32].

The biosynthesis begins with the formation of the nucleotide sugar, uridine 5-diphosphate D-Glucose (UDP-G), uridine 5-diphosphate D-Glucuronic Acid (UDP-GA) and thymidine 5-diphosphate L-rhamnose (TDP-R). Therefore, glucose-6-phosphate seems to be an important key to start two routes, one resulting in uridine-5-diphosphate glucose and the other leading to thymine-5-diphosphate rhamnose [33].

Thus, the genes (the *pgmG* and *ugpG* genes encoding a phosphoglucomutase and glucose-1-phosphate uridyltransferase, respectively) and enzymes involved in the synthesis of gellan precursors, which are necessary for the synthesis of UDP-G, catalyse the reversible conversion of glucose-6-phosphate into glucose-1-phosphate and glucose-1-phosphate and UTP (Uridine 5-

Triphosphate) into UDP-G and diphosphate [34, 35]. The *ugdG* gene encoding UDP-glucose dehydrogenase, converting it into UDP-GA [36], and *rmlA* encodes glucose-1-phosphate thymidilyltransferase and convert glucose-1-phosphate and TTP in thymidine 5-diphosphate glucose (TDP-G), essential in the formation of TDP-R [37]. The *pgmG* protein has a fundamental function, being an ideal target to metabolic engineering, since it catalyses a step representative of a branch point in the carbohydrate metabolism. Thus, glucose-6-phosphate enters in catabolic processes to produce energy and reduce the power, while glucose-1-phosphate is a precursor of sugar nucleotides which are used by cells in the synthesis of diverse polysaccharides [30].

1.2.4. Gellan gum production

The production of *Sphingomonas paucimobilis* bacterium is isolated from the surface of an aerobic plant from the *Elodea* genus, in a rod-shaped with a single flagellum and forms mucoid and yellow pigmented colonies in the medium [38]. These production can be influenced by factors such as the composition, structure or the properties of gellan, culture conditions such as oxygen transfer, temperature [39] and medium compounds, particularly the carbon [40] and the nitrogen sources [41].

The optimal temperature for the cell growth is between 30 ºC to 35 ºC, however the gellan yield reaches its peak at 20 ºC, remaining quite high to 25 ºC. On the other hand, these yield decreases when the fermentation is run at 30 ºC or 35 ºC. Additionally, the synthesis of this biopolymer at 20 ºC raises the viscosity of the medium [39].

Rheological studies discovered how the functionality of gellan is affected by variations in acyl substitution. Thus, the viscosity values are directly associated to the level of glycerate present in the polysaccharide [42]. Also, the pH value of the medium growth affects the production of gellan being the recommended pH ranges of 6.5 to 7.0 [9, 43].

Agitation rate is another condition that influences the production of this polysaccharide. A lower agitation level is insufficient for homogeneous conditions and the broth exhibits gelling characteristic, thus an agitation rate of 250 rpm is suitable for mixing the gellan broth [43].

A vital parameter for gellan synthesis is the oxygen. Oxygen is transferred to the cells making it a key player role in fermentation and closely related in bulk mixing. Thus, a high oxygenation rates, which promote an great gellan synthesis, is in distinct contrast with the low or limiting oxygen levels that contributes to high concentrations of fungal glucans [43].

Finally, nitrogen can also influence the growth of gellan. The addition of nitrate in the grown broth prolonged the fermentation time, once it was the only nitrogen source [44]. However, the specific product yield is very high and the biomass content of broth is lower. Also, the broth

is less viscous and the mixing capacity of the fermenter is lesser limited by the polysaccharide formation [44].

1.2.5. Recovery of gellan gum

An optimization of fermentative parameters is very important but is not enough to guarantee a high yield of the exopolysaccharide gellan gum. The recovery of this biopolymer is crucial and two distinct methods can be used. The first is leading to gellan gum, containing divalent cations, and the other is a short process for the preparation of monovalent cation salts of gellan.

In the first process, the gellan is separated from the cells by filtration, using chemical compounds [9], while in the second process the filtration is replaced by a centrifugation [45]. In both cases a pre-treatment stage is necessary to kill the bacterial cells, deactivate the enzymes and improve the gelling properties of gellan gum through its deacetylation [45].

The first process starts with a pre-treatment which consists in heat the fermentative broth to 95 ºC, in water bath, and then, cool it to 80 ºC and adjust the pH to 10 for 10 minutes, using potassium hydroxide (KOH) or sodium hydroxide (NaOH). The cells are removed by filtration with a filter of 0.2 µm (the cells remaining in the filter). Finally, the filtrate is precipitated using 2 volumes of 99 % isopropanol to obtain a clarified and deacetylated gellan gum. The gellan recovered was dried at 55 ºC for 1 hour [9].

The second method for gellan recovery is similar to the first one. The fermentative broth is heated to 100 ºC in a water bath, for 15 minutes, and then cooled to 85 ºC to adjust the pH to 10, for 10 minutes, using 2 M NaOH. Finally, the broth is neutralized at pH 7.0, using 2 M sulfuric acid (H_2SO_4). These broth is dissolved in distilled water and centrifuged at 38 000 *g* for 1 hour, to sediment the cells, and the supernatant is once again centrifuged. To precipitate the gellan, 4 volumes of 99 % isopropanol are added to the biopolymer to acquire a clarified and deacetylated gellan gum [45]. After the recovery of gellan gum, the product was dried for 1 hour, at 55 ºC [9]. Behind the recovery of gellan gum, the product is freeze-dried to offer another alternative for formulating a dry gellan powder. The production and the recovery steps of gellan gum are represented in figure 5.

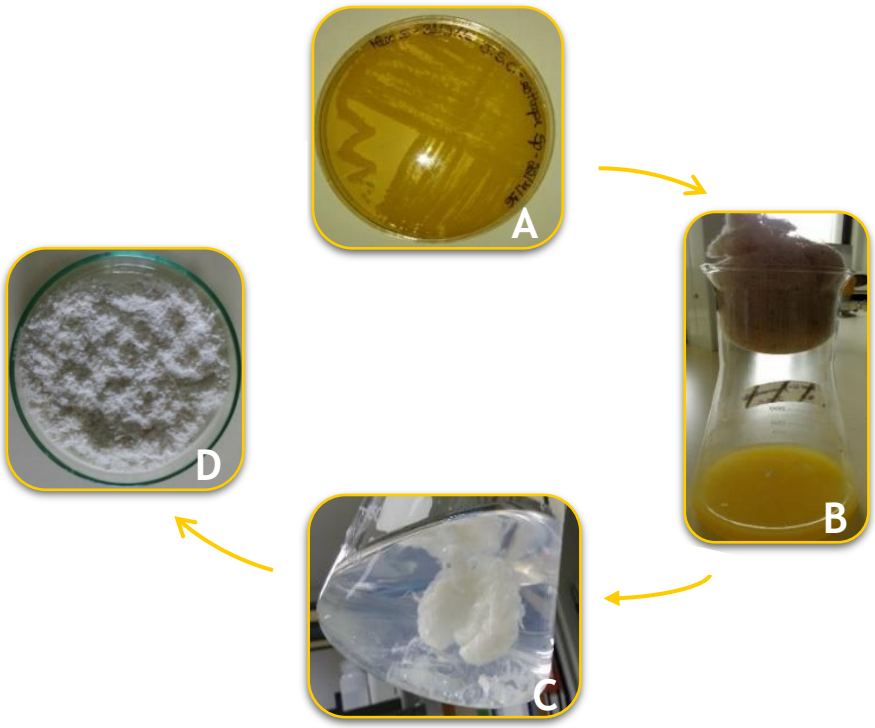

Figure 5 - Schematic model of production and recovery of gellan gum. **(A)** The mucoid solid culture of *Sphingomonas paucimobilis* ATCC 31461**; (B)** Fermentative broth medium at 48 hours; **(C)** Precipitation of gellan gum with isopropanol; **(D)** Gellan gum lyophilized.

1.2.6. Applications

Gellan gum has numerous applications in the food and pharmaceutical industries, as an emulsifier, stabilizer, gelling agent, coagulant, lubricant, thickening and suspending agents [46].

Initially, gellan was used for the preparation of water-based desserts and aspics [27]. The gelatin products have desirable organoleptic properties; however, they are unstable, susceptible to proteolysis and can melt at room temperature. Thus, the combination of gelatin with gellan produce gels with desirable organoleptic properties and thermal stability [47]. This biopolymer not only enhances thermal stability when used as gelling agent but also provides an excellent clarity, similar to water, which is an important characteristic for jellies or sugar icings [12]. Therefore, the addition of gellan to fruit or milk drinks has been very useful in creating stable and homogeneous products [48].

This biopolymer can also be applied in confectionery products and the major advantage here is the pronounced reduction in the setting time of the product. An example of these is the starch jellies that normally take 24 to 48 hours to set, however with the introduction gellan gum reduces the setting time for 10 or 12 hours [27].

Still in food applications, a wide variety of pet foods are commercially obtainable in dry, semisolid or canned form. Thus, gellan is very efficient at low concentrations, making it a good material for pet food application, such as canned and gelled pet food, due to gellan gelling properties in different media [27].

In dairy products, gellan gum can be also applied, for example in cheese. The interaction of gellan with milk proteins increases the yield of cheese and reduces the loss of solids in whey. Also, during the cheese making process, water retention is enhanced after the addition of gellan to milk. Therefore, ice cream is another dairy product that can be improved by the addition of gellan, acting as an effective bulking agent [27].

Table 2 are lists the major food applications of gellan gum, mainly the gelling and thickening agents that this biopolymer can replace.

Table 2 - Food applications of gellan gum [27].

Food area	Products examples	Conventional gelling and thickening agents
Water-based gels	Dessert gels, aspics	Gelatin, alginate, carrageenan
Icings and toppings	Bakery icings, canned toppings	Agar, starches, pectin, xanthan/guar gum
Jams and marmalades	Diet-jams, imitation jams, bakery filings	Pectin, algin, carrageenan
Pie filings and puddings	Instant desserts, pie filings, canned/pre-cooked puddings	Starches, carrageenan, alginate
Confectionery	Starch pellets, pectin jellies, filings, marshmallow	Pectin, starches, gelatin, agar, xanthan/locust bean gum
Fabricated foods	Restructured meat, fruits and vegetables	Alginate, carrageenan/ locust bean gum
Pet foods	Canned/gelled pet food	Alginate, carrageenan/ locust bean gum
Dairy products	Yogurt, milk shakes, gelled milk ice cream	Carrageenan, gelatin, alginate

Beyond applications in food, gellan gum can also be used as a substitute of agar, in plant tissue cultivation, production of capsules, miscellaneous films and fibers and in dental and personal care products as well [9, 49].

The application of gellan gum in pharmaceutical products is presented in table 3. Numerous pharmaceutical formulations have been studied in different applications such as for oral drug delivery, mainly as a disintegrating agent in immediate release drugs [50] or a matrix-forming excipient for sustained release [51], in ophthalmic, as a thickening and gelling agent [52], or for nasal administration, mainly used on local treatment for nasal congestion, infections or

allergic symptoms [53]. Also, gellan-based materials are investigated in the field of tissue regeneration [54], dental care [55], bone repair [56] or biosensor synthesis [57]. Therefore, this biopolymer has potential to control drug release and adsorption in the stomach, in cell immobilization and in microencapsulation techniques [58].

Table 3 - Application of gellan in pharmaceutical products [59].

Drug used	Formulation	Action	Application
Clarithromycin	Floating in *situ* gel	Anti-bacterial	Gastric ulcers
Levofloxacin hemihydrates	Floating in *situ* gel	Anti-bacterial	Helicobacter pylori infections, peptic ulcers
Naproxen	Floating in *situ* gel	Anti-pyretic and nonsteroidal anti-inflammatory drugs (NSAID)	Rheumatic arthritis, inflammation
Cimetidine	Floating in *situ* gel	H_2 receptor antagonist	Peptic ulcer
Acetohydroxamic acid	Floating sphere	Anti-bacteria	Helicobacter pylori infections
Mometasone furoate	Nasal in *situ* gel	Corticosteroid	Allergic rhinitis
Metoclopramide HCl	Intranasal microspheres	Anti-emetic	Cancer therapy, nausea, vomiting, pregnancy migraine
Glipizide	Gellan gum spheres	Hypoglycaemic agent	Diabetes
Gellan gum and beverage or food component	Spherical flavoured gel sphere	Flavourant	Food industry
Carvedilol	Hydrogel microspheres	Anti-hypertensive	Hypertension, Angina pectoris
Gatifloxacin	Ocular inserts	Fluoroquinolone antibiotic	Bacterial conjunctivitis
Indomethacin	Ophthalmic *in situ* gel	NSAID	Uveitis, inflammation of eyes
Metformin	Gum cordial/ gellan spheres	Hypoglycaemic agent	Diabetes
Propranolol	Gellan spheres	ß-blocker	Hypertension
Paracetamol	Oral *in situ* gel	-	-
Ascorbic acid	Gellan gum films	Nutritional and antioxidant property	Food industry

In addition, gellan gum has very important characteristic to be applied in chromatography, due to its hydrophilicity, porosity, high binding capacity and negative charge to establish ionic interactions with charged biomolecules [42, 60–62].

1.3. Magnetization

In recent years, magnetic separation has been widely apply to diverse aspects in biotechnology and biomedical engineering, such as cell separation [63], enzymes immobilization [64], protein separation [65], target drugs [66], and also antibody immobilization [67]. Therefore, are multiple properties associated to magnetic particles such as a relatively quick and easy separation, require a simple apparatus when compared to centrifugal separation [68], and can be derivatised with any ligand used in chromatography, like affinity, ion-exchange or hydrophobic chromatography.

In general, magnetic resins are compound by two parts. The first is the magnetic core made up of inorganic magnetic nanoparticles, like ferrate (FeO_4), manganese ferrite ($MnFe_2O_4$). The second part is the polymeric shell to recover the magnetic core [69]. Briefly, from a physical standpoint the particles should be non-porous relatively to the target molecule, monodisperse relatively to their size, easily separated with the help of a low-to-moderate strength magnetic field and possess a highly specific surface area [70, 71]. Small affinity ligands such as divalent metal ions (for instance Co^{2+}, Zn^{2+}, Ni^{2+} or Cu^{2+}), can be used to obtain high binding capacities for proteins bearing surface-exposed cysteine, tryptophan and especially histidine residues [72].

One of the two older basic designs of commercially magnetic adsorbents are the superparamagnetic iron oxide nanoparticles coated with organofunctional silane coupling agents or silica. The other type of base particles have a nearly perfect spherical shape and are compound of magnetic nanoparticles embedded into a polymeric matrix [72]. Nowadays, magnetic particles are frequently used as magnetic microspheres (figure 6) to separate, capture or purify proteins.
On the other hand, magnetized spheres can also be prepared by subsequent addition of iron and manganese reagents to the spheres previously prepared by the chemical co-precipitation method. This method consists on the recovering of the spheres with an iron chloride and manganese chloride solution and then, the spheres will react with sodium hydroxide to precipitate the ferrite present in the spheres [73].

Figure 6 – Magnetic spheres [73].

1.4. Chromatography

Chromatography is a very frequently studied and applied methodology due to its versatility, simplicity and high reproducibility to separate, identify and purify biomolecules for further different applications. The chromatography principle is based on mixture of molecules applied to the solid surface of stationary phase, which are separated from each other by passing the mobile phase. The factors involved in the separation process include molecular characteristic associated to adsorption, partition and affinity [74, 75]. Thus, the basis of this technique rests in three components. The stationary phase that is composed by a solid phase or a layer of a liquid adsorbed on the surface of a solid support. The mobile phase that is always a compound of a liquid or a gaseous component. Finally, the last component is the sample that contain the target molecule separation [74].

Chromatography procedures can be divide in two categories. The first is analytical chromatography that has as main principal objective the detection of defined components through direct signal acquisition to determine its concentrations by a calibration curve. The second is the preparative chromatography that requires the injection of massive quantities of sample into the column to acquire a certain amount of pure product with high recuperation yield [76].

Additionally, chromatographic processes present five stages, the equilibrium phase, sample injection, washing of non-retained species, elution of molecules adsorbed to the matrix and regeneration [77], as it is presented in figure 7. Firstly, the equilibrium phase confers optimal conditions at the mobile phase, allowing the binding of the target biomolecule to the stationary phase. Then, the sample injection subsists in the insertion of a complex mixture, containing the target molecule, into the stationary phase. The sample is transported by the mobile phase and is distributed between the mobile and the stationary phase. The impurities, which do not interact in the stationary phase, are removed from the column using the equilibrium buffer,

denominated the washing step. To elute the retained species, a buffer that decreases the strength of the interactions between the matrix and the target biomolecule is applied. At last, a very important cleaning process is the regeneration stage which preserves the binding capacity, selectivity and applicability of the chromatographic support and depends on the matrix type [78, 79].

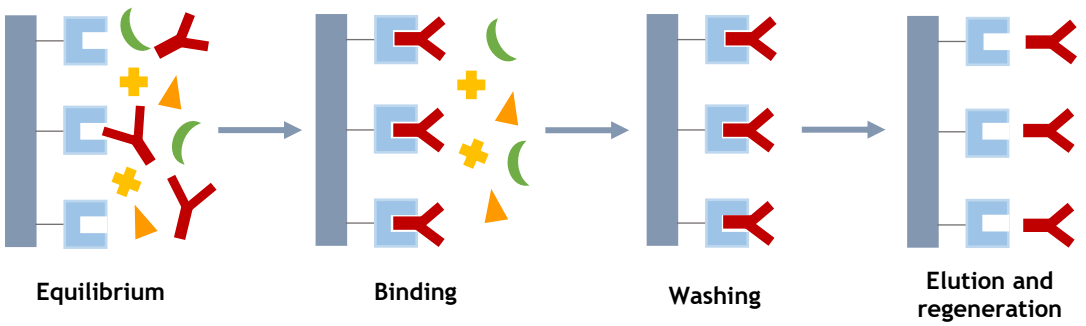

Figure 7 - Schematic chromatography stages: the equilibrium phase, binding, washing and, finally, elution and regeneration.

There are many types of chromatography, which are studied according to diverse types of interactions promoted between ligands in the stationary phase and molecules transported by the mobile phase [80, 81]. Chromatographic methods can be classified as ion-exchange chromatography (IEC), size-exclusion chromatography (SEC), affinity chromatography (AC), reverse phase chromatography (RPC) and hydrophobic interaction chromatography (HIC). The chromatographic methods based on partition are very effective at separating and identifying small molecules like amino acids, carbohydrates and fatty acids. However, affinity chromatography is more efficient to separate macromolecules like nucleic acids and proteins [81]. In table 4 are listed several types of chromatography and their separation principle.

Table 4 - Different types of chromatography and heir principle of action and separation [77].

Name	Separation principle	Separation by
Size-exclusion chromatography	Size exclusion	Molecular size and shape
Ion-exchange chromatography	Ionic binding	Surface charge
Hydrophobic interaction chromatography	Hydrophobic complex formation	Hydrophobicity and hydrophobic patches
Reversed-phase chromatography	Hydrophobic complex formation	Hydrophobicity
Affinity chromatography	Biospecific adsorption/desorption	Molecular structure and chemical structure

1.4.1. Ion-exchange chromatography

Ion- exchanged chromatography is based on electrostatic interactions between charged molecule groups and the charged ligands of the matrix. The matrix contains ions with opposite charge to the target molecule in order to establish an interaction and the affinity of the molecule to the column is achieved with ionic bonds. The target molecule can be further eluted from the column by changing the pH, or the ionic strength of the buffer solution [82].

Ion-exchange matrices can be positively or negatively charged. The positively charged ion-exchange matrices are called anion-exchange matrices and adsorb the negative charged molecules (figure 8). On the other hand, the matrices negatively charged are denominated as cation-exchange matrices and adsorb the positive charged molecules [83, 84].

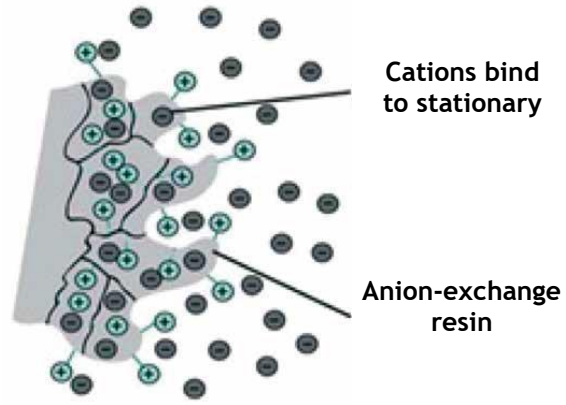

Figure 8 - Ion-exchange chromatographic matrix [84].

1.4.2. Size exclusion chromatography

The principle of size exclusion chromatography is the use of porous particles containing materials to separate the macromolecules based on their different molecular sizes. This type of chromatography is used to determine the molecular weight of proteins and to desalting samples [85].

During size exclusion chromatography, the solution containing molecules of different dimensions passes continuously, with a constant flow rate, through the column. The larger molecules cannot permeate into gel particles and will pass through spaces between porous particles and moves rapidly inside the column. On the other hand, the smaller molecules are diffused into the pores and leave the column with proportionally longer retention times, as demonstrated in figure 9 [86].

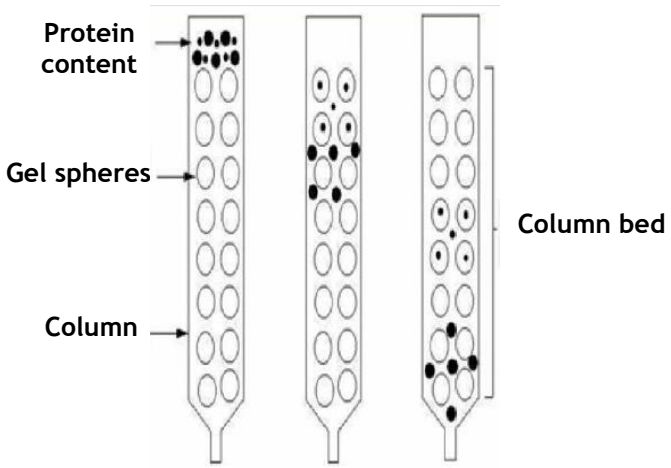

Figure 9 - Size exclusion chromatography [84].

1.4.3. Reverse phase chromatography

This chromatographic process separates molecules according to differences in their hydrophobicity by using organic solvents in the mobile phase (figure 10). Briefly, reverse phase chromatography is a high-resolution method that is more used to purity check analysis (analytical chromatography) when the activity and tertiary structure are not a focus. Given that some biomolecules are denatured by organic solvents, this chromatographic technique is not recommended for preparative biomolecules purification because the recovery of activity and native structure can be compromised. The biomolecules tend to denature and bind strongly to the stationary phase being more difficult to achieve their elution. Therefore, due to its high resolving power, when the most impurities are removed, this chromatography is very appropriate, especially for small target proteins [87].

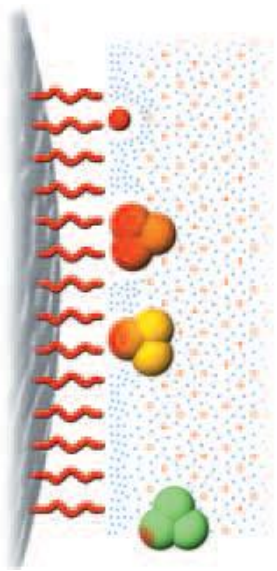

Figure 10 - Reverse phase chromatography [79]

1.4.4. Hydrophobic interaction chromatography

Hydrophobic interaction chromatography is a separation technique based on hydrophobic interactions between hydrophobic ligands immobilized on a matrix and non-polar areas on the surfaces of molecules to be purified [88] (represented in figure 11). The interactions of the molecules in this chromatography are usually promoted by kosmotropic salts, like ammonium sulphate or sodium citrate, which interact with water molecules to reduce solvation of protein molecules in solution and expose their hydrophobic patches to promote binding. The elution step is performed by decreasing of salt concentration or using organic mobile phase modifiers [89, 90]. The major factors that affect the behaviour of the target molecule are hydrophobicity, surface hydrophobicity distribution and molecular size [88, 91].

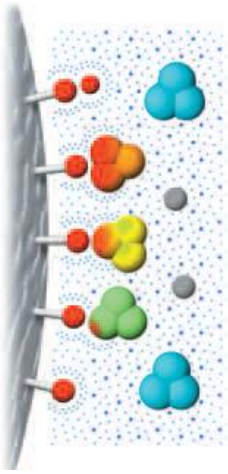

Figure 11 - Hydrophobic interaction chromatography [79].

1.4.5. Affinity chromatography

Affinity chromatography is another technique that can be defined as a type of liquid chromatography, which uses a biologically-related agent or "affinity ligand" as a stationary phase to selectively retain analytes or to study biological interactions [92]. This type of chromatography is used for the purification of enzymes, hormones, antibodies, nucleic acids and specific proteins [93]. Separation of a desired molecule using this technique relies on the reversible interactions between the molecule to be purified and the affinity ligand coupled to chromatographic matrix [94]. This chromatographic process starts with the binding of a specific molecule to the ligand, which can make a complex molecule-ligand. The specific molecule is recognized by the ligand by establishing different type of interactions and being retained in the column, while free molecules exits to the column. Finally, the bonded molecules leave the column by changing the pH, increasing or decreasing the ionic strength or adding competing agents [95], as schematized in figure 12.

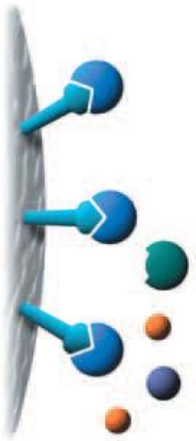

Figure 12 – Affinity chromatography [79].

1.4.5.1. Immobilized Metal Ion Affinity Chromatography

Immobilized metal ion affinity chromatography (IMAC) is a type of affinity chromatography based on specific interactions, which can occur between immobilized metal ions and targets, like amino acids, peptides, proteins, or nucleic acids that contain constituent based on histidine [96].

The metal ions (Ni^{2+}, Zn^{2+}, Cu^{2+} or Fe^{2+}) are immobilized in a column through the use of chelating agents, such as iminodiacetic acid, nitrilotriacetic acid or L-glutamic acid [97, 98]. Thus, the sample passes through an IMAC column and the targets, which can bind to the immobilized metal ions, will be retained and later will be eluted over the addition of a competing agent, like imidazole, and/or by changing the pH and increase of ionic strength [96, 97]. IMAC has become a powerful tool for analysing membrane proteins, histidine-tagged proteins and phosphorylated proteins, in the detection of biomarkers for disease diagnosis and, also, in protein purification [97, 99].

1.4.6. Batch method

The batch method is an alternative chromatographic procedure to a column chromatographic, mostly used for the capture and purification of biomolecules [100].

This method can be applied at any scale and involves three steps. The binding step, where the target biomolecules bind to the particles. Then, the washing step by using the equilibrium buffer to remove the impurities that do not interact with the particles. Finally, the elution step to elute the retained species in the particles, as illustrated in figure 13. The binding, washing and elution stages are divided by a centrifugation step or a magnetic capture step (depending on the nature of the particles) [101].

The major disadvantage of the batch method combined with the centrifugation steps is the waste of liquid, since these cannot be removed completely because some of the volume remains in the pellet [100].

Despite this, the batch method has great advantages like the reduced costs, comparatively to a column chromatography. It is also a faster procedure and has presented very good results compared to the results obtained with a column chromatography [100].

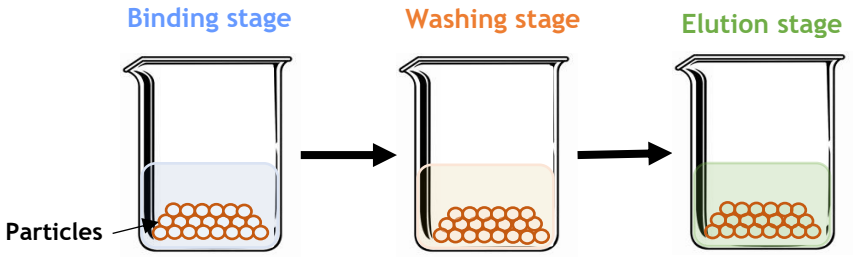

Figure 13 - Schematization of a batch method.

1.5. Catechol - *O* - methyltransferase (COMT)

Catechol-*O*-methyltransferase (COMT, E.C. 2.1.1.6) was first described in the late 1950´s [102]. Since 1980, COMT started to gain interest when the potent and selective second generation of COMT inhibitors were developed. Quickly, this protein presents two isoforms (soluble and membrane), whose structure and gene were discovered and characterized, and the COMT polypeptide cDNAs were cloned [103, 104].

COMT is a magnesium-dependent enzyme that catalyse the methylation of catechol substrates using S-adenosyl-L-methionine (SAM), as a methyl donor and yielding, as reaction products, *O*-methylated catechol and S-adenosyl-L-homocysteine (SAH) [105], represented in figure 14. The substrates of COMT include a large diversity of catechol´s, denominated as catecholamine's, their hydroxylated metabolites, catecholestrogens, ascorbic acid, dietary phytochemicals and medical compound [105, 106].

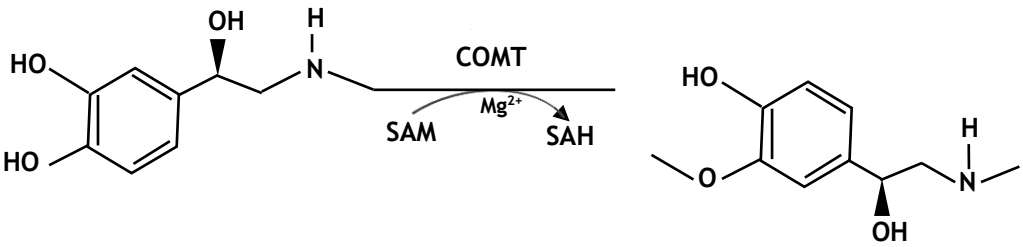

Figure 14 - Reaction catalysed by COMT. COMT in the presence of magnesium (Mg^{2+}) transfers a methyl group from S-adenosyl-L-methionine (SAM) to a hydroxyl group of the substrate.

The principal role of COMT is to eliminate biologically active or toxic catechol's and is especially important the methylation of levodopa to 3-*O*-methyldopa (3-OMD) in levodopa/aromatic amino acid decarboxylase (AADC) inhibitor-treated PD patients [107, 108].

1.5.1. COMT structure

The three-dimensional structure of COMT consists in one single domain with α/ß folds, containing eight α-helices arranged around a central mixed ß-sheet, as illustrated in figure 15. This topology is characteristic of the catalytic domain of other SAM-dependent methyltranferases [109, 110]. The COMT active sites involved the actual catalytic site, where occurs the binding of one magnesium ion and the substrate, and the SAM-binding region. Thus, while SAM is buried into the structure of the enzyme, the catalytic site is a superficial groove located on the surface of COMT. Additionally, the magnesium ions are essential to COMT activity, once that they are coordinated to catecholic hydroxyls, water molecular and the three amino acids residues in the catalytic site of COMT [111, 112].

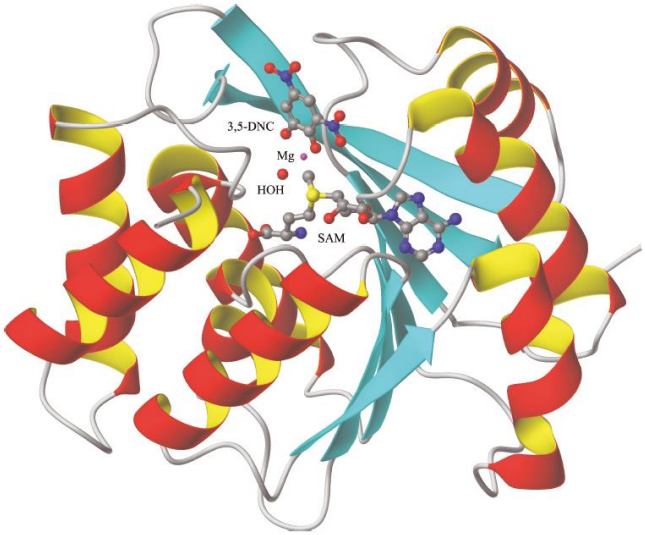

Figure 15 - Schematic representation of the three-dimensional structure of COMT. It is illustrated the S-adenosyl-L-methionine co substrate (SAM), the inhibitor 3,5-dinitrocatechol (3,5-DNC), the Mg^{2+} and coordinated water molecules [112].

1.5.2. The two isoforms of COMT: SCOMT and MBCOMT

COMT has one single gene that codes his two protein isoforms, the soluble COMT (SCOMT) and the membrane-bound COMT (MBCOMT), produced by Escherichia coli bacterium [104].

SCOMT is a nonglycosylated protein dominant containing 221 aminoacids, with a molecular weight of 24.4 kDa. On the other hand, MBCOMT is an integral membrane protein containing 50 additional aminoacids, with a molecular weight of 30 kDa [111, 113].

Nowadays, SCOMT e MBCOMT have been very study and submitted to different purification processes, such as ion-exchange chromatography [114], affinity chromatography [80] or hydrophobic interaction chromatography [115].

In the literature, diverse studies are described to purify the both COMT isoforms through ion-exchange chromatography. Thus, the structural and functional variances between the two isoforms can be reflected in the interactions established with the ligand and, consequently, in the chromatographic conditions applied for each isoform. Studies developed by our research group demonstrate that a lower ionic strength is required to adsorb SCOMT comparatively with MBCOMT, which requires the application of a salt linear gradient. Moreover, the elution steps of these isoforms are different once that the elution of SCOMT is only promoted by an increase in ionic strength, contrary to MBCOMT that needs detergent application in the mobile phase [114]. This technique has a great advantage once that new strategies were established to recover the COMT isoforms, using Q-Sepharose as ion exchanger, which not occurs in other chromatographic techniques and, also, allows to maintain the biological activity, after ion-exchange chromatography.

Also, the affinity chromatography was study to purify proteins and more recently, the complex protein SCOMT. Thus, strategies have been developed to study the effect of adjusting the pH in the mobile phase, in order to elute constituent proteins from recombinant host by using AAIL (amino acids as immobilized ligands) chromatographic matrices. This approach leads to the chromatographic COMT retention, while possess a higher specificity, comparatively with other chromatographic methods. However, the pH manipulation should be controlled in order to avoid the loss of bioactivity of this enzyme. [80].

Recently, hydrophobic interaction chromatography has been used as an efficient method to isolate SCOMT protein, using elution conditions by decreasing stepwise gradients of ammonium sulphate to guarantee intermediate purification and the SCOMT capture step from cell culture supernatant, ensuring that the enzyme retains its native conformation and biological activity. A viable alternative to the elution with ammonium sulphate is the use of sodium citrate, an anti-chaotropic ion described as a powerful protein stabilizer and used to isolate several biomolecules and small proteins. Also, the temperature of the chromatographic system is crucial to improve hydrophobic interaction chromatography selectivity. However, the

improvement of hydrophobic interactions with the adjusting of the temperature can modify the protein conformation and increase or decrease the hydrophobic contact area as well as its bioactivity. This can be advantageous in complex protein extracts, which promotes the elimination of contaminants and, also, can destabilize the bioactivity of target protein [115].

1.5.3. Inhibitors of COMT in Parkinson´s disease

Parkinson´s disease (PD) is characterized by tremor, rigidity, bradykinesia and postural instability. It is a chronic degenerative disease whose principal symptoms are slowness, stiffness and the inability to initiate movements [112].

The design of inhibitors of COMT appeared with its discovery. The first generation of inhibitors, such as tropolone, catechol or 2-hydroxylated oestrogens, showed a low efficacy *in vivo*, lacked selectively and were quite toxic and short acting. In the second-generation, the most commonly inhibitors were nitrocatechols like entacapone, nitecapone or tolcapone [116].

In recent decades, dopamine has been linked to Parkinson´s disease. Thus, levodopa and dopamine agonists are usually the drugs chosen for this disease, when a significant symptomatic effect needs to be achieved [117]. The combination of levodopa with a peripheral AADC inhibitor remains the most effective treatment for PD [112].

COMT inhibitors prevent the normal-*O*-methylation of levodopa to its metabolite 3-OMD and increase the availability of levodopa for conversion to dopamine in the brain by limiting this metabolic route [112].

Chapter II - Objectives

The main objectives of this project are to produce, isolate and magnetize biosynthetic gellan gum spheres to capture therapeutic proteins, mainly the soluble catechol-*O*-methyltransferase protein, containing a polyhistidine tag.

Thus, the first task consists in the biosynthesis of the gellan gum by *Sphingomonas paucimobilis* fermentation, in the recovery of the produced polymer from the extracellular medium by using several techniques, and analysis of its purity level by Fourier-transform infrared (FTIR) and nuclear magnetic resonance (NMR) methodologies.

The second task involves the dissolution of biotechnological gellan gum at high temperatures and the preparation of gellan spheres through the water-in-oil emulsion technique, combined with several divalent metal ions and with and without magnetization. After the oil removal, the formed structures will be characterized by scanning electron microscopy (SEM) and energy-dispersive X-ray spectroscopy (EDX).

Finally, the third task comprises to evaluate the application of gellan gum spheres with model proteins and in real crude *Pichia pastoris* lysates to capture the soluble catechol-*O*-methyltransferase protein.

Chapter III – Material and methods

3.1. Materials

Ultrapure reagent-grade water for all the solutions was obtained with a Mili-Q system from Milipore/Water (Billerica, MA, USA). Sodium phosphate dibasic (Na_2HPO_4) and Manganese (II) chloride tetrahydrate ($MnCl_2.4H_2O$) were purchased in Acrós organics (Geel, Belgium). Potassium phosphate monobasic (KH_2PO_4) and sodium hydroxide (NaOH) were obtained by Chem-labs (Nairobi, Kenya) and Vencilab (Serzedo, Portugal), respectively. Yeast extract, peptone, tryptone and agar were acquired from Biokar Diagnostics (France). Sodium chloride (NaCl), glycose, acetonitrile, ether, sucrose, Tris (hydroxymethyl) aminomethane, urea and imidazole were purchased in Fisher scientific (Epson, United Kingdom).

Sodium sulphate (Na_2SO_4), magnesium sulphate ($MgSO_4$), magnesium sulphate heptahydrate ($MgSO_4.7H_2O$), iron (II) sulphate heptahydrate ($FeSO_4.7H_2O$), casein hydrolysate, 4-Morpholineethanesulfonic acid (MES), gellan gum (Gelrite ®), nickel chloride ($NiCl_2$), cobalt chloride ($CoCl_2$), copper chloride ($CuCl_2$), Iron (III) Chloride Hexahydrate ($FeCl_3.6H_2O$), lysozyme, bovine serum albumin (BSA), deuterated water (D_2O) were obtained by Sigma- Aldrich (St. Louis, MO).

Calcium chloride ($CaCl_2$) and barium chloride ($BaCl_2$) were requested from Panreac (Barcelona, Spain). Acrylamide 30%/Bis was obtained from BioRad (Hercules, CA). Sodium dodecyl sulphate (SDS) and glycerol were acquired from Himedia (Mumbai, India). Ammonium persulfate (PSA) was obtained from Eurobio (Courtaboeuf, France). N,N,N',N'-tetramethylethylenediamine (TEMED) and ß-mercaptoethanol were purchased from Merck (Darmstadt, Germany).

Protein Marker II was purchased from NZYTech (Lisboa, Portugal). Monoclonal rabbit anti-COMT antibody and anti-rabbit IgG alkaline phosphatase secondary antibody were purchased from BIAL (S. Mamede do Coronado, Portugal) and GE Healthcare Biosciences (Uppsalla, Sweden), respectively. All other chemicals were of analytical grade and used without further purification.

3.2. Gellan gum biosynthesis

For the gellan gum biosynthesis through *Sphingomonas Paucimobilis* ATCC 31461, two different mediums were tested. The produced polymer was quantified and the cell growth was measured.

3.2.1. N medium

Production of gellan gum was previously described by Zhang *et al.* [118]. The plates medium (LB) composed by 5 g/L yeast extract, 10 g/L tryptone, 10 g/L NaCl and 20 g/L agar, at pH 7.0, was kept for 72 hours in an incubator at 30 ºC, with the bacterium *Sphingomonas paucimobilis* ATCC 31461.

To promote the adaptation of the bacterium to the N liquid medium, composed by 40 g/L sucrose, 3 g/L tryptone, 3.20 g/L $MgSO_4$, 7.5 g/L Na_2HPO_4, 9.2 g/L KH_2PO_4 and 4.3 g/L Na_2SO_4, at pH 7, a loop of cells of the bacterium were inoculated into 50 mL of the liquid medium in 250 mL flasks and incubated for 24 hours at 30 ºC, 250 rpm, using an orbital shaker. Then, 5 mL of culture medium were centrifuged at 10 000 *g* for 10 minutes and the pellet was resuspended in 50 mL of liquid medium in 250 mL shake flasks, to achieve an initial optical density, at 640 nm (OD_{640nm}), of 0.2±0.01. The fermentation was maintained in the orbital shaker under 250 rpm, for 48 hours, at 30 ºC.

3.2.2. S medium

The biosynthesis of gellan gum was described by Fialho *et al.* [40]. *Sphingomonas paucimobilis* ATCC 31461 was maintained in agar containing S medium, compound by 10g/L of Na_2HPO_4, 3 g/L of KH_2PO_4, 1 g/L of Na_2SO_4, 1 g/L of NaCl, 0.2 g/L of $MgSO_4.7H_2O$, 0.01 g/L of CaCl2, 0.001 g/L of $FeSO_4.7H_2O$, 1 g/L of casein hydrolysate, 1 g/L of yeast extract, 20 g/L of glucose and 20 g/L of Agar. The solid culture was maintained for 72 hours in an incubator at 30 ºC.

For the adaptation step of bacterium to the liquid medium, a loop of *Sphingomonas paucimobilis* from the solid culture was transferred to a culture of 50 mL of S medium in 250mL shake flasks, incubated in an orbital shaker with an agitation of 250 rpm, at 30 ºC, overnight. Then, the culture was centrifuged at 10 000 *g* for 10 minutes, and the pellet was resuspended in growth medium, in order to obtain an initial culture (OD_{640nm}), of 0.2±0.01. The bacterial strain fermentation occurred in 50 mL of S medium in 250 mL shake flasks incubated under 250 rpm, at 30 ºC, for 48 hours.

3.2.3. Quantification of growth bacteria and gellan gum

In order to evaluate the gellan gum produced and the growth of bacteria during the fermentative process, samples of 10 mL of fermentation medium were collected from each flask of 250 mL containing 50 mL of medium recovered at different times (every 8 hours). The samples were placed in a boiling water bath at 95 ºC, for 15 minutes [118] and centrifuged at 16 000 *g*, for 30 minutes. The supernatant free of bacterial content and pellet were separated. The pellet was resuspended in 50 mL of medium to access the cell growth by measuring the OD_{640nm}, by using a spectrophotometer [40].

To determine the gellan gum produced in 10 mL of sample, 30 mL of acetonitrile were added to the supernatant (proportion 1:3). The solution obtained was kept overnight, at 4 ºC, to improve the gellan precipitation and the pellet obtained was dried in an incubator at 60 ºC, for 12 hours [118]. The dry pellet was weighted to determine gellan gum mass.

3.3. Recovery of gellan gum

The biosynthetic gellan gum should be recovered with a satisfactory purity degree to be further used in different applications. Multiple processes were combined and tested to recover the biosynthetic gellan gum in the present project, such as precipitation with acetonitrile, washing with acetone and ether, dissolution in distilled water, dialysis and filtration.

3.3.1. Precipitation, washing, dissolution and precipitation

The first procedure to recover gellan gum was tested in a sample previously precipitated with acetonitrile (proportion 1:3). The pellet was washed several times with acetone and ether and to remove their excess, the gellan gum was centrifuged at 16 000 *g* for 10 minutes. Finally, the biosynthetic gellan was dissolved in distilled water and precipitated overnight with three volumes of acetonitrile, and the pellet, obtained after a centrifugation at 16 000 *g* for 10 minutes was dried in an incubator at 60 ºC for 12 hours. The dry sample was recovered for further analysis.

3.3.2. Precipitation, washing, dissolution, dialysis and precipitation

This method was performed after precipitate the sample from the broth medium [119]. Thus, the sample previously precipitated was, also, washed multiple times with acetone and ether and, finally, dissolved in water. The supernatant was placed within the 3 500 MWCO dialysis cassette, which in turn was placed in a glass with 1 L of distilled water. The sample was dialysed for 3 days with a constant agitation and the water was changed six times. The dialysed gellan gum supernatant was precipitated with 3 volumes of acetonitrile, as previously mentioned.

3.3.3. Dialysis and precipitation

Briefly, after fermentation and the removal of bacterial content by centrifugation, the supernatant was added into a Slide-A-Lyzer 3 500 molecular weight cut off (MWCO) dialysis cassette, according to the procedure described above. Finally, the dialysed gellan gum supernatant was precipitated with acetonitrile as previously described.

3.3.4. Filtration and precipitation

For the recovery of gellan gum, the fermentative broth without bacterial content was directly filtered, with the help of a vacuum pump, using a 2.2 µm cut off filter. Then, the filtered sample was precipitated with acetonitrile as previously referred.

3.3.5. Filtration, washing and precipitation

The supernatant without bacterial content was filtered through a vacuum pump, using a 2.2µm filter, and washed with acetone, ether and distilled water, directly in the filter. The sample was precipitated with acetonitrile as previously indicated.

3.3.6. Filtration, washing, dissolution and precipitation

This technique is very similar to the previous one. The only difference is that after the filtration and washing steps, the sample was dissolved in distilled water for further precipitation with acetonitrile (as already mentioned above).

3.3.7. FTIR and NMR analysis

The recovered pellets of biosynthetic gellan gum were freeze-dried and analysed by Fourier-transform infrared (FTIR) spectroscopy and nuclear magnetic resonance (NMR), in order to be compared to the commercial gellan gum.

The FTIR analysis was performed in a FTIR spectrophotometer (Nicolet iS10) (Thermo Scientific, Waltham, USA). The samples were placed in contact with a diamond window and the spectra were obtained after 128 scans on a wavenumber ranging from 700 to 4000 cm^{-1}, at a resolution of 32 cm^{-1}. The data was processed in the OMNIC Spectra software (Thermo Scientific).

Proton ^{1}H NMR spectroscopy was recorded on a model Brüker Advance III 400 MHz spectrometer (Brüker Scientific Inc, USA). The recovered gellan gum was dissolved in D_2O, in a concentration of 5 mg/mL, and heated at 95 ºC. The solution was transferred to 5 mm outside diameter tubes and the spectra were acquired at 90 ºC. The data was processed using TOPSPIN 3.5 software (Brüker Scientific Inc.).

3.4. Gellan spheres formation with water-in-oil emulsion

The water-in-oil emulsion technique for the formation of gellan gum spheres was described by Narkar *et al.* [120] and optimized through experimental design [121]. Briefly, the solution of gellan gum was prepared with a concentration of 1.41 % (w/v) and heated at 100 ºC with a stirring of 300 rpm, for 30 minutes. Then, this solution was transferred to a syringe, with a 21 G needle (Medoject, United Kingdom), attached to a laboratory support, and was trickled in individual drops into a 100 % vegetable cooking oil solution with a 750 rpm stirring, at 100 ºC.

The resultant mixture was transferred to different solutions (counter-ion) of 200 mM $BaCl_2$, $CaCl_2$, $CoCl_2$, $CuCl_2$ and $NiCl_2$ with a stirring of 750 rpm for 30 minutes, at room temperature. Then, the spheres were washed with ethanol 70% and dried with distilled water in a vacuum filtration system with a filter paper (VWR, EUA). Finally, the spheres were recovered and reserved in a 10 mM MES buffer, pH 6.2, at 4 ºC.

3.4.1. Zeta-potential analysis

The measurement of zeta-potential was performed in a Zetasizer Nano ZS (Malvern Instruments, UK) in order to evaluate the global charge of gellan spheres and data acquisition was performed by the Zetasizer software. One millilitre of gellan spheres, suspended in distilled water, was

flushed through a folded capillary cell (DTS 1070). Then, the cell was placed into the Zetasizer and three replicas of the measurement were made.

3.4.2. Magnetization of gellan spheres

Magnetic particles were prepared through the chemical co-precipitation method [73] of the gellan gun spheres previously prepared. The spheres were added to a solution of 0.25 M $MnCl_2.4H_2O$ and 0.5 M $FeCl_3.6H_2O$, overnight, to make them swell. Then, the spheres were reacted with a 5 M NaOH solution with a constant stirring, to precipitate the ferrite. Finally, the spheres were washed with distilled water in order to remove unreacted chemicals and stored in 10 mM MES buffer, pH 6.2.

3.4.3. Semi-optical and SEM analysis of gellan spheres

A semi-optical microscope was used to determine the mean diameter of the spheres. The spheres stored in a 10 mM MES buffer, pH 6.2, were visualized in a hydrate state and a sample of each formulation was transferred to microscope slides. The samples were visualized at different magnification lens, 5x and 10x and five replicas of each assay were obtained in order to determine the average sphere size (n=5).

The gellan spheres were also visualized through a Hitachi S-3400 N (Tokyo, Japan) scanning electron microscopy (SEM), to view their morphology and surface topography. The spheres were removed from the MES solution, placed in adequate aluminium support and frozen to -20 ºC. The photomicrographs from the surface of spheres were obtained with an acceleration voltage of 15 kV by a Bruker 129 eV (Bruker, USA), at different degrees of magnification.

3.4.4. EDX analysis of gellan spheres

To identify the chemical elements presents in the various formulations of gellan spheres, they were analysed by the energy-dispersive X-ray spectroscopy (EDX). In a frozen state, after the SEM analysis, the spheres were analysed at 15kV and the data acquisition were obtained through QUANTAX 400 (Bruker, USA).

3.5. SCOMT production and extraction

The production of the soluble catechol-O-methyltransferase isoform and recovery from *Pichia pastoris* lysate was made as described by Pedro *et al.* [122]. Briefly, *Pichia pastoris* X-33 cells were grown during 72 hours at 30 ºC in YPD plates and a single colony was inoculated in 100 mL of BMGH medium (100 mM potassium phosphate buffer, pH 6.0, 1.34 % yeast nitrogen base, 4×10^{-5} % biotin and 1 % glycerol) in 500 mL shake flasks, at 250 rpm, 30 ºC, overnight. The cells were reached at OD (600 nm) of 6. Then, an aliquot of the previous fermentation was centrifuged at 500 *g*, for 5 minutes, at room temperature and the cells were resuspended in 125 mL of BMHH medium (100 mM potassium phosphate buffer, pH 6.0, 1.34 % yeast nitrogen base, 4×10^{-5} % biotin and 0.5 % methanol) to start the culture with a OD of 1. The fermentation was induced with methanol and kept at 30 ºC with a stirring of 250 rpm for 24 hours. Finally, the cells were collected by a centrifugation at 1500 *g*, 4 ºC, for 10 minutes and stored at - 20 ºC.

Finally, the cells were lysed in a proportion of 1:2:2, that corresponds to 1 g of cells, 2 g of glass spheres and 2 mL of lysis buffer. The lysis was achieved by a sequential procedure of 7 vortex cycles, of 1 minute, each one with intervals of 1 minute on ice. Then, the mixture was centrifuged at 500 *g*, for 5 minutes at 4 ºC, and the pellet was resuspended in the binding MES buffer.

3.6. Batch method to capture model and SCOMT proteins

The batch method [101], an alternative process to a chromatographic column, was applied using two standard proteins, 5 mg/mL BSA and 10 mg/mL lysozyme and to a more complex extract containing the SCOMT protein.

Initially, the model proteins were prepared with 5 mg/mL BSA dissolved in 10 mM MES buffer, pH 6.2, and 10 mg/mL lysozyme dissolved in 10 mM MES, pH 6.2. The beads (500 µL) were equilibrated with 10 mM MES buffer, pH 6.2, and after the removal of the binding buffer 1 mL of each model protein solution, compound by 250 µL of protein solution with 750 µL of 10 mM MES buffer, pH 6.2, was added to gellan beads. The mixture was incubated with a constant agitation during 1 hour, at room temperature. Then, the supernatant was separated from the spheres by gravity and recovered for further analysis and in order to remove the excess of protein that did not bind with the beads, a washing step with MES buffer was made. To elute the protein bonded to the beads, 1 mL of 0.5 M NaCl in 10 mM MES buffer, pH 6.2 was added and after an incubation of 15 minutes with a constant stirring, the supernatant was collected for further analysis. Therefore, the beads were washed with distilled water.

In the assays with a more complex extract containing the SCOMT protein, different conditions for binding and elution strategies were tested, at room temperature. The recombinant soluble catechol-*O*-methyltransferase was obtained from *Pichia pastoris* X-33 fermentation and the cells were collected by a centrifugation step. As described above, these cells were lysed, through sequential intervals of vortex cycles and ice [122].

The first strategy explored for the capture of SCOMT protein from the lysate consisted in the same conditions used to capture the model proteins.

The second strategy used 8 M of urea during the SCOMT extraction in order to promote a higher binding of the protein with the beads by exposing the histidine tag. Thus, after the equilibration of spheres with 10 mM MES buffer, pH 6.2, it was added 1 mL of sample (compound by 250 µL of SCOMT lysate and 750 µL of MES buffer, containing 8 M urea), was added to 500 µL of beads and maintained for 1 hour with constant agitation. The supernatant was removed from the beads as described previously. To elute the protein that bonded to the beads, 1 mL of 0.5 M NaCl in 10 mM MES buffer, pH 6.2 was added to beads and incubated during 15 minutes, with constant agitation, and the supernatant was recovered for further analysis. Finally, the beads were washed with distilled water.

Other strategy was tested with a larger volume of beads. Thus, at 3 mL of beads, equilibrated with 10 mM MES buffer, pH 6.2, was added 4 mL of sample (compound by 1 mL of SCOMT lysate and 3 mL of MES buffer, containing 8 M urea), and incubated during 1 hour at constant agitation. The supernatant was recovered and 10 mM MES buffer, pH 6.2, was added to the beads to wash them. The elution step was performed with 4 mL of 0.5 M NaCl in 10 mM MES buffer, pH 6.2, and after an incubation for 15 minutes with constant agitation, the supernatant was collected for further analysis. The beads were washed with distilled water.

Once that, the binding of the protein to the beads is very small, a new strategy with a higher volume of beads was tested. Thus, to 10 mL of gellan beads (previously equilibrated with 10 mM MES buffer, pH 6.2) were added 4 mL of SCOMT lysate solution in 10 mM MES and 8 M urea (with the same concentration of lysate described before) and the mixture was incubated for 1 hour at constant agitation. The supernatant was recovered and the beads were washed with 10 mM MES buffer, pH 6.2. To elute the protein that bound to the beads, 4 mL of 0.5 M in NaCl in 10 mM MES buffer, pH 6.2 was added, and after an incubation for 15 minutes with a constant agitation, the supernatant was recovered for further analysis. Finally, the beads were washed with distilled water.

The next strategy was performed with a higher salt concentration in the elution step, in order to increase the recovery of SCOMT protein that bound to the beads. Therefore, after the equilibrium of the beads with 10 mM MES buffer, pH 6.2, 4 mL of SCOMT lysate solution, 10 mM MES buffer and 8 M urea, prepared with the same conditions described before, was added to 10 mL of beads and the mixture was maintained for 1 hour, at a constant agitation. The

supernatant was recovered and the beads were washed with 10 mM MES buffer, pH 6.2. Finally, the bonded protein was eluted from the beads with 4 mL of 1.5 M NaCl solution (10 mM MES, pH 6.2), during 15 minutes, at constant agitation, and the supernatant was recovered. The beads were washed with distilled water.

Thereafter, a strategy was tested using imidazole in the elution step, in order to study its effect on the interaction of proteins bonded to the beads, once that imidazole competes with the his-tag proteins and thus, it is used in IMAC assays to elute any proteins that were weakly bound [123]. Therefore, to 10 mL of beads were added 4 mL of a solution of SCOMT lysate, 10 mM MES buffer, pH 6.2, (with the same concentration of protein as described previously) and 8 M urea. The mixture was kept for 1 hour with a constant agitation, the supernatant was recovered and the beads were washed with 10 mM MES buffer solution, pH 6.2. To elute the protein, 4 mL of 0.5 M NaCl and 0.5 M imidazole were added to the beads, the supernatant was recovered and finally, the beads were washed with distilled water.

After this test, increased NaCl concentrations were tested in the elution step, at pH 6.2 in order to improve the SCOMT recovery. Thus, the beads were equilibrated with 10 mM MES buffer, pH 6.2, and, then, 4 mL of SCOMT lysate solution, 10 mM MES buffer, pH 6.2, and 8 M of urea (with the same concentration described before), was added to 10 mL of beads with a constant agitation, for 1 hour. The supernatant was recovered and the beads were washed with MES buffer, pH 6.2. Then, the elution step was performed with different salt concentrations (0.1 M NaCl, 0.750 M NaCl and 1.5 M NaCl, pH 7.0) added sequentially to the beads, with an incubation of 15 minutes for each concentration and the respective supernatant was recovered and, finally, the beads were washed with distilled water.

Posteriorly, in order to study the influence of pH at 7.5 on the binding of the protein to the beads, an equilibrium step was performed with 10 mM Tris buffer, pH 7.5. After, 4 mL of SCOMT lysate solution, in 10 mM of Tris buffer, pH 7.5, and 8 M of urea (prepared with the same concentration of protein as describe in the previously strategies) was added to 10 mL of beads and the mixture was kept for 1 hour at a constant agitation. The supernatant was removed from the beads, which were washed with 10 mM Tris buffer, pH 7.5. The elution step was made with change of pH to 5.2 by addition of 4 mL of 10 mM MES buffer, pH 5.2, follow by two elution steps with 100 mM and 750 mM NaCl in 10 mM MES buffer, pH 5.2. Each elution step was incubated during 15 minutes, with constant agitation, and the respective supernatant were collected. The beads were washed with distilled water.

Lastly, the influence of acidic pH was tested in the binding step. Thus, after the equilibrium of the beads with 10 mM of citrate buffer, pH 4.0, 4 mL of SCOMT lysate solution in citrate buffer, pH 4.0, and 8 M urea, (with the same concentration of protein as mentioned before) was added to 10 mL of beads, and incubated during 1 hour, in a constant agitation. The supernatant was recovered and the beads were washed with 10 mM citrate buffer, pH 4.0. The elution of the protein that bond to the beads was made with the addition of 4 mL of 10 mM of MES buffer pH

6.2 and then with 100 mM NaCl and 750 mM NaCl in 10 mM MES bffer, pH 7.0, consecutively, with an incubation of 15 minutes, for each concentration and the respective supernatant was preserved. Finally, the beads were washed with distilled water.

All the assays were tested with gellan spheres containing nickel as a cross-linker and the same spheres that were additionally magnetized. The recovered supernatants were concentrated for a volume of 200 µL, and desalted with Vivaspin concentrators (10.000 MWCO) using 10 mM of MES, citrate or Tris buffer, depending on the samples, and stored at - 20 ºC, for further analysis. Also, the OD of all samples were measured at 280 nm wavelength, through a Pharmacia Biotech Ultraspec 3000 spectrophotometer.

3.6.1. Total protein quantification

The protein contained in lysate SCOMT and the recovered supernatants were quantified by a Pierce BCA Protein Assay Kit (Thermo Scientific, USA) on a 96 well plate. To determine protein concentration, a specific volume of working reagent (W_R) was prepared from the kit and BSA was used as the standard and calibration control samples. The absorbance was measured at 562 nm wavelength.

To determine the total protein in the sample three standard curves were taken into account, the standard curve of MES buffer, citrate buffer and Tris buffer.

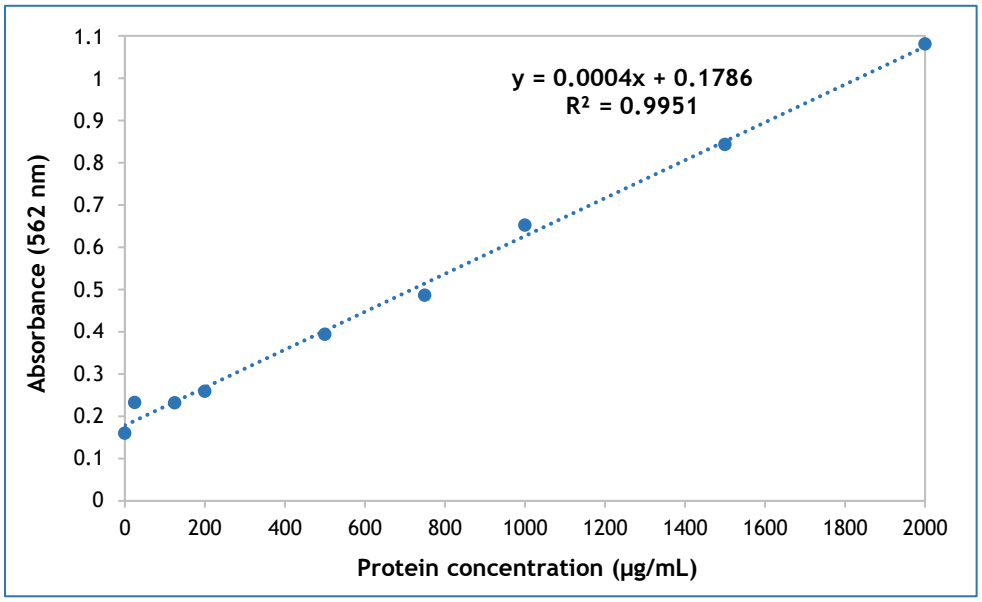

Figure 16 - Standard curve for MES buffer, using BCA protein assay kit.

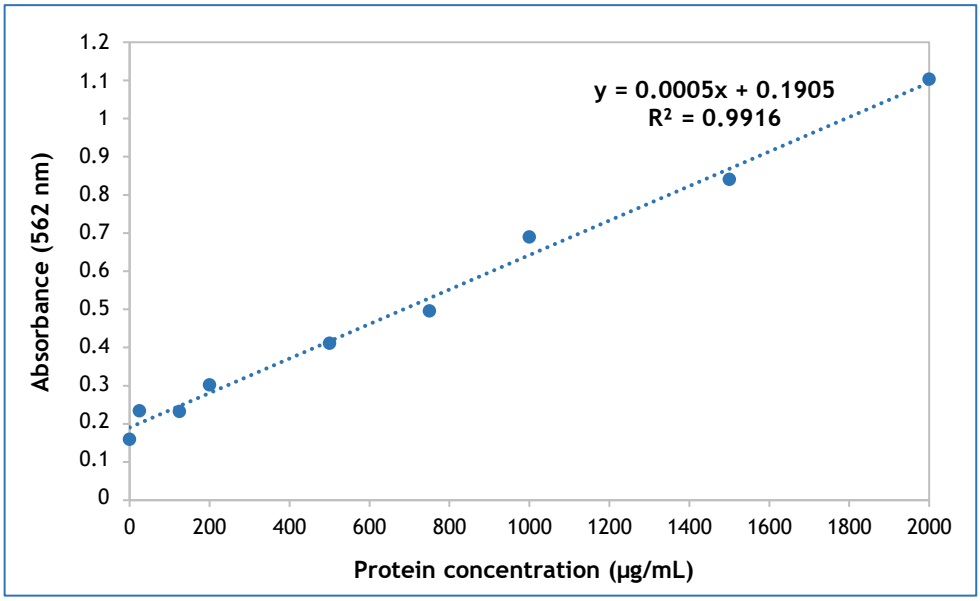

Figure 17 - Standard curve for citrate buffer, using BCA protein assay kit.

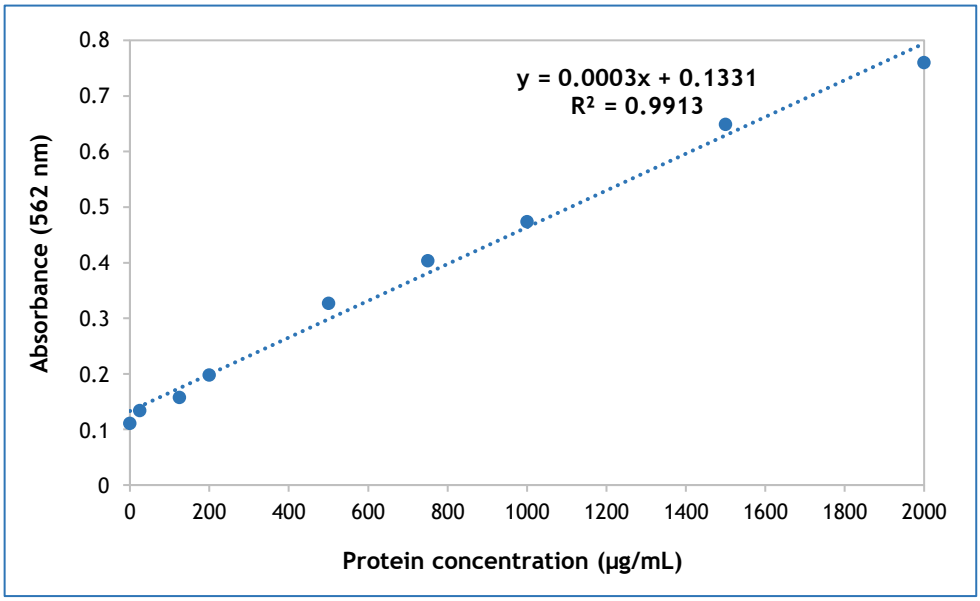

Figure 18 - Standard curve for Tris buffer, using BCA protein assay kit.

3.6.2. DOT-BLOT and SDS-PAGE electrophoresis analysis

Dot-Blot analysis was performed with a polyvinylidene (PVDF) membrane activated with pure methanol and treated with Mili-Q water and TBS (20 mM Tris-HCl, 150 mM NaCl). Then, 80 µL of concentrated samples were applied to the membrane and after the drying of these samples the membrane was again activated with methanol 40% and treated with water and TBS, for 5 minutes. To block non-specific sites, the membrane was placed in a 5 % (w/v) solution of non-fat powered milk dissolved in TBS-T (20 mM Tris-HCl, 150 mM NaCl, Tween 20) for 1 hour. After

this, the membrane was washed three times with TBS-T and incubated with a primary antibody (monoclonal rabbit anti-COMT antibody, at 1:4000 dilution in TBS-T), overnight, at 4 ºC. Then, the membrane was washed three time with TBS-T and the adhering antibody was detected after being incubated with an anti-rabbit IgG alkaline phosphatase secondary antibody, at 1:40 000, during 1 hour. The PVDF membrane was washed three times with TBS-T, during 15 minutes, incubated with 1 mL of ECL, for 5 minutes, and enhanced by exposure to chemiluminescence detector.

Sodium Dodecyl Sulphate-Polyacrylamide Gel Electrophoresis (SDS-PAGE) was performed by the Laemmli method [124]. Briefly, 30 µL of samples were treated with 10 µL of a reduction buffer (500 mM Tris-HCl (pH 6.8)), 10 % (w/v) SDS, 0.02 % bromophenol blue (w/v), 0.2 % glycerol (v/v), 0.02 % ß-mercaptoethanol (v/v)) and denatured at 100 ºC, for 5 minutes. The electrophoretic assay was performed on 12.5 % resolving and 4.5 % stacking gels with a running buffer containing 25 mM, 192 mM glycine, 0.1 % (w/v) SDS, at 120 V for 1h 40 minutes. After the running, the gel was placed in Comassie brilliant blue.

Chapter IV – Results and discussion

Gellan gum is a microbial exopolysaccharide that can be applied in the food, pharmaceutical and other industries, as a thickening, stabilizing, emulsifying and gelling agents, due to its diverse properties [32]. Also, as chromatographic matrix, this polysaccharide shows some important properties, like porosity, hydrophilicity, high binding capacity and negative charge to establish ionic interactions with positively charged model proteins. Additionally, in the presence of metallic ions, this biopolymer forms clear gels, resistant to temperature and extreme acidic conditions [42, 60–62].

Presently, the capturing, separation and purification of proteins has been very studied and new strategies have been reported and used with that finality. Magnetization has been thoroughly applied in cell separation [63], protein separation [65], target drugs [66] and others, once that promotes a quick and easy separation, and can be derivatised with ligands used in chromatography in order to be more specific.

Thus, the main goal of this project is to produce biosynthetic gellan gum and formulate gellan spheres. The spheres will be magnetized by the chemical co-precipitation method and used to capture SCOMT lysate, through the batch method.

4.1. Gellan gum biosynthesis

The production of gellan gum is often described in literature and differences in the medium, temperature, oxygen, carbon source or cation concentrations can be determinant factors for obtaining a better production of this biopolymer [40, 118]. In the present work, to produce biosynthetic gellan gum, two different medium cultures were applied in the fermentation of *Sphingomonas paucimobilis* ATCC 31461 strain. These procedures were chosen based in articles that relate the achievement of high production of gellan gum (19.91 g/L and 14 g/L, using the N medium and S medium, respectively) [40, 118]

The fermentation process obtained for each medium is presented in figure 19. The bacteria grown in N medium demonstrate a higher OD measure over the 48 hours, indicating that the bacteria have a better adaptation to this liquid medium.

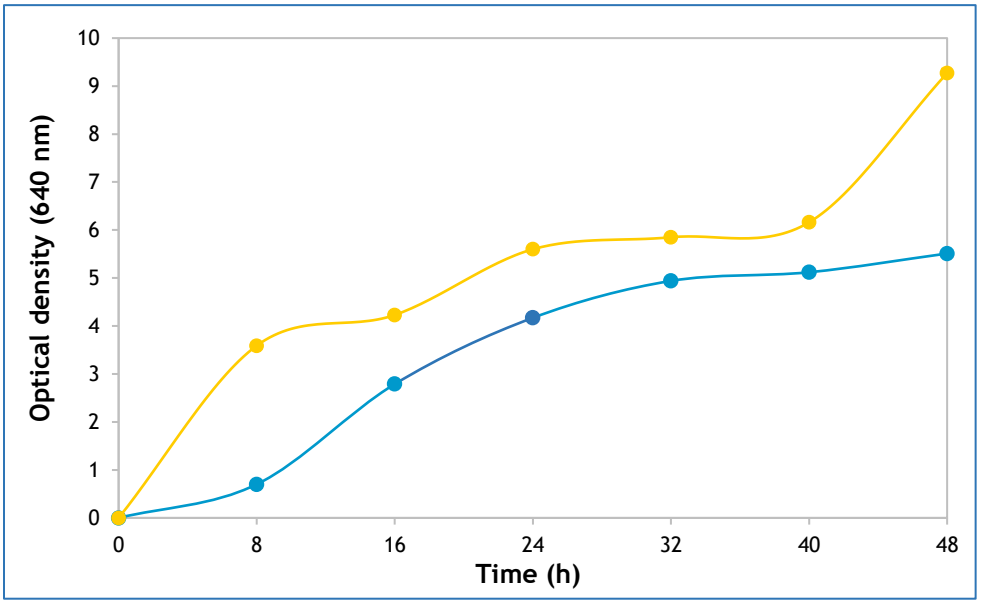

Figure 19 - Bacteria growth for 48 hours in relation with the optical density (640 nm). N medium (●) and S medium (●).

Therefore, the production of gellan gum shows better concentrations for the S medium, with 23.84 g/L gellan gum, at 48 hours, while N medium achieve 0.11 g/L, as can be seen in figure 20.

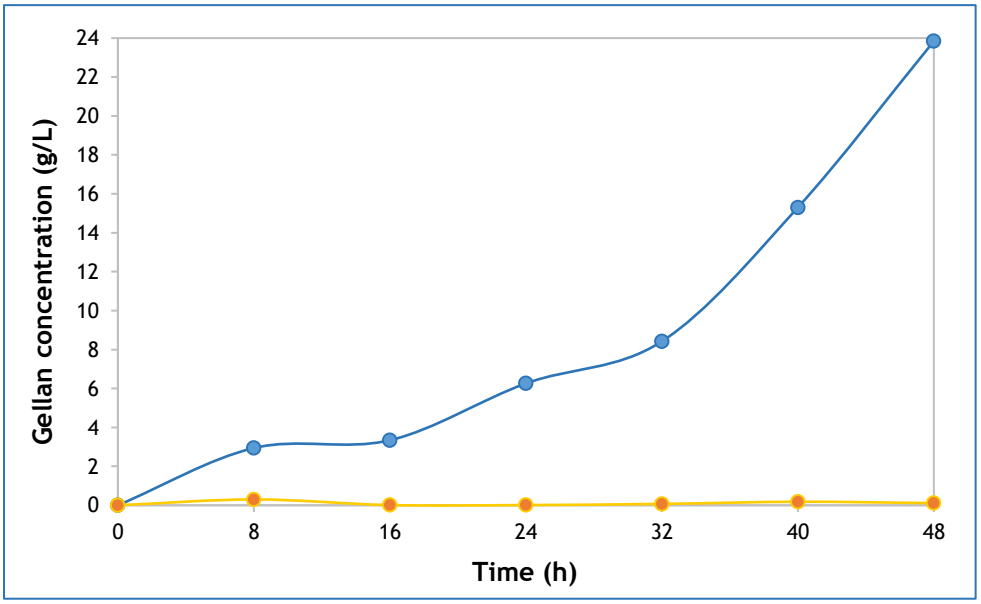

Figure 20 - Gellan gum production by *Sphingomonas paucimobilis* ATCC 31461, for 48 hours. N medium (●) and S medium (●).

Thus, the results obtained in this work contradict what it is described in literature [40, 118]. Comparing the results, it is perceptible that the best yield was obtained with the S medium. The results obtained with the N medium may be related to the fact that the values of gellan

gum, described in the literature, were obtained by bioreactor production, while in this work were obtained by small-scale fermentation. Also, it is noticeable that in this work a higher concentration of gellan gum was obtained using the S medium, comparatively with the described in literature [40], maybe due to the difference of proportion used between the medium volume and the Erlenmeyer flask capacity. In this work 50 mL of medium in 250 mL flask (1:5 proportion) were used, while in the literature 250 mL of medium were inoculated into a 500 mL Erlenmeyer flask (1:2 proportion). According to the results obtained in the present work it can be suggested that oxygen is a vital parameter for gellan synthesis.

4.2. Recovery of gellan gum

After to identify the best procedure to produce gellan gum, it is necessary to recover this biopolymer by removing the bacterial content from the fermentative broth. Thus, several procedures were tested in order to eliminate contaminants present in bacteria free-supernatant and to increase the purity of the recovered gellan gum.

All the samples obtained during the procedures used for gellan recovery were compared with the commercial gellan gum (Gelrite ®) through FTIR and NMR analysis [125–129].

FTIR spectrum of commercial gellan gum is represented in figure 21 and has five characteristic peaks, the broad band centred at 3320 cm^{-1} due to the O-H stretching vibration (peak A), at 2900.66 cm^{-1} the C-H stretching (peak B), at 1602.60 cm^{-1} the asymmetric COO^- stretching (peak C), at 1400.95 cm^{-1} the symmetric COO^- stretching (peak D), and finally, at 1023.64 cm^{-1} the hydroxylic C-O stretching (peak E).

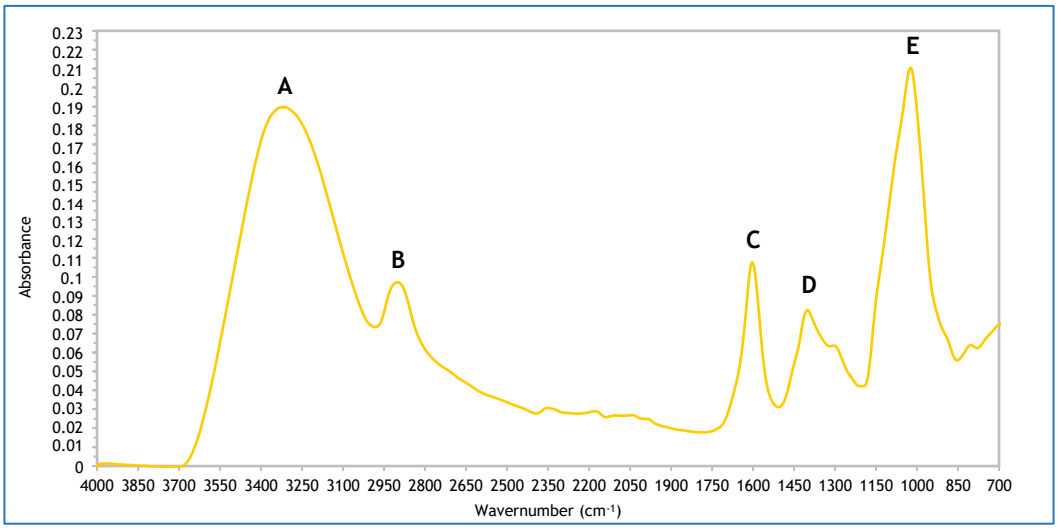

Figure 21 - FTIR spectrum of commercial gellan gum. **A** - 3320 cm^{-1}; **B** - 2900.66 cm^{-1}; **C** - 1602.60 cm^{-1}; **D** - 1400.95 cm^{-1}; **E** - 1023.64 cm^{-1}.

The NMR spectrum of the commercial gellan gum, presented in figure 22, exhibits four characteristic signals at 5.7410 ppm, at 5.3017 ppm, at 5.1398 ppm and at 1.9021 ppm, which corresponds to -CH of rhamnose, -CH of glucuronic acid, -CH of glucose and -CH_3 of rhamnose, respectively.

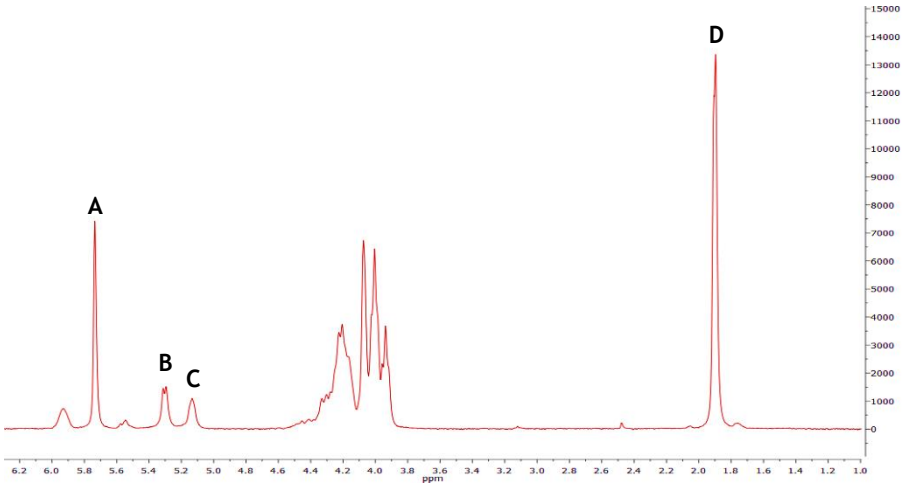

Figure 22 - ^{1}H-NMR spectrum of commercial gellan gum. **A -** 5.7410 ppm; **B -** 5.3017 ppm; **C -** 5.1398 ppm; **D -** 1.9021 ppm.

The FTIR and NMR spectra of commercial gellan gum were used as a pattern to compare with the spectra obtained for the different biosynthetic gellan gum samples obtained by different recovery procedures, after removing the bacterial content from the fermentative broth.

Different procedures were tested to recover the gellan gum, such as washes with acetone and ether, dialysis, precipitation, dissolution in distilled water and a combination of some of these techniques in order to obtain high purity of recovered gellan gum. So, the recovery method starts with a precipitation of the gellan gum sample, once that after the step of the bacteria removal the sample was precipitated with acetonitrile. The use of acetonitrile to precipitate the sample, contrary to that described in literature, was optimized by Emanuel *et al.* [130].

4.2.1. Precipitation, washing, dissolution and precipitation

Firstly, the precipitated sample was washed multiple times with acetone and ether, dissolved in distilled water and, finally precipitated with acetonitrile. After the lyophilization step, the sample was analysed by FTIR and NMR.

In figure 23, the FTIR spectrum demonstrates five characteristic peaks of gellan gum and four peaks from the constituents of the grown medium. The characteristic peaks present in the spectrum below are the O-H stretching (peak A), the C-H stretching (peak B), the asymmetric COO^- stretching (peak D), the symmetric COO^- stretching (peak E) and the hydroxylic C-O stretching (peak G). Therefore, other peaks are evidenced, such as the C=O stretching of ester

group, at 1729.59 cm^{-1} (peak C), the ethereal C-O stretching, at 1144.73 cm^{-1} (peak F), and the bending vibration of C-H appears at 947.41 and 851.42 (peaks H and I). The peaks F, H and I are provided from glucose contamination (whose FTIR spectrum is presented in annex II).

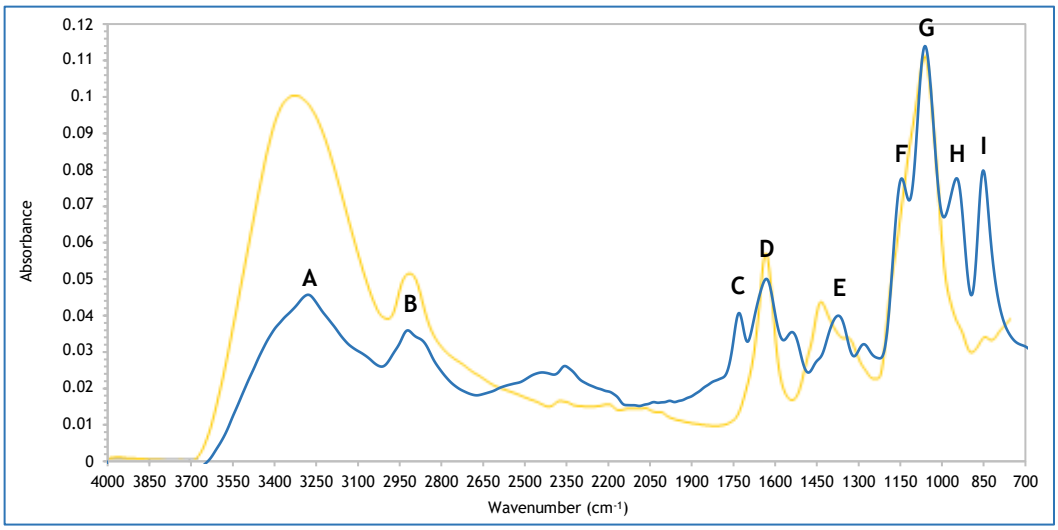

Figure 23 - FTIR spectra of commercial gellan gum (●) and recovered gellan gum (●). **A** - 3279.30 cm^{-1}; **B** - 2920.72 cm^{-1}; **C** - 1729.59 cm^{-1}; **D** - 1631.60 cm^{-1}; **E** - 1372.83 cm^{-1}; **F** - 1144.73cm^{-1}; **G** - 1081.44cm^{-1}; **H** - 947.41 cm^{-1}; **I** - 851.42 cm^{-1}.

The NMR spectrum represented in figure 24, show some contaminants that are not present in the commercial gellan spectrum. Thus, the characteristic signals of gellan are present in that spectrum, those being the -CH of rhamnose (peak A), the -CH of glucuronic acid (peak B), the -CH of glucose (peak C) and the $-CH_3$ of rhamnose (peak G). Beyond these, other signals appear at 3.1197 ppm (peak D) and 2.4766 ppm (peak F) that corresponds to casein and yeast extract, respectively (whose NMR spectrum is presented in annex III and IV, respectively). The signal at 2.7260 ppm (peak E) is characteristic of the methyl group (CH_3), allowing to evaluate the acetylation of the sample and, in this case, it is confirmed that the sample is acetylated.

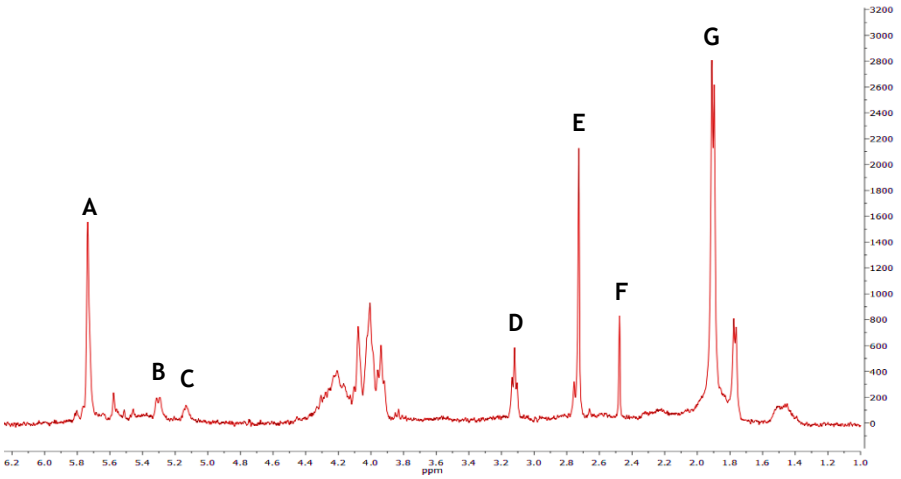

Figure 24 - ^{1}H-NMR spectrum of gellan gum recovered. **A** - 5.7359 ppm; **B** - 5.2939 ppm; **C** - **5**.1339 ppm; **D** - 3.1197 ppm; **E** - 2.7260 ppm; **F** - 2.4766 ppm; **G** - 1.8962ppm.

Take into account the results obtained in this process is necessary test another technique to improve the purity degree of the recovered gellan gum. Thus, it was introduced the dialysis procedure after the washing step and instead of the dissolution with water.

4.2.2. Precipitation, washing, dissolution, dialysis and precipitation

The FTIR spectrum of this procedure is represented in figure 25 and has only two peaks characteristic comparing with the commercial gum. The first peak at 3366.32 cm^{-1}, corresponds to O-H stretching (peak A) and at 1638.94 cm^{-1} is represented the asymmetric COO^- stretching (peak B). The peak at 620.04 cm^{-1} corresponds to the C-H stretching (peak C), from glucose (whose FTIR spectrum is presented in annex II).

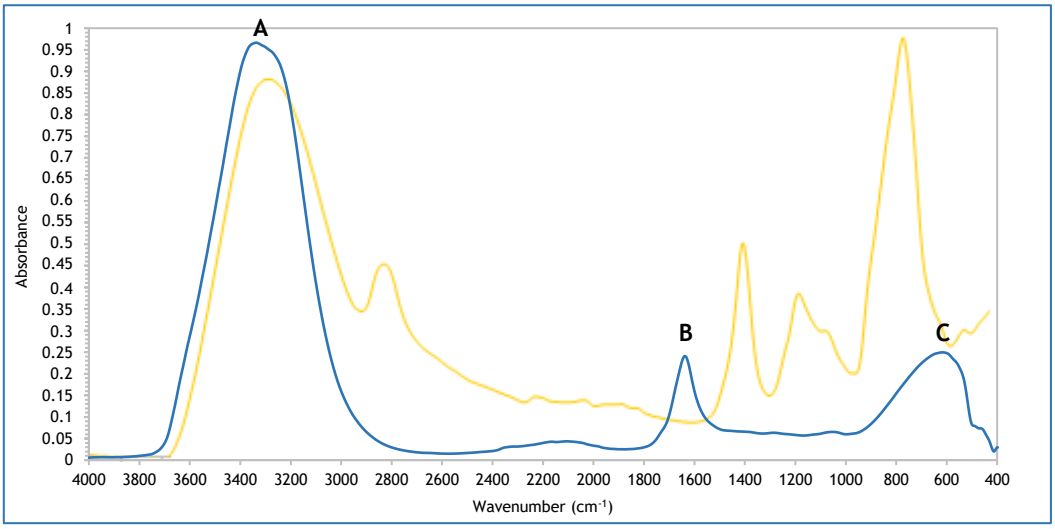

Figure 25 - FTIR spectra of commercial gellan gum (●) and gellan gum precipitated and dialysed (●). **A** - 3366.32 cm^{-1}; **B** - 1638.94 cm^{-1}; **C** - 620.04 cm^{-1}.

Analysing the NMR spectrum pictured in figure 26, the characteristic signals are less intense than in commercial gellan gum. Thus, the characteristic signals are represented in peaks A and E. The signals at 3.1227 ppm and 2.4832 ppm corresponds to casein and yeast extract, respectively (whose NMR spectrum is presented in annex III and IV, respectively), while at 2.6631 ppm is characterized the acetylation degree of the sample through the intensity of the signal, which in this case is deacetylated.

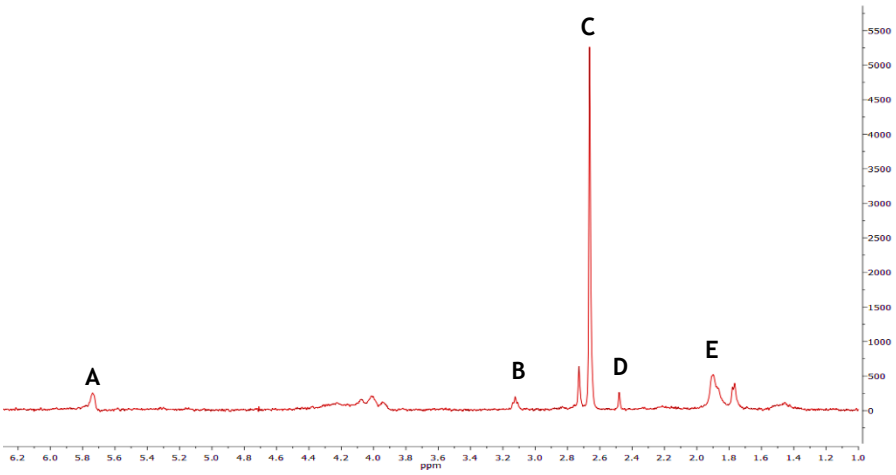

Figure 26 - ^{1}H-NMR spectrum of gellan gum precipitated and dialysed. **A -** 5.7308 ppm; **B -** 3.1227 ppm; **C -** 2.6631 ppm; **D -** 2.4832 ppm; **E -** 1.8902 ppm.

The NMR results corroborate with the FTIR results and it was observed that almost does not exist characteristic peaks of gellan gum in both spectra. As it can be seen, the recovery of gellan gum was not very efficient with this recovery procedure. Thus, the next step was performed in order to understand the influence of isolated dialysis procedure and for that a sample was only centrifuged to remove the cells for further dialysis.

4.2.3. Dialysis and precipitation

After three days of dialysis, the sample was precipitated with acetonitrile and lyophilized for further analysis by FTIR and NMR. Comparing the FTIR spectrum of this sample, presented in figure 27, with the spectrum of commercial gellan gum it is observed that the first have three more peaks than the second one. The spectrum of dialysis has the characteristic peaks of gellan gum, the O-H stretching vibration (peak A), the C-H stretching (peak B), the asymmetric COO^- stretching (peak D), the symmetric COO^- stretching (peak F), and the hydroxylic C-O stretching (peak H). Beyond these, at 1726.02 cm^{-1} is represented the C=O stretching of ester group (peak C), at 1530.18 cm^{-1} are present the acetyl substituents, CH_2, (peak E) and at 1274.64cm^{-1} is the C-O stretching (peak G). The peaks E and G derive from the constituents of the fermentation medium and corresponds to the casein and glucose, respectively (whose FTIR spectrum is presented in annex I and II, respectively).

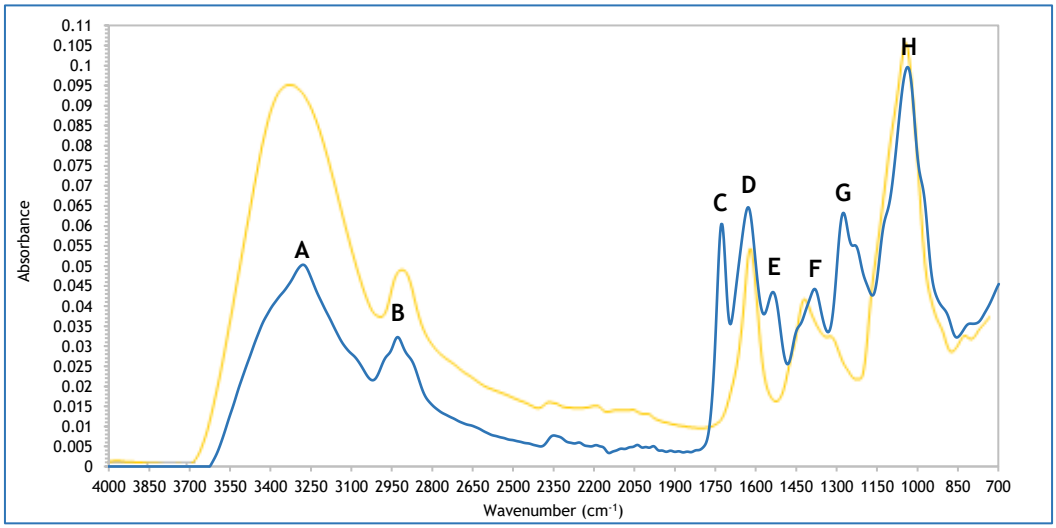

Figure 27 - FTIR spectra of commercial gellan gum (●) and dialysed gellan gum (●). **A** - 3279.29cm^{-1}; **B** - 2926.22 cm^{-1}; **C** - 1726.02 cm^{-1}; **D** - 1626.07 cm^{-1}; **E** - 1530.18 cm^{-1}; **F** - 1381.58 cm^{-1}; **G** - 1274.64cm^{-1}; **H** - 1036.58 cm^{-1}.

Regarding to the NMR analysis, some differences in the spectra are also noticeable. In the dialysis spectrum, presented in figure 28, the characteristic signals of gellan gum are present the -CH of rhamnose (peak A), the -CH of glucuronic acid (peak B), the -CH of glucose (peak C) and the -CH_3 of rhamnose (peak F). The other two signals, at 3.1249 ppm (peak D) and at 2.7439 ppm (peak E) correspond to casein, a constituent of grown medium (whose NMR spectrum is presented in annex III), and to a methyl group, CH_3, which corresponds to the acetylated gellan gum.

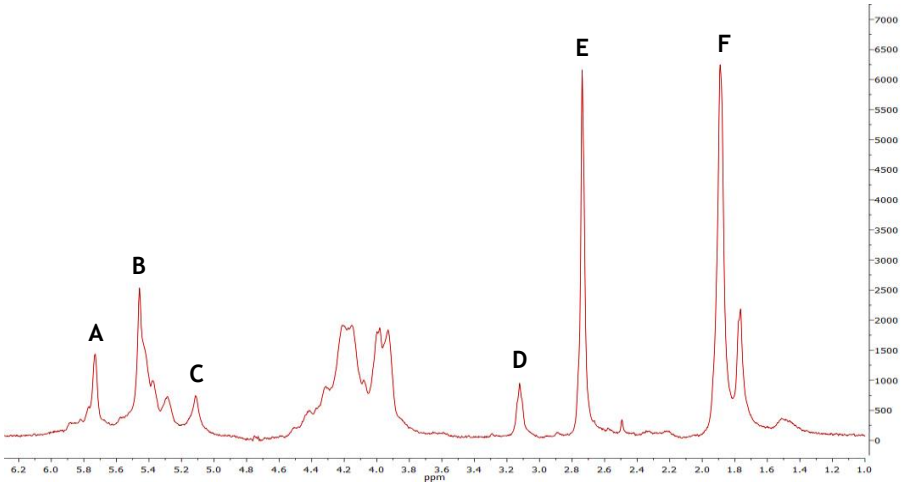

Figure 28 - ^{1}H-NMR spectrum of gellan gum recovered by dialysis. **A -** 5.7361 ppm; **B -** 5.2900 ppm; **C -** 5.1225 ppm; **D -** 3.1249 ppm; **E** - 2.7439 ppm; **F -** 1.8902 ppm.

These results indicated that the recovery of gellan gum with a simple procedure of dialysis without a previous precipitation can also allow interesting results. In this way, the isolated filtration procedure was also tested.

4.2.4. Filtration and precipitation

The filtration technique was used to recovery this biopolymer and the FTIR spectrum, schematized in figure 29, shows that this method is not enough to guarantee the recovery of pure gellan gum. Three characteristic peaks are present in the spectrum, the O-H stretching (peak A), the asymmetric COO^- stretching (peak B) and the hydroxylic C-O stretching (peak C), however, are missing two important characteristic peaks of gellan gum.

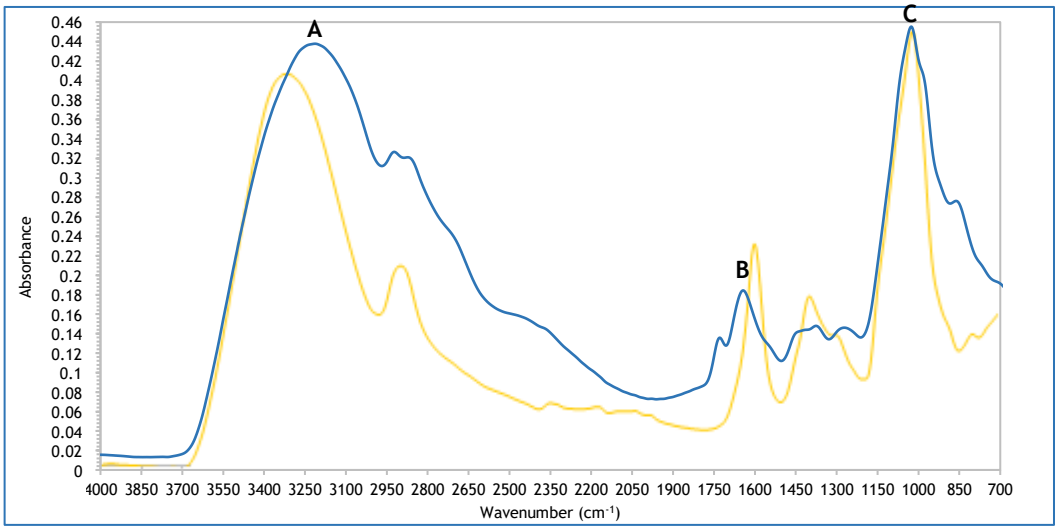

Figure 29 - FTIR spectra of commercial gellan gum (●) and gellan gum filtered (●). **A** - 3213.20 cm^{-1}; **B** - 1643.06 cm^{-1}; **C** - 1026.49 cm^{-1}.

In figure 30, the NMR spectrum shows the characteristic signals of gellan gum, the -CH of rhamnose (peak A), the -CH of glucuronic acid (peak B), the -CH of glucose (peak C) and the $-CH_3$ of rhamnose (peak G). However, some interference still appears at 3.1198 ppm and 2.4773 ppm which corresponds to the casein and yeast extract, respectively (whose NMR spectrum is presented in annex III and IV, respectively). Also, the signal at 2.7258 ppm (CH_3) shows that this sample is acetylated.

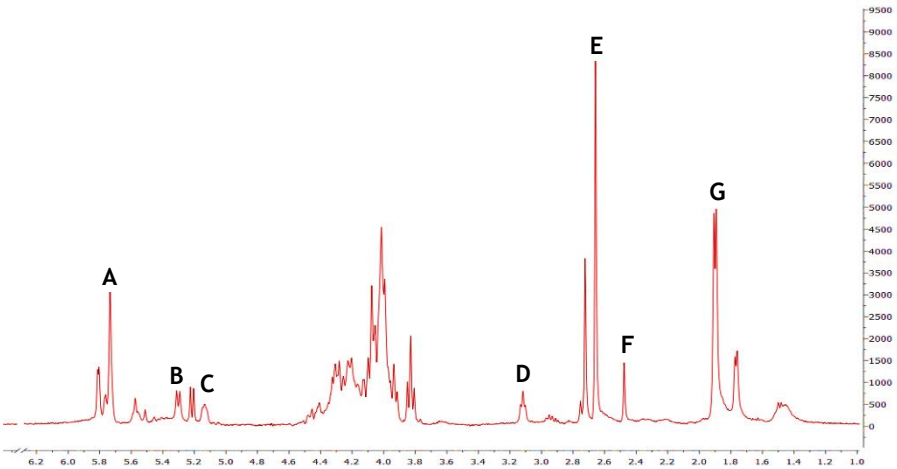

Figure 30 - ^{1}H-NMR spectrum of gellan gum recovered by filtration. **A -** 5.7379 ppm; **B -** 5.2958 ppm; **C - 5**.1222 ppm; **D -** 3.1198 ppm; **E** - 2.7258 ppm; **F -** 2.4773 ppm; **G** - 1.8944 ppm.

Considering these results, it is noticeable that filtration is not enough to recover gellan gum. Thus, the acetone and ether were tested in the filtration technique to wash the gellan gum and then, the sample was dissolved in distilled water.

4.2.5. Filtration, washing and precipitation

In order to improve the previous results, the filtration step was combined with a washing step with acetone, ether and distilled water. By analysis of the FTIR spectrum, illustrated in figure 31, all the characteristic peaks are presented, such as the O-H stretching vibration (peak A), the C-H stretching (peak B), the asymmetric COO^- stretching (peak D), the symmetric COO^- stretching (peak E), and finally, the hydroxylic C-O stretching (peak G). Beyond that, there are two more peaks, one at 1728.05 cm^{-1}, which corresponds to C=O stretching of ester group (peak C), and at 1276.05 cm^{-1}, which characterize the presence of acetyl constituents, CH_2 (peak F), derivative from glucose (whose FTIR spectrum is presented in annex II).

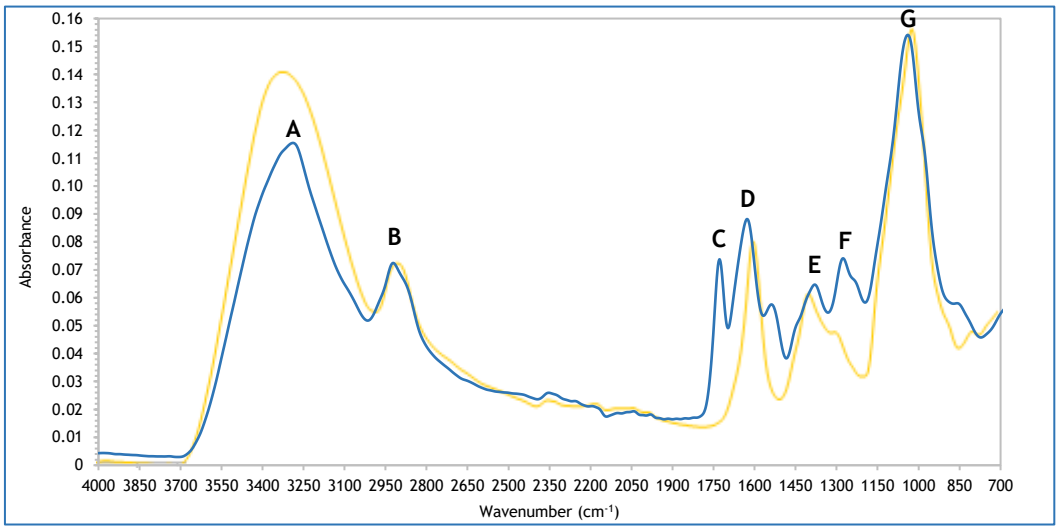

Figure 31 - FTIR spectra of commercial gellan gum (●) and gellan gum filtered with acetone, ether and distilled water (●). **A** - 3266.52 cm^{-1}; **B** - 2921.79 cm^{-1}; **C** - 1728.05 cm^{-1}; **D** - 1627.11 cm^{-1}; **E** - 1379.79 cm^{-1}; **F** - 1276.05cm^{-1}; **G** - 1039.36 cm^{-1}.

The NMR spectrum, represented in figure 32, is very similar to the spectrum of commercial gellan gum. These spectra present seven signals, being that four corresponds to the characteristic signals of gellan gum. The signals at 3.1237 ppm (peak D) and 2.4808 ppm (peak F) characterize the casein and the yeast extract, respectively (whose NMR spectrum is presented in annex III and IV, respectively). Therefore, this sample is acetylated, due to the methyl group (CH_3) present at 2.7288 ppm (peak E).

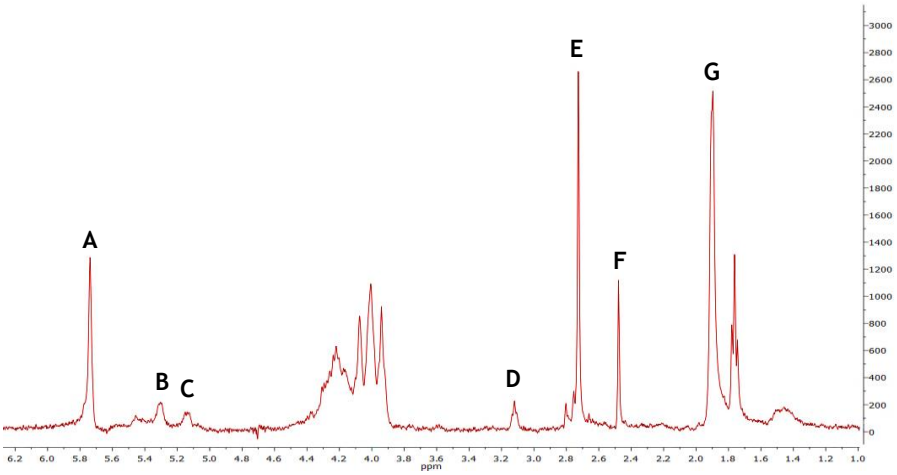

Figure 32 - ^{1}H-NMR spectrum of gellan gum filtered with acetone, ether and distilled water. **A -** 5.7390 ppm; **B -** 5.2975 ppm; **C - 5**.1140 ppm; **D -** 3.1237 ppm; **E -** 2.7288 ppm; **F -** 2.4808 ppm; **G -** 1.8944 ppm.

The results obtained by the addition of the washing step to the filtration technique improved the recovery of gellan gum and, also, its purity degree. However, there is observed a loss of the gellan during the filtration, probably due to the final washing with distilled water that could dissolve the gellan, reducing its yield. Therefore, the next strategy was similar to the previous one but instead of a final wash with water, it was included a dissolution step before the final precipitation.

4.2.6. Filtration, washing, dissolution and precipitation

To overcome the loss of gellan gum through filtration, a new technique was used that consists in the gellan gum filtration, washing with acetone and ether, and then removing this biopolymer from the filter and dissolution with distilled water.

Analysing the spectrum obtained through FTIR, in figure 33, it is very similar to the previous spectrum. The characteristic bands of gellan gum are present in the peaks A, B, D, E and G, which characterize the O-H stretching vibration, the C-H stretching, the asymmetric COO^- stretching, the symmetric COO^- stretching and the hydroxylic C-O stretching, respectively, while the peaks C and F corresponds to C=O stretching of ester group and to acetyl constituents, CH_2, characteristic from glucose (whose FTIR spectrum is presented in annex II).

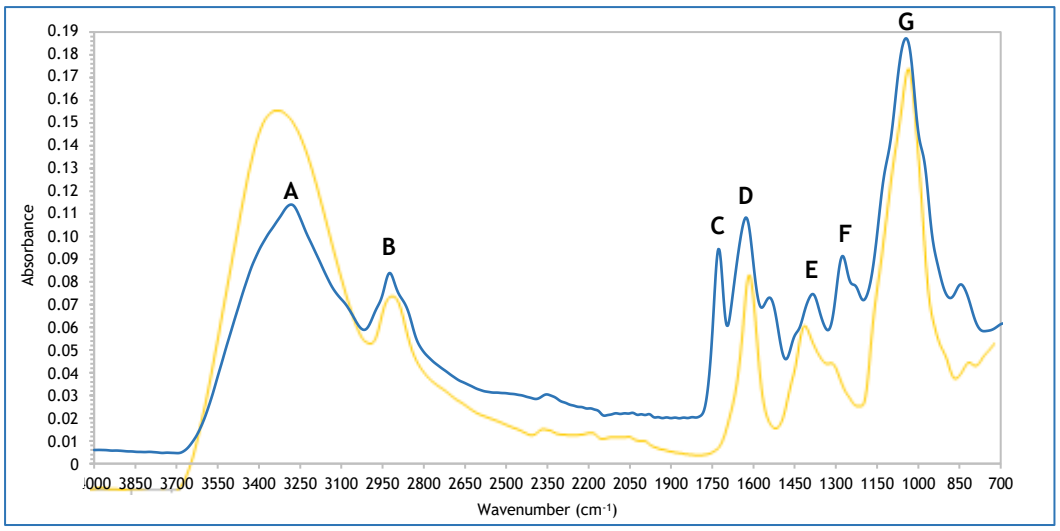

Figure 33 - FTIR spectra of commercial gellan gum ( ) and gellan gum filtered, washed and dissolved with distilled water ( ). **A** - 3262.66 cm^{-1}; **B** - 2923.69 cm^{-1}; **C** - 1726.36 cm^{-1}; **D** - 1627.14cm^{-1}; **E** - 1364.50 cm^{-1}; **F** - 1275.31 cm^{-1}; **G** - 1044.62 cm^{-1}.

The NMR spectrum is presented in figure 34, and the four characteristic signals of gellan gum are present at A, B, C and G peaks, while at D and F peaks characterize the casein and yeast extract, respectively (whose NMR spectrum is presented in annex III and IV). Beyond that, the signal at 2.7306 ppm (peak E) shows that the gellan gum recovered is acetylated, once that this signal represents the methyl group, CH_3.

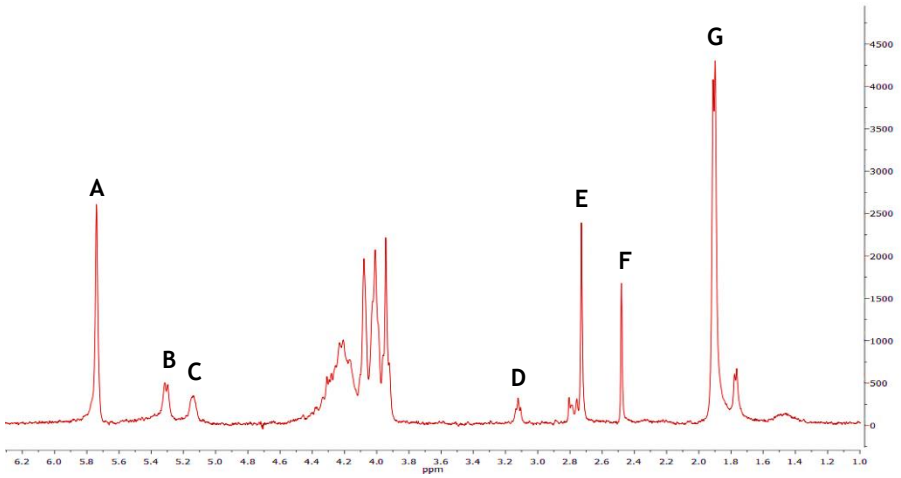

Figure 34 - ^{1}H-NMR spectrum of gellan gum filtered and washed with distilled water. **A** - 5.7410 ppm; **B** - 5.3004 ppm; **C** - **5**.1269 ppm; **D** - 3.1249 ppm; **E** - 2.7306 ppm; **F** - 2.4817 ppm; **G** - 1.8983 ppm.

After the analysis of FTIR and NMR spectra, it is noticeable that for a better recovery of gellan gum, with a major purity degree, the best methods are the last two. However, considering these spectra, the peaks intensity and the noise present, and also the losses of gellan gum in one of the methods, it is possible conclude that the best procedure to recover the gellan gum is the filtration, washing with acetone and ether, dissolution with distilled water and precipitation.

4.3. Gellan spheres formulation with water-in-oil emulsion

The formulation of gellan gum spheres through water-in-oil emulsion was tested using the commercial and biosynthetic gellan gum. Firstly, the gellan was dissolved at 100 ºC using a stirring of 300 rpm. Then, the oil was heated with a stirring of 750 rpm, the gellan solution was dripped into the oil, through a 21 G needle. In order to reinforce the polymer solution to form solid structures and promote the stabilization of gellan spheres, they were transferred to different solutions with divalent ions, at room temperature. Finally, the oil was removed by vacuum filtration and the spheres were washed with ethanol 70 % and rinsed with distilled water.

To reinforce the polymer solution, several counter-ions were used, such as barium chloride, calcium chloride, cobalt chloride, copper chloride and nickel chloride, since those divalent cations are very effective in the gelation of gellan gum. Also, the positive charge of these counter-ions binds electrostatically to the negatively charged of gellan gum, contributing to the formation of spherical spheres [131].

After the spheres formulation with a gellan gum concentration of 1.41 % (w/v), through the water-in-oil emulsion with a stirring of 750 rpm, at 100 ºC, which was optimized by experimental design [121], the spheres were evaluated relatively to its diameter by semi-optical microscopy, to its charge by zeta-potential, to its structure by SEM, and, finally, to its chemical composition by EDX.

4.3.1. Zeta-Potential

The zeta-potential of the microspheres was measured in order to determine the global charge of the commercial and biosynthetic spheres. Thus, three replicas were measured and the values vary between – 25 to - 35 mV and – 38 to – 44 mV for commercial and biosynthetic gellan spheres, respectively. The values obtained from the three replicas are represented in table 5 and it is noticeable that the biosynthetic spheres have a bigger negative charge comparatively with the commercial spheres, and these results indicate that the global superficial charge of the spheres is negative, being considered potential spheres to bind molecules with positive charge.

Table 5 - Mean value of zeta-potential measurements for commercial and biosynthetic gellan spheres.

	Commercial	**Biosynthetic**
Replica 1	- 25,4 mV	- 38,1 mV
Replica 2	- 28,4 mV	- 39,3 mV
Replica 3	- 34,4 mV	- 43,6 mV

4.3.2. Semi-optical microscopy analysis

The produced spheres were visualized on a semi-optical microscope and the mean diameter was calculated. This average was determined for the commercial and biosynthetic gellan spheres and five replicas of each type of gellan gum were considered, for each counter ion used.

An example of the images observed at semi-optical microscope for the commercial and biosynthetic gellan gum spheres is illustrated in figure 35, along with the diameter measured through this microscope to determine the mean diameter.

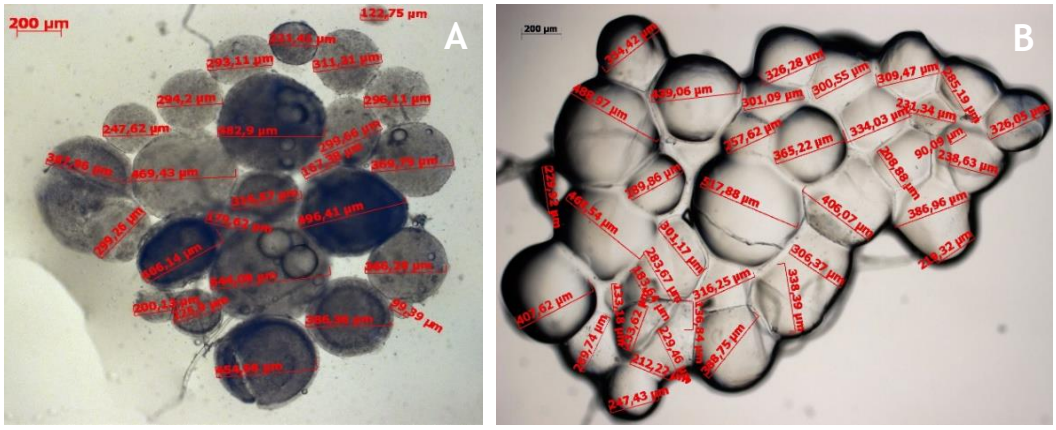

Figure 35 - Gellan gum spheres visualized at semi-optical microscope. **A** - Biosynthetic gellan gum spheres. **B** - Commercial gellan gum spheres.

In table 6 is represented the mean diameter for each replica (n=5), of each counter ion used to prepare commercial and biosynthetic gellan gum spheres. As can be seen by the values obtained for the average of the spheres, the biosynthetic gellan spheres are a little bigger than the spheres obtained with the commercial gellan gum. However, the mean diameter of spheres is not altered with the counter ion used between the commercial and biosynthetic gellan spheres. The counter ion that formulate smaller spheres is nickel (303.12 µm and 320.07 µm for commercial and biosynthetic spheres, respectively), while calcium forms bigger spheres (320.60 µm and 412.62 µm for commercial and biosynthetic spheres, respectively).

Table 6 – Mean diameter of commercial and biosynthetic gellan gum spheres take into account the counter ion.

		Barium	Calcium	Cobalt	Copper	Nickel
Commercial gellan spheres	**Replicas (µm)**	284.20	330.70	318.37	287.22	334,58
		343.24	286.18	297.05	295.68	280,38
		279.84	327.46	319.44	302.81	314.68
		348.70	355.47	324.16	328.43	269.37
		273.53	303.21	333.39	326.93	316.61
	Average of replicas (µm)	**305.90**	**320.60**	**318.60**	**308.21**	**303.12**
Biosynthetic gellan spheres	**Replicas (µm)**	307.89	423.23	379.98	354.88	257.24
		343.39	414.64	330.33	416.91	325.76
		326.65	428.28	419.18	432.87	337.04
		333.41	395.19	385.03	381.26	361.66
		347.40	401.76	390.95	368.91	318.64
	Average of replicas (µm)	**331.75**	**412.62**	**381.09**	**390.96**	**320.07**

4.3.3. SEM and EDX analysis

The SEM was used to acquire a more detailed information of the structure of gellan gum spheres, regarding to parameters such as reticulation and porosity. Thus, it is possible to access their surface morphology and topography. To visualize the commercial and biosynthetic spheres with different counter ions, the samples were frozen at – 20 ºC.

In figure 36, 37, 38, 39 and 40 are illustrated the commercial and biosynthetic spheres with the counter ions barium, calcium, cobalt, copper and nickel, respectively, with different degrees of magnification.

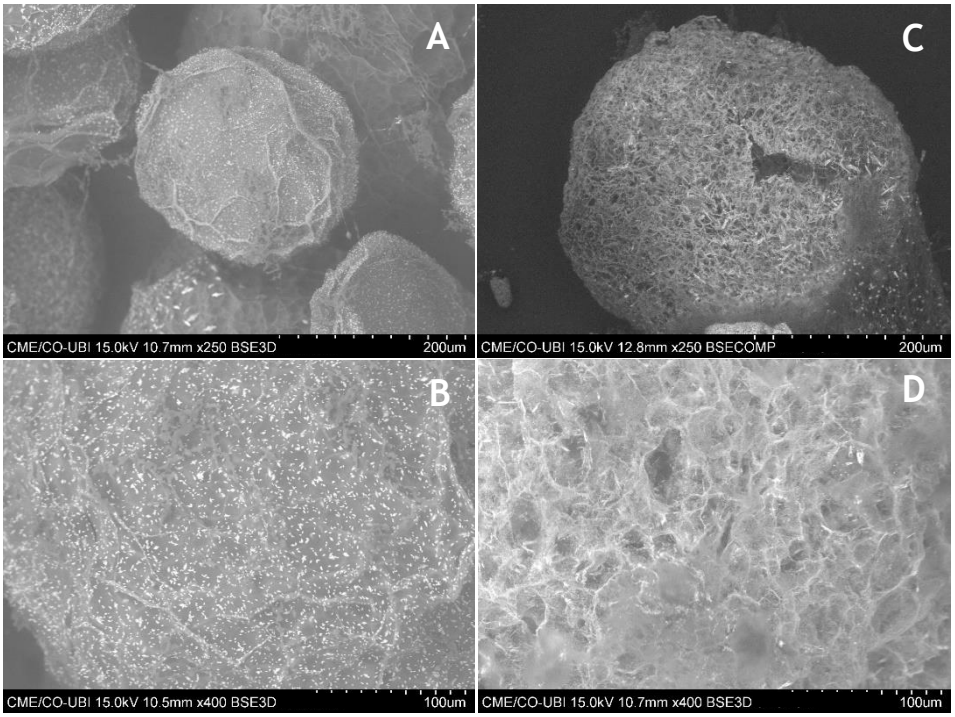

Figure 36 – Schematic representation of gellan gum spheres with barium as a cross-linker, visualized at SEM. **A and B** – Commercial gellan gum spheres with a magnification of x250 and x400, respectively. **C and D-** Biosynthetic gellan gum spheres with a magnification of x250 and x400, respectively.

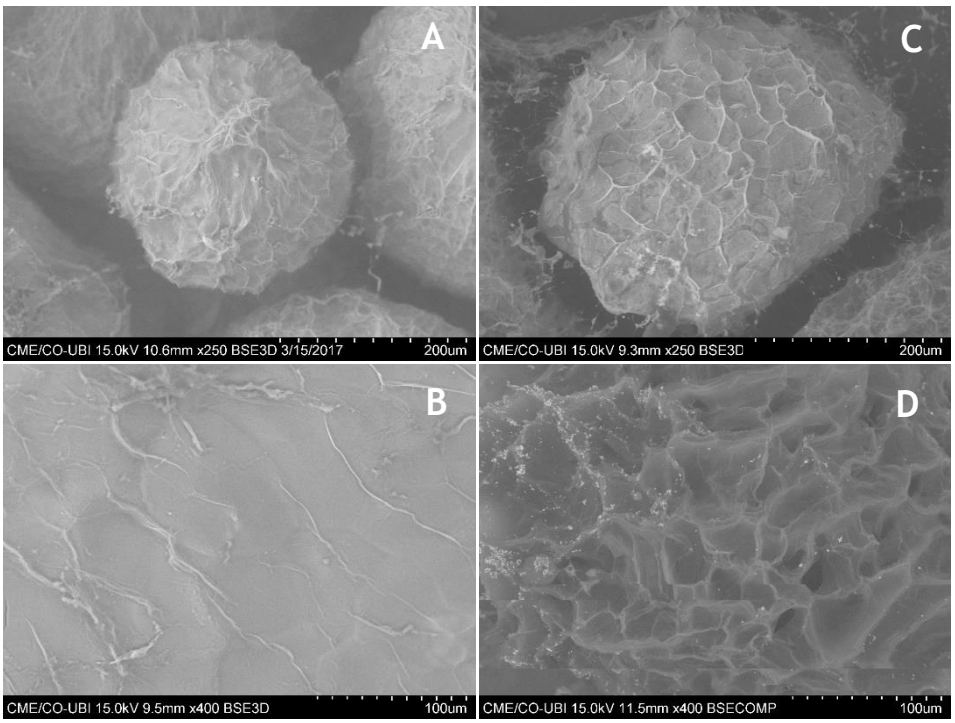

Figure 37 - Schematic representation of gellan gum spheres with calcium as a cross-linker, visualized at SEM. **A and B** – Commercial gellan gum spheres with a magnification of x250 and x400, respectively. **C and D-** Biosynthetic gellan gum spheres with a magnification of x250 and x400, respectively.

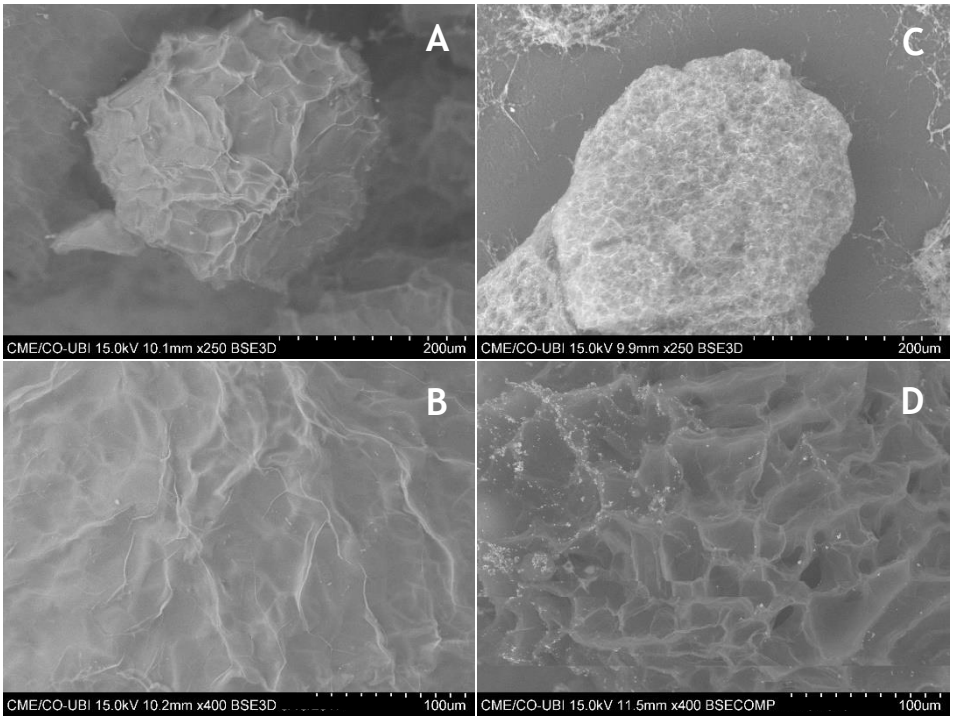

Figure 38 - Schematic representation of gellan gum spheres with cobalt as a cross-linker, visualized at SEM. **A and B** - Commercial gellan gum spheres with a magnification of x250 and x400, respectively. **C and D -** Biosynthetic gellan gum spheres with a magnification of x250 and x400, respectively.

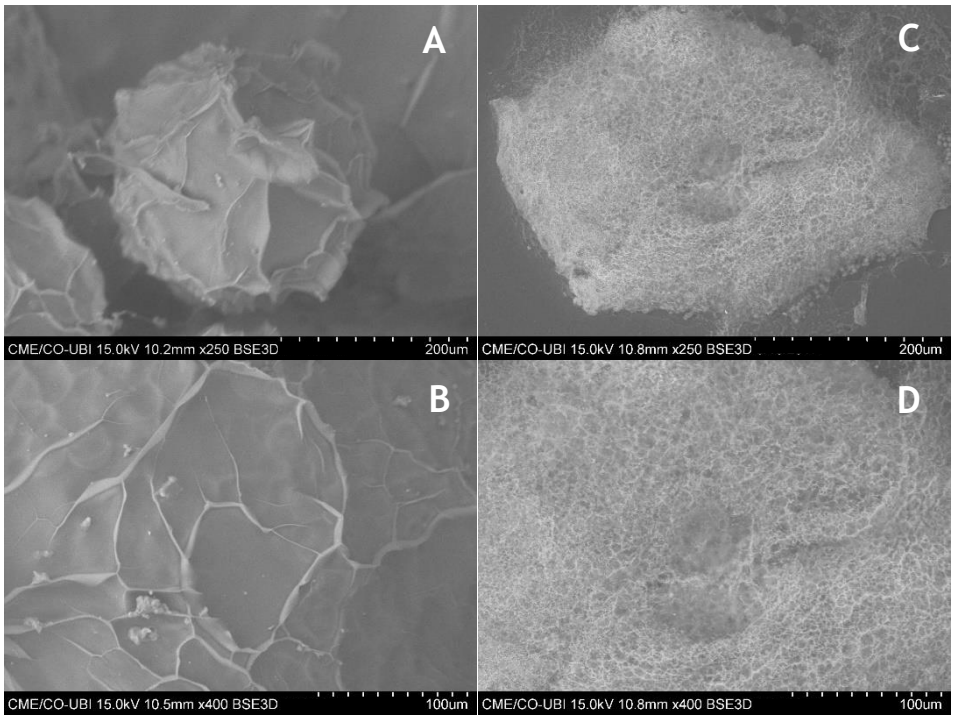

Figure 39 - Schematic representation of gellan gum spheres with copper as a cross-linker, visualized at SEM. **A and B** - Commercial gellan gum spheres with a magnification of x250 and x400, respectively. **C and D-** Biosynthetic gellan gum spheres with a magnification of x250 and x400, respectively.

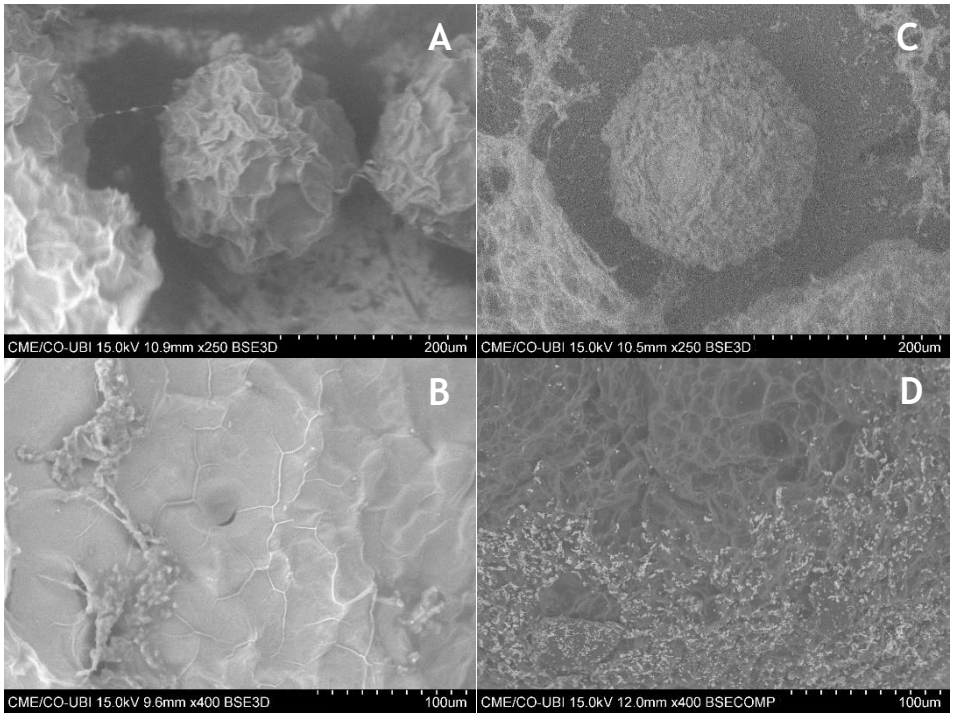

Figure 40 - Schematic representation of gellan gum spheres with nickel as a cross-linker, visualized at SEM. **A and B** – Commercial gellan gum spheres with a magnification of x250 and x400, respectively. **C and D-** Biosynthetic gellan gum spheres with a magnification of x250 and x400, respectively.

It can be observed that biosynthetic and commercial gellan gum spheres differ depending on the nature of gellan gum, whether they are commercial or biosynthetic, and on the cross-linkers used. The commercial gellan spheres show a consistent structure, with big cavities in the structures. The outer rough surface illustrated in these spheres can be associated with the porosity degree and these cavities containing a vast number of porous channels which confers a rough surface to the spheres [132]. However, the fact that the spheres not presents inner channels also means that the molecules will only be able to bind to its surface, and not to its interior. On the other hand, the biosynthetic spheres demonstrate a surface more reticulated with deeper pores. Thus, due to the vast number and larger size of pores present in the surface of the sphere, it can be suggested that the proteins can bind in higher number to the surface of the sphere increasing the binding capacity.

Comparing the shape of the spheres, it is noticeable that for commercial spheres all of them presents a uniform spherical structure, however, only the biosynthetic spheres with barium, calcium and nickel as cross-linker presents a uniform spherical structure.

The EDX analysis was performed in order to make a chemical characterization and determine the constituent elements of the spheres. Relatively to EDX analysis, in tables 7 to 18 are represented the elementary constituents of commercial and biosynthetic spheres, for the different cross-linkers and the magnetic spheres, as well as the normalised concentration in weight percent of each element (C norm. [wt. %]), the atomic weigh percent (C Atom. [at. %]) and the error in the weight percent concentration at the 2 Sigma level (C Error (2 sigma) [wt. %]).

Table 7 - Elementary analysis of commercial gellan spheres with barium as a cross-linker, through EDX.

	C norm. [wt. %]	C Atom. [at. %]	C Error (2 sigma) [wt. %]
Carbon	29.84	37.55	7.08
Nitrogen	58.83	55.57	13.14
Oxygen	3.02	3.26	1.14
Sodium	1.80	1.18	0.28
Aluminium	2.75	1.54	0.31
Sulphur	1.21	0.57	0.14
Chloride	0.14	0.06	0.06
Barium	2.41	0.27	0.21
Total	**100.00**	**100.00**	

Table 8 - Elementary analysis of commercial gellan spheres with calcium as a cross-linker, through EDX.

	C norm. [wt. %]	C Atom. [at. %]	C Error (2 sigma) [wt. %]
Carbon	37.82	45.26	8.49
Nitrogen	-	-	-
Oxygen	59.57	53.52	13.05
Sodium	0.71	0.44	0.14
Aluminium	0.28	0.15	0.08
Sulphur	0.46	0.21	0.09
Chloride	0.11	0.04	0.06
Calcium	1.05	0.38	0.12
Total	**100.00**	**100.00**	

Table 9 - Elementary analysis of commercial gellan spheres with cobalt as a cross-linker, through EDX.

	C norm. [wt. %]	C Atom. [at. %]	C Error (2 sigma) [wt. %]
Carbon	24.15	30.31	5.98
Nitrogen	2.21	2.38	0.94
Oxygen	68.64	64.68	15.30
Sodium	1.07	0.70	0.20
Aluminium	2.68	1.50	0.31
Sulphur	0.48	0.23	0.09
Chloride	0.04	0.02	0.06
Cobalt	0.72	0.18	0.12
Total	**100.00**	**100.00**	

Table 10 - Elementary analysis of commercial gellan spheres with copper as a cross-linker, through EDX.

	C norm. [wt. %]	C Atom. [at. %]	C Error (2 sigma) [wt. %]
Carbon	38.20	51.71	11.47
Nitrogen	3.38	3.92	1.70
Oxygen	26.93	27.36	7.95
Sodium	1.74	1.23	0.32
Aluminium	21.39	12.39	2.46
Sulphur	2.15	1.09	0.24
Chloride	1.07	0.49	0.15
Copper	5.14	1.32	0.53
Total	**100.00**	**100.00**	

Table 11 - Elementary analysis of commercial gellan spheres with nickel as a cross-linker, through EDX.

	C norm. [wt. %]	C Atom. [at. %]	C Error (2 sigma) [wt. %]
Carbon	31.28	38.60	7.57
Nitrogen	2.66	2.81	1.14
Oxygen	60.29	55.86	13.70
Sodium	0.99	0.64	0.19
Aluminium	2.49	1.37	0.29
Sulphur	0.61	0.28	0.10
Chloride	0.06	0.02	0.06
Nickel	1.63	0.41	0.19
Total	**100.00**	**100.00**	

The EDX obtained from the commercial gellan spheres are characterised in tables 7 to 11, demonstrate that all of them have in common the presence of carbon, nitrogen, oxygen, sodium, aluminium, sulphur and chloride chemical elements, except for spheres with calcium as a cross-linker that does not have nitrogen present in its constitution.

In addition, by the results obtained by EDX, it is noticeable that according to the cross-linker used, their capacity to bind to spheres is variable, being present in different percentages in each type of spheres. As can be observed, the counter ions with a major capacity to bind to the spheres are barium, copper and, with a major concentrations of weight percentage and atomic percentage, being that copper has the highest concentration, then barium and finally nickel.

In the EDX analysis of biosynthetic gellan spheres, the common chemical constituents are carbon, oxygen, sodium, aluminium, silicon, phosphorus and sulphur and the weight percentage and atomic percentage concentrations are listed in tables 12-16.

Table 12 - Elementary analysis of biosynthetic gellan spheres with barium as a cross-linker, through EDX.

	C norm. [wt. %]	C Atom. [at. %]	C Error (2 sigma) [wt. %]
Carbon	48.00	62.32	11.86
Oxygen	33.02	32.19	8.39
Sodium	1.32	0.90	0.24
Aluminium	2.50	1.44	0.31
Silicon	0.11	0.06	0.06
Phosphorus	1.81	0.91	0.21
Sulphur	1.78	0.87	0.19
Barium	11.45	1.30	0.80
Total	**100.00**	**100.00**	

Table 13 - Elementary analysis of biosynthetic gellan spheres with calcium as a cross-linker, through EDX.

	C norm. [wt. %]	C Atom. [at. %]	C Error (2 sigma) [wt. %]
Carbon	56.63	65.28	2.69
Oxygen	36.05	31.20	8.43
Sodium	1.89	1.14	0.29
Aluminium	1.48	0.76	0.19
Silicon	0.05	0.02	0.06
Phosphorus	0.42	0.19	0.09
Sulphur	2.42	1.04	0.23
Calcium	1.05	0.36	0.12
Total	**100.00**	**100.00**	

Table 14 – Elementary analysis of biosynthetic gellan spheres with cobalt as a cross-linker, through EDX.

	C norm. [wt. %]	C Atom. [at. %]	C Error (2 sigma) [wt. %]
Carbon	55.28	63.28	12.02
Oxygen	39.71	34.13	8.93
Sodium	2.78	1.66	0.40
Aluminium	0.30	0.15	0.08
Silicon	0.05	0.02	0.06
Phosphorus	0.19	0.08	0.07
Sulphur	1.36	0.58	0.15
Cobalt	0.34	0.08	0.08
Total	**100.00**	**100.00**	

Table 15 - Elementary analysis of biosynthetic gellan spheres with copper as a cross-linker, through EDX.

	C norm. [wt. %]	C Atom. [at. %]	C Error (2 sigma) [wt. %]
Carbon	52.67	68.10	13.51
Oxygen	26.05	25.28	7.02
Sodium	0.46	0.31	0.12
Aluminium	0.55	0.32	0.11
Silicon	0.01	0.01	0.05
Phosphorus	3.56	1.78	0.37
Sulphur	0.52	0.25	0.10
Copper	16.18	3.95	1.27
Total	**100.00**	**100.00**	

Table 16 - Elementary analysis of biosynthetic gellan spheres with nickel as a cross-linker, through EDX.

	C norm. [wt. %]	C Atom. [at. %]	C Error (2 sigma) [wt. %]
Carbon	43.47	52.31	9.82
Oxygen	49.11	44.27	11.04
Sodium	1.27	0.80	0.21
Aluminium	1.38	0.74	0.18
Silicon	0.05	0.03	0.06
Phosphorus	0.93	0.43	0.13
Sulphur	1.88	0.85	0.19
Nickel	1.91	0.47	0.20
Total	**100.00**	**100.00**	

The results obtained for the biosynthetic spheres is very similar to the commercial spheres. As it happens in the concentrations acquired from EDX analysis of commercial spheres, the weight and atomic percentage concentrations of biosynthetic spheres differs with the counter ions, and so the concentrations are higher to barium, copper and nickel cross-linkers.

Comparing to the EDX results of biosynthetic and commercial spheres, it is perceptible that the chemical elements present in both spheres are not the same, only carbon, oxygen, sodium, aluminium and sulphur are common. This can be related to the different production methodology of gellan gum used in this work, which in the case of biosynthetic gellan gum it was obtained by fermentation of *Sphingomonas paucimobilis* ATCC 31461, the different elements constitution can be related to the medium composition. It is also noticeable that the concentration of the cross-linkers is higher for the biosynthetic gellan gum spheres, which can indicate the possibility to explore additional interactions with the divalent ions beyond the electrostatic interactions with negative gellan polymer.

4.4. Magnetic spheres formulation

In order to take advantage of capture proteins by using a magnetic field instead of centrifugation, the magnetization of the spheres is essential and for that it is necessary choose one of the cross-linkers used. Therefore, it was considered the mean diameter, the morphology and the surface topography, the concentrations of weight percentage and atomic percentage of the different counter ions and its applicability in chromatography. So, the cross-linker chosen for the magnetized spheres was the nickel, once that the spheres obtained with this cross-linker have the smaller diameter, comparing with barium, calcium, copper and cobalt and presents a spherical and rigid structure and morphology, in contrast with the spheres with cobalt and copper as a cross-linker, where it is visible a fragile and non-spherical structure. Also, the high concentration of nickel present in the spheres and because this ion is very used in IMAC, were considered important factors to this choice.

Also, the gellan beads with nickel as a cross-linker magnetized by the chemical co-precipitation method, were frozen at –20 ºC and, then, visualized by SEM. In figure 41 it is presented the magnetized gellan spheres. The magnetized commercial gellan spheres present an “open” structure and are apparently more fragile, comparing to the commercial spheres, inversely to the magnetized biosynthetic gellan spheres, which exhibit a stronger structure, without any pores on its surface.

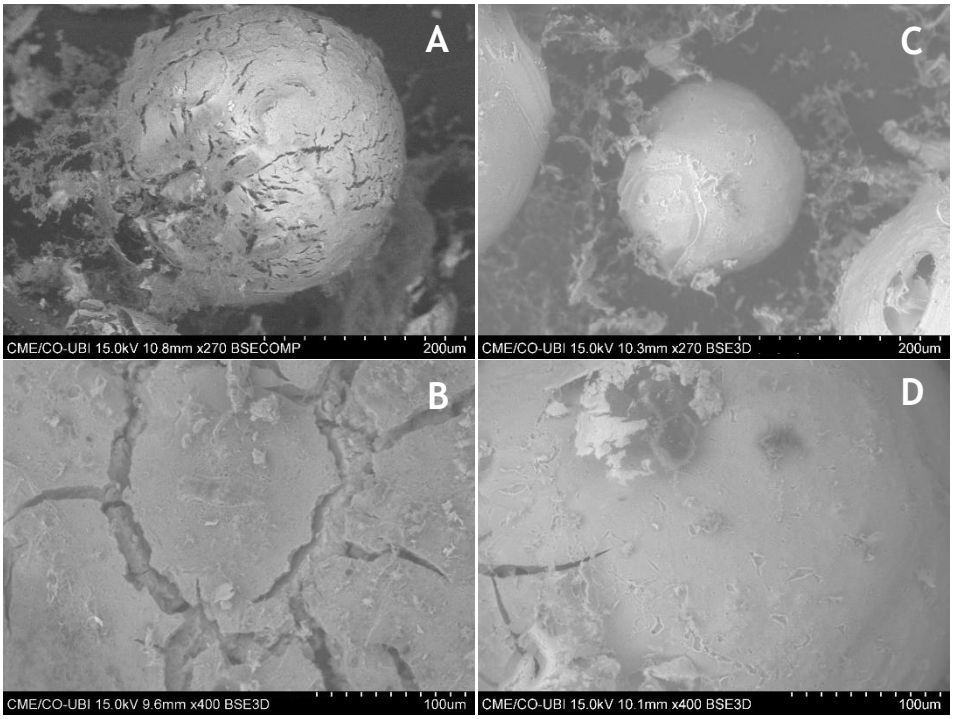

Figure 41 - Schematic representation of magnetized gellan gum spheres, visualized at SEM. **A and B** - Commercial gellan gum spheres with a magnification of x270 and x400, respectively. **C and D -** Biosynthetic gellan gum spheres with a magnification of x270 and x400, respectively.

In tables 17 and 18 are listed the EDX analysis to commercial and biosynthetic magnetic gellan spheres.

Table 17 - Elementary analysis of commercial magnetic gellan spheres, through EDX.

	C norm. [wt. %]	C Atom. [at. %]	C Error (2 sigma) [wt. %]
Carbon	27.31	43.50	7.34
Oxygen	32.41	38.75	8.31
Sodium	6.37	5.30	0.96
Aluminium	1.22	0.86	0.18
Silicon	0.47	0.32	0.10
Sulphur	0.78	0.47	0.12
Manganese	6.53	2.28	0.49
Iron	24.91	8.53	1.72
Total	**100.00**	**100.00**	

Table 18 - Elementary analysis of biosynthetic magnetic gellan spheres, through EDX.

	C norm. [wt. %]	C Atom. [at. %]	C Error (2 sigma) [wt. %]
Carbon	19.30	34.97	5.12
Oxygen	33.89	46.10	8.07
Sodium	0.42	0.40	0.12
Aluminium	0.56	0.45	0.11
Silicon	0.15	0.12	0.07
Sulphur	0.26	0.18	0.08
Manganese	12.52	4.96	0.82
Iron	32.91	12.83	2.07
Total	**100.00**	**100.00**	

Analysing these tables, in both spheres are present the carbon, oxygen, sodium, aluminium, silicon, sulphur, manganese and iron chemical elements in their constitution and is notorious that exists a high concentration of manganese and iron, once that are the two ions used in the magnetization of spheres. However, the nickel ion is not listed in EDX analysis, maybe due to the x-ray issued by spheres, which cannot detect nickel due to the high concentrations of other elements.

Comparing the results obtained, it is possible to conclude that biosynthetic spheres present higher concentrations of manganese and iron ions, suggesting that these spheres can promote more cationic interactions with negatively charged molecules.

4.5. Batch method assays to capture model proteins

The application of these spheres was initially tested with model proteins in order to study the sustainability and performance of gellan spheres in a capture step using the batch method by exploring its ionic nature and establishing the elution profiles of the proteins considering their surface charge under the established elution conditions. Thus, two model proteins were tested, BSA and lysozyme, using equilibrium and elution buffers with pH 6.2, in order to acquire different global charge, positive and negative charges respectively, due to its isoelectric points (which are 5.4 and 11, respectively) [133].

In table 19 it is presented the absorbance values at 280 nm from the recovered supernatants (obtained with the 500 µL of spheres that were previously equilibrated with 10 mM MES buffer, pH 6.2), resultant from the binding solution (250 µL of 5 mg/mL BSA and 10 mg/mL lysozyme with 750 µL of 10 mM MES buffer, pH 6.2), the protein content that did not bind to the spheres, the elution of protein that bound to the spheres (0.5 M NaCl in 10 mM MES buffer, pH 6.2) and

the washing with distilled water, for spheres with nickel as a cross-linker and for magnetic spheres.

Table 19 - Absorbance obtained from the recovered supernatant, at 280 nm, with 1 mL of 5 mg/mL BSA and 10 mg/mL lysozyme, in 10 mM MES buffer, pH 6.2, added to 500 µL of spheres.

	Spheres with nickel as a cross-linker		Magnetic spheres	
	BSA	**Lysozyme**	**BSA**	**Lysozyme**
Binding solution	0.980	5.00	0.980	5.00
Protein that did not bind to the spheres, pH 6.2	0.712	3.90	0.659	1.94
Elution of bound protein with 0.5 M NaCl, pH 6.2	0.078	0.865	0.038	0.400
Washing with distilled water	0.035	0.047	0.010	0.088

In figures 42 and 43 are illustrated the SDS-PAGE electrophoresis obtained for the samples recovered from the spheres prepared with nickel as the cross-linker and for magnetic spheres, respectively.

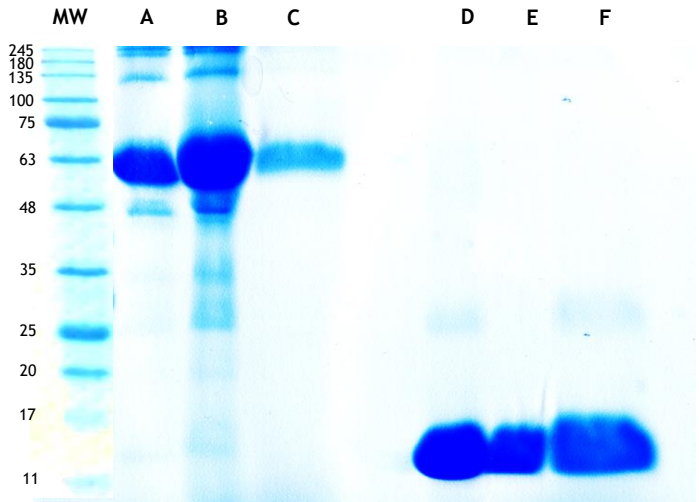

Figure 42 - SDS-PAGE electrophoretic analysis of the recovered supernatant from spheres with nickel as a cross-linker, through batch method using model proteins. **MW** - Molecular weight standards. **A** - BSA standard; **B** - BSA that did not bind to the spheres; **C** - Elution of BSA that was bound to the spheres; **D** - Lysozyme standard; **E** - Lysozyme that did not bind to the spheres; **F** - Elution of lysozyme that was bound to the spheres.

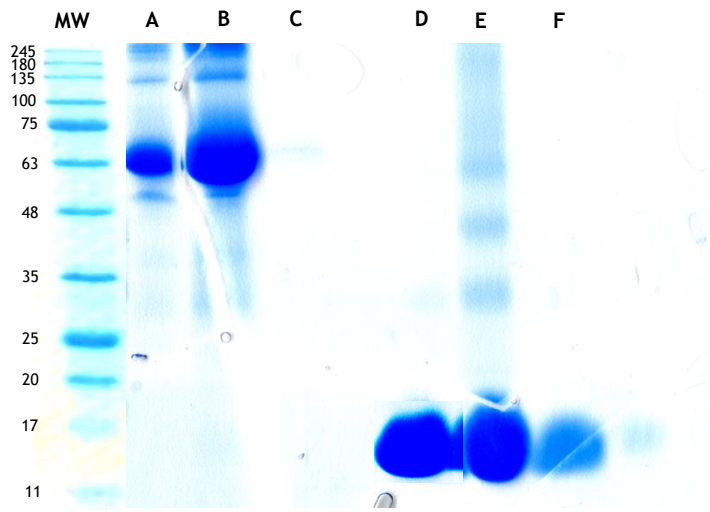

Figure 43 - SDS-PAGE electrophoretic analysis of the recovered supernatant from magnetic spheres, through batch method using model proteins. **MW** - Molecular weight standards. **A** - BSA standard; **B** - BSA that did not bind to the spheres; **C** - Elution of BSA that was bound to the spheres; **D** - Lysozyme standard; **E** - Lysozyme that did not bind to the spheres; **F** - Elution of lysozyme that was bound to the spheres.

By analysis of the electrophoresis and the absorbances of supernatants, it is possible observe that BSA protein, with a molecular weight of 66 kDa, does not bind to the beads with nickel as a cross-linker and to the magnetic beads, since the presence of the protein is almost inexistent in lanes C (elution step) in the SDS-PAGE electrophoresis. At pH 6.2 this protein is negatively charged, once that the isoelectric point of the protein is 5.4. Thus, the complete binding did not occur probably because the beads are mostly negatively charged, as well as the protein.

However, it is noticeable that some of lysozyme protein, with a molecular weight of 14 kDa, binds to both beads. Given that the isoelectric point of lysozyme is 11 and the pH of the binding solution is 6.2, the lysozyme is positively charged, and consequently, favours the protein binding to the beads. The elution of the protein was also visible, through the absorbances measured and the lane F of the electrophoresis, revealing that the lysozyme bound to the beads was recovered with 0.5 M NaCl.

Overall, these results allowed to conclude that gellan gum beads can be used for the selective capture of proteins, though the batch method and by manipulation of ionic strength of the binding and elution buffers. Therefore, the next step will be the application of these beads for the capture of the COMT protein from a complex lysate solution.

4.6. Batch method assays to capture SCOMT protein

The COMT protein is an important protein that can be obtained by recombinant production and chromatographic purification for further therapeutic studies. However, some purification procedures did not allow the required purity degree and apply aggressive conditions that can be compromise the bioactivity of this enzyme. Thus, the development of capture steps that allow the direct isolation of COMT protein from the lysate sample or can be used as an intermediate step to simplify and improve the purification step, can be fundamental for this biotechnological process. In the present study, the isoform of interest is the SCOMT and different conditions were tested in order to capture this protein.

Initially, the capture of SCOMT was tested with the same conditions used to capture the model proteins. Briefly, the spheres were equilibrated with 10 mM MES buffer, pH 6.2, and after, 1 mL of a binding solution (250 µL of SCOMT lysate with 750 µL of 10 mM MES buffer, pH 6.2) was added to 500 µL of spheres and the elution step was performed with 0.5 M NaCl, in 10 mM MES buffer, pH 6.2. Therefore, in table 20 are represented the absorbances obtained from the recovered supernatants of the binding solution of SCOMT lysate, the SCOMT protein that did not bind to the spheres, the elution of SCOMT with NaCl and the washing of the spheres with distilled water.

Table 20 - Absorbance obtained from the recovered supernatant, at 280 nm, with 1 mL of SCOMT lysate solution, in 10 mM MES buffer, pH 6.2, added to 500 µL of spheres with nickel as a cross-linker.

Binding solution	126
SCOMT lysate that did not bind to the spheres, pH 6.2	40.9
Elution of SCOMT lysate with 0.5 M NaCl, pH 6.2	0.868
Washing with distilled water	0.015

Also, in figure 44 is illustrated the DOT-BLOT obtained from the recovered supernatants.

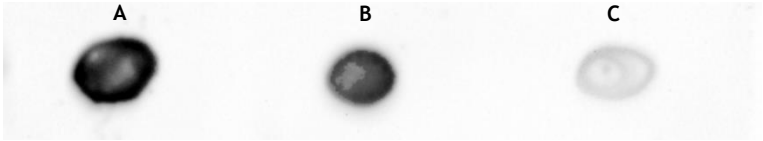

Figure 44 - DOT-BLOT analysis of the recovered supernatant from 500 µL of spheres with nickel as a cross-linker, through the batch method. **A** - SCOMT lysate; **B** - SCOMT that did not bind to the spheres; **C** - Elution of SCOMT that bonded to the spheres.

After the obtained results, it is noticeable that SCOMT bound in small extension to the spheres (lane C of figure 44), maybe due to the pH used in this assay. Knowing that the isoelectric point of SCOMT is 5.2, the protein can be negatively charged at pH 6.2 and explore some interactions with the cationic divalent ions but in small extension.

Thus, another assay was performed in order to promote a higher binding of the protein to the spheres with the addition of urea to the SCOMT lysate. Urea is a chaotropic agent described in literature and can be used to dissolve protein aggregates. For instance, it can be useful in IMAC, by increasing the exposition of protein histidine tags and improving the affinity binding between the histidine tags and the metallic ions [123]. So, after equilibrating the spheres with 10 mM MES buffer, pH 6.2, 1 mL of SCOMT lysate containing urea (250 µL of SCOMT lysate with 750 µL of 10 mM MES buffer, pH 6.2) was added to 500 µL of spheres and using the same conditions described previously.

In table 21, they are expressed the absorbances of the recovered supernatants and in figure 45 is illustrated the SDS-PAGE of these supernatants.

Table 21 - Absorbance obtained from the recovered supernatant, at 280 nm, with 1 mL of SCOMT lysate solution, containing urea, in 10 mM MES buffer, pH 6.2, added to 500 µL of spheres with nickel as a cross-linker.

Binding solution	126
SCOMT lysate that did not bind to the spheres, pH 6.2	38.8
Elution of SCOMT lysate with 0.5 M NaCl, pH 6.2	0.690
Washing with distilled water	0

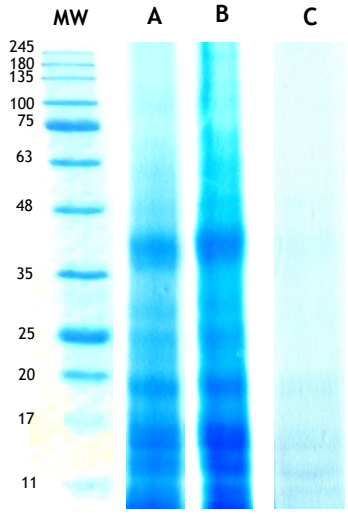

Figure 45 - SDS-PAGE electrophoretic analysis of the recovered supernatant from spheres with nickel as a cross-linker, through batch method in SCOMT lysate. **MW** - Molecular weight standards. **A** - SCOMT lysate; **B** - SCOMT lysate that did not bind to the spheres; **C** - Elution of SCOMT lysate that bonded to the spheres.

Also in these results was observed a small retention of lysate sample, that was eluted with 0.5 M NaCl (present in lane C of figure 45) containing also the SCOMT protein, with a molecular weight of 24.4 kDa. However, a large quantity of protein still not bind to the spheres, probably due to the negative charge of the protein at the pH used in the assay, which avoid the establishment of interactions with gellan polymer also negatively charged.

Therefore, a new assay with a higher volume of spheres was made to understand if a major volume of spheres makes the difference in the binding step. Briefly, the spheres were equilibrated with 10 mM MES buffer, pH 6.2. After that, 4 mL of a binding solution, with the same concentration of protein lysate containing urea (1 mL of SCOMT lysate with 3 mL of 10 mM MES buffer, pH 6.2) were added to 10 mL of spheres and to elute the protein bound, 4 mL of 0.5 M NaCl in 10 mM MES buffer, pH 6.2, were added. The absorbance obtained from the supernatants of the binding solution, the SCOMT lysate that did not bind to the spheres, the protein eluted from the spheres and the residues that kept in the spheres after a washing stage with distilled water, are listed in table 22 and in figures 46 and 47 are presented the DOT-BLOT and the SDS-PAGE analysis, respectively.

Table 22 - Absorbance obtained from the recovered supernatant, at 280 nm, with 4 mL of SCOMT lysate solution, containing urea, in 10 mM MES buffer, pH 6.2, added to 10 mL of spheres with nickel as a cross-linker.

Binding solution	148
SCOMT lysate that did not bind to the spheres, pH 6.2	18
Elution of SCOMT lysate with 0.5 M NaCl, pH 6.2	1.80
Washing with distilled water	0.050

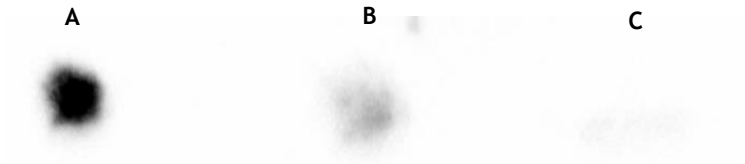

Figure 46 - DOT-BLOT analysis of the recovered supernatant from 10 mL of spheres with nickel as a cross-linker, through the batch method. **A** - SCOMT lysate; **B** - SCOMT lysate that did not bind to the spheres; **C** - Elution of SCOMT lysate that bound to the spheres.

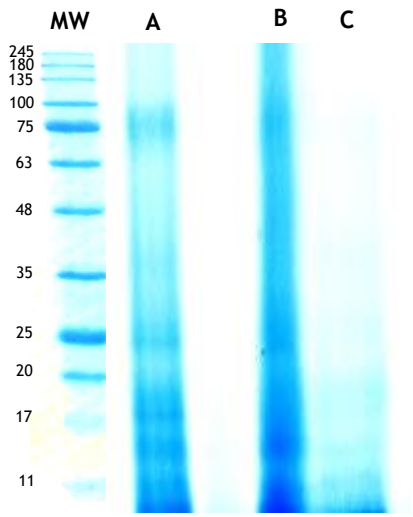

Figure 47 - SDS-PAGE electrophoretic analysis of the recovered supernatant from 10 mL of spheres with nickel as a cross-linker, through batch method in SCOMT lysate. **MW** - Molecular weight standards. **A** - SCOMT lysate; **B** - SCOMT lysate that did not bind to the spheres; **C** - Elution of SCOMT lysate that bound to the spheres.

The results present in table 22 show a small increase of protein retention, being eluted 1.80, since in the previous result was only eluted 0.69 (table 21). However, the absorbance of the SCOMT lysate that did not bind to the spheres was lower (18) comparing to the previous result (38.8), suggesting that a higher content of protein was retained but did not elute with 0.5 M of NaCl. Probably 0.5 M of NaCl cannot be enough ionic strength to recover the total protein bound to the spheres.

These three last assays were only tested in spheres with nickel as a cross-linker, but the following assays were all performed with these spheres and with magnetic spheres.

In order to promote the elution of the protein that bound to the spheres, a higher salt concentration was tested in the elution step. Once that the amount of SCOMT that bind to the spheres is very low, a larger was also tested. Therefore, 10 mL of spheres, previously equilibrated with 10 mM MES buffer, pH 6.2, were added to 4 mL of SCOMT lysate, with the same concentration and conditions described previously. After to recover the supernatant and in order to improve the elution of the protein bound, 1.5 M NaCl, in 10 mM MES buffer, pH 6.2, was added to the spheres.

In table 23 are presented the measured absorbances of the supernatants for spheres with nickel as a cross-linker and to magnetic spheres and in figures 48 and 49 are illustrated the DOT-BLOT and the electrophoresis, respectively, obtained with the supernatants recovered from the distinct steps of batch method.

Table 23 - Absorbance obtained from the recovered supernatant, at 280 nm, with 4 mL of SCOMT lysate solution, containing urea, in 10 mM MES buffer, pH 6.2, added to 10 mL of spheres.

	Spheres with nickel as a cross-linker	Magnetic spheres
Binding solution	97.6	
SCOMT lysate that did not bind to the spheres, pH 6.2	18.8	9
Elution of SCOMT lysate with 1.5 M NaCl, pH 6.2	32.6	5.91
Washing with distilled water	0.009	0.008

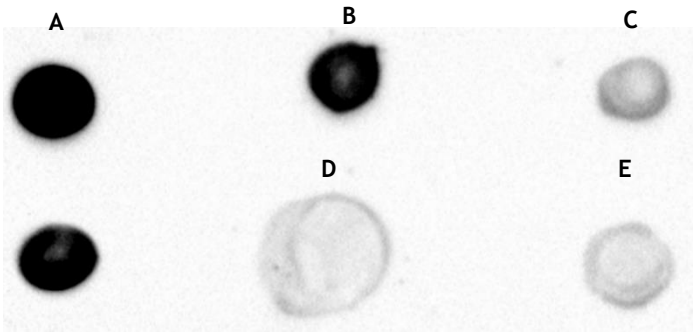

Figure 48 - DOT-BLOT analysis of the recovered supernatant from 10 mL of spheres with nickel as a cross-linker and from magnetic spheres, through the batch method. **A** - SCOMT lysate; **B** - SCOMT lysate that did not bind to the spheres with nickel as a cross-linker; **C** - Elution of SCOMT lysate that bound to the spheres with nickel as a cross-linker; **D** - SCOMT lysate that did not bind to the magnetic spheres; **E** - Elution of SCOMT lysate that bound to the magnetic spheres.

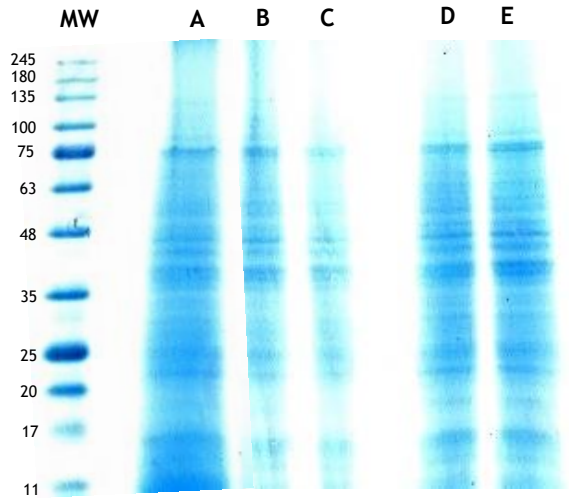

Figure 49 - SDS-PAGE electrophoretic analysis of the recovered supernatant from 10 mL of spheres with nickel as a cross-linker and from magnetic spheres, through batch method in SCOMT lysate. **MW** - Molecular weight standards. **A** - SCOMT lysate; **B** - SCOMT lysate that did not bind to the spheres with nickel as a cross-linker; **C** - Elution of SCOMT lysate that bound to the spheres with nickel as a cross-linker; **D** - SCOMT lysate that did not bind to the magnetic spheres; **E** - Elution of SCOMT lysate that bound to the magnetic spheres.

These results show that in general, a major quantity of SCOMT lysate was retained to the spheres probably due to the increase of spheres quantity. In particular, the retention was higher in magnetic spheres (9.00), comparatively to the spheres with nickel as a cross-linker (18.8), as can be seen in the lanes D and B respectively, probably due to the high presence of magnesium and iron in the surface of these spheres. Also, the addition of a higher concentration of salt promotes a better protein elution. As it can be seen in table 22, from the protein that bound to the spheres was eluted 1.80, with 0.5 M NaCl, while with 1.5 M NaCl was eluted 32.6 (table 23). Beyond SCOMT, there are several protein contaminants present in the electrophoresis, being necessary to optimize the capture process aiming to isolate the SCOMT protein.

In order to explore some selectivity, a new test was performed with the addition of imidazole to the elution buffer. Imidazole disrupts the coordination bonds between the histidine and transition metals, favouring the elution of proteins bound by polyhistidine residues [123]. Briefly, 4 mL of SCOMT lysate solution (with the same concentration described previously), containing urea, in 10 mM MES buffer, pH 6.2, were added to 10 mL of spheres (previously equilibrated with 10 mM MES buffer, pH 6.2) and the bound protein was eluted with 0.5 M NaCl and 0.5 M imidazole, in 10 mM MES buffer, pH 6.2. The absorbance results of the recovered supernatants obtained with both spheres are presented in table 24, and the DOT-BLOT and electrophoresis analysis are represented 50 and 51, respectively.

Table 24 - Absorbance obtained from the recovered supernatant, at 280 nm, with 4 mL of SCOMT lysate solution, containing urea, in 10 mM MES buffer, pH 6.2, added to 10 mL of spheres.

	Spheres with nickel as a cross-linker	**Magnetic spheres**
Binding solution	142.8	
SCOMT lysate that did not bind to the spheres, pH 6.2	28.6	5.9
Elution of SCOMT lysate with 0.5 M NaCl and 0.5 M imidazole, pH 6.2	9.93	4.63
Washing with distilled water	0.015	0.017

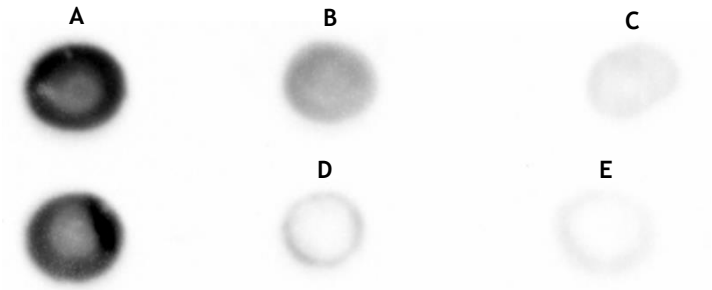

Figure 50 - DOT-BLOT analysis of the recovered supernatant from 10 ml of spheres with nickel as a cross-linker and from magnetic spheres, through the batch method. **A** - SCOMT lysate; **B** - SCOMT lysate that did not bind to the spheres with nickel as a cross-linker; **C** - Elution of SCOMT lysate that bound to the spheres with nickel as a cross-linker; **D** - SCOMT lysate that did not bind to the magnetic spheres; **E -** Elution of SCOMT lysate that bound to the magnetic spheres.

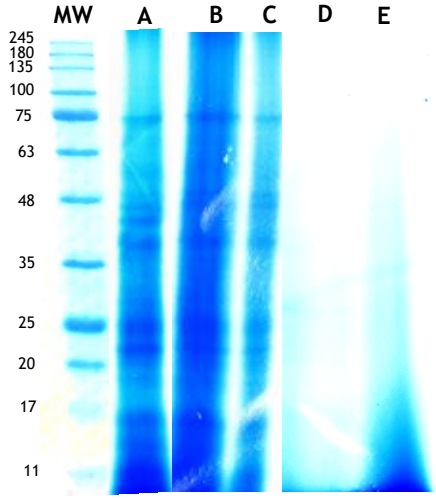

Figure 51 - SDS-PAGE electrophoretic analysis of the recovered supernatant from 10 mL of spheres with nickel as a cross-linker and from magnetic spheres, through batch method in SCOMT lysate. **MW** - Molecular weight standards. **A** - SCOMT lysate; **B** - SCOMT lysate that did not bind to the spheres with nickel as a cross-linker; **C** - Elution of SCOMT lysate that bound to the spheres with nickel as a cross-linker; **D** - SCOMT lysate that did not bind to the magnetic spheres; **E -** Elution of SCOMT lysate that bound

The obtained results demonstrate that magnetic spheres bind a higher content of SCOMT lysate than the spheres with nickel as a cross-linker, once the absorbance measured is lower. The results obtained with addition of imidazole in the elution buffer, did not show a significant increase in the elution of SCOMT protein. By the electrophoresis gel and the poor marking obtained in the DOT-BLOT of the eluted fraction (lane C and E) it is visible that SCOMT is not present in higher content. Thus, it is possible to conclude that the inclusion of imidazole did not improve the selectivity, neither the elution of the protein of interest.

The next assay was performed in order to evaluate the influence of the elution of SCOMT protein that bound to the spheres, at different salt concentrations. So, 4 mL of SCOMT lysate (with the same concentration described before), containing urea, in 10 mM MES buffer, pH 6.2, were added to 10 mL of spheres (previously equilibrated with 10 mM MES buffer, pH 6.2). The elution of the protein was teste with different concentrations of salt (100 mM NaCl, 750 mM NaCl and

1.5 m NaCl, in 10 mM MES, pH 6.2) to study the effect that it causes in the sequential elution of the bound protein and in the isolation of SCOMT. The absorbance results of the different supernatants recovered from magnetic spheres and from spheres with nickel as a cross-linker are listed in table 25. In figures 52 and 53 are illustrated the DOT-BLOT and the SDS-PAGE, respectively, of the binding solution and the different salts concentration used.

Table 25 - Absorbance obtained from the recovered supernatant, at 280 nm, with 4 mL of SCOMT lysate solution, containing urea, in 10 mM MES buffer, pH 6.2, added to 10 mL of spheres.

	Spheres with nickel as a cross-linker	**Magnetic spheres**
Binding solution	95.8	
SCOMT lysate that did not bind to the spheres, pH 6.2	17.2	10.0
Elution of SCOMT lysate with 100 mM NaCl, pH 6.2	8.65	14.0
Elution of SCOMT lysate with 750 mM NaCl, pH 6.2	1.12	2.83
Elution of SCOMT lysate with 1.5 M NaCl, pH 6.2	1.698	0.895
Washing with distilled water	0.009	0.008

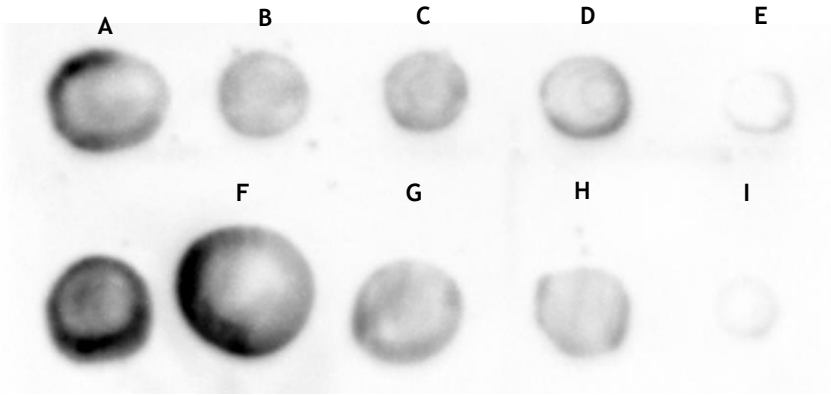

Figure 52 - DOT-BLOT analysis of the recovered supernatant from 10 mL of spheres with nickel as a cross-linker and from magnetic spheres, through the batch method. **A** - SCOMT lysate; **B** - SCOMT lysate that did not bind to the spheres with nickel as a cross-linker; **C** - Elution of SCOMT lysate, with 100 mM NaCl, that bound to the spheres with nickel as a cross-linker; **D** - Elution of SCOMT lysate, with 750 mM NaCl, that bound to the spheres with nickel as a cross-linker; **E** - Elution of SCOMT lysate, with 1.5 M NaCl, that bound to the spheres with nickel as a cross-linker; **F** - SCOMT lysate that did not bind to the magnetic spheres; **G** - Elution of SCOMT lysate, with 100 mM NaCl, that bound to the magnetic spheres; **H** - Elution of SCOMT lysate, with 750 mM NaCl, that bound to the magnetic spheres; **I** - Elution of SCOMT lysate, with 1.5 M NaCl, that bound to the magnetic spheres.

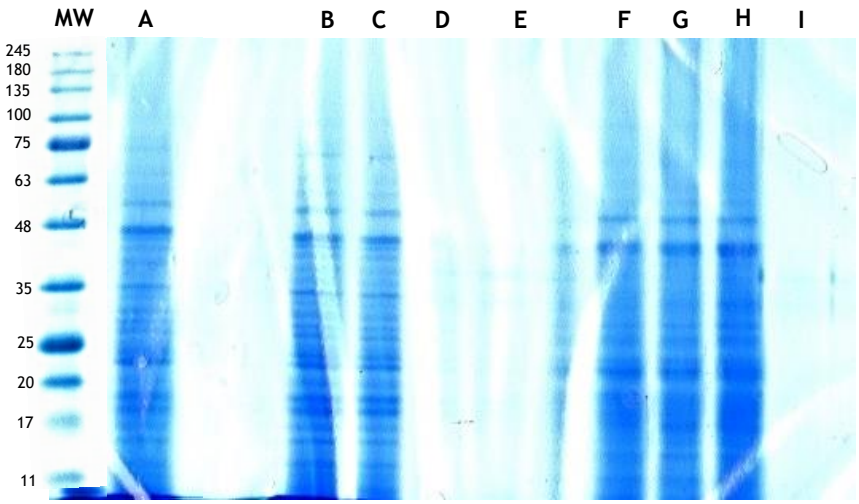

Figure 53 - SDS-PAGE electrophoretic analysis of the recovered supernatant from 10 mL of spheres with nickel as a cross-linker and from magnetic spheres, through batch method in SCOMT lysate. **MW** - Molecular weight standards; **A** - SCOMT lysate; **B** - SCOMT lysate that did not bind to the spheres with nickel as a cross-linker; **C** - Elution of SCOMT lysate, with 100 mM NaCl, that bound to the spheres with nickel as a cross-linker; **D** - Elution of SCOMT lysate, with 750 mM NaCl, that bound to the spheres with nickel as a cross-linker; **E** - Elution of SCOMT lysate, with 1.5 M NaCl, that bound to the spheres with nickel as a cross-linker; **F** - SCOMT lysate that did not bind to the magnetic spheres; **G** - Elution of SCOMT lysate, with 100 mM NaCl, that bound to the magnetic spheres; **H** - Elution of SCOMT lysate, with 750 mM NaCl, that bound to the magnetic spheres; **I** - Elution of SCOMT lysate, with 1.5 M NaCl, that bound to the magnetic spheres.

By analysis of the results, it is possible to observe that the spheres can capture the protein of interest (absorbances of 10 and 17.2 for gellan spheres with nickel as a cross-linker and magnetize spheres, respectively). Observing the table 25, it is possible to conclude that almost of the protein, that bound to the spheres, elute with 100 mM NaCl (absorbances of 8.65 and 14 for gellan spheres with nickel as a cross-linker and magnetize spheres, respectively). Also, with 750 mM NaCl, the protein was eluted in the gellan spheres with nickel as a cross-linker (1.12) and in the magnetic spheres (2.83), while with 1.5 M NaCl almost no protein is eluted (absorbances of 1.698 and 0.895 for gellan spheres with nickel as a cross-linker and magnetize spheres, respectively), indicating that part of the interactions established with both spheres can be the ionic character since they are established with lower ionic strength. However, by DOT-BLOT and electrophoresis analysis, it is perceptible the presence of contaminants in the elution steps, which indicates that the isolation of the protein has not been yet achieved at these conditions.

The next two assays were performed in order to evaluate the influence of pH on the retention and elution of SCOMT protein to the spheres.

Thus, the next assay was performed with a binding solution, at pH 7.5, to create an effective negative charge of the protein and to study the capacity of the spheres, also negatively charged, to bind to the protein at this pH. Also, the pH of the elution solution was changed to a lower pH to understand the effect of pH variations to elute the protein and finally different salt concentrations were applied. Therefore, after equilibrating the spheres with 10 mM Tris

buffer, pH 7.5, were used 4 mL of SCOMT lysate solution (with the same concentration of lysate described previously), containing urea, in 10 mM Tris buffer solution, pH 7.5, to bind to 10 mL of spheres. In order to elute the protein that bound to the spheres and promoting its isolation, a solution of 10 mM MES buffer, pH 5.2, and solutions of 100 mM NaCl and 750 mM NaCl, in 10 mM MES buffer, pH 5.2, were added to the spheres, sequentially. The concentrations of salt were choose considering the prior results. The pH used in the binding step intends to promote an effective negative charge of the SCOMT protein considering its isoelectric point (5.2) and the elution step only by change the pH to 5.2 pretends to observe if most of SCOMT protein is eluted by the neutralization of its global charge.

In table 26 are represented the absorbances obtained from the supernatants resultants of the binding (10 mM Tris buffer pH 7.5), elution (10 mM MES buffer pH 5.2) and washing steps and the DOT-BLOT and the electrophoresis analysis are presented in the figures 54 and 55, respectively.

Table 26 - Absorbance obtained from the recovered supernatant, at 280 nm, with 4 mL of SCOMT lysate solution, containing urea, in 10 mM Tris buffer, pH 7.5, added to 10 mL of spheres.

	Spheres with nickel as a cross-linker	**Magnetic spheres**
Binding solution	95.9	
SCOMT lysate that did not bind to the spheres, pH 7.5	25.88	15.28
Elution of SCOMT lysate without salt addition, pH 5.2	8.80	14.76
Elution of SCOMT lysate with 100 mM NaCl, pH 5.2	2.69	13.22
Elution of SCOMT lysate with 750 mM NaCl, pH 5.2	0.67	3.85
Washing with distilled water	0.009	0.013

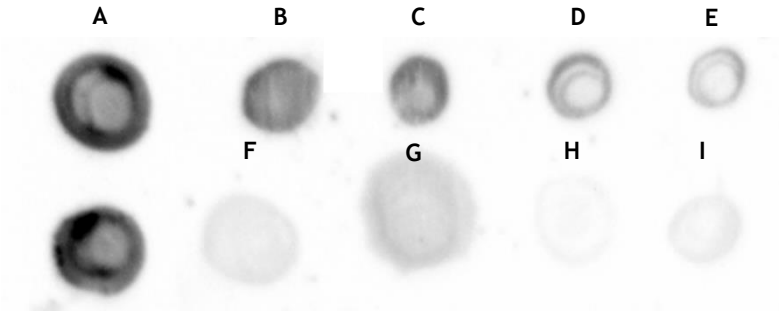

Figure 54 - DOT-BLOT analysis of the recovered supernatant from 10 mL of spheres with nickel as a cross-linker and from magnetic spheres, through the batch method. **A** - SCOMT lysate; **B** - SCOMT lysate in 10 mM Tris buffer pH 7.5 that did not bind to the spheres with nickel as a cross-linker; **C, D and E** - Elution of SCOMT lysate with 10 mM MES buffer pH 5.2, with 100 mM NaCl and 750 mM NaCl in 10 mM MES buffer pH 5.2, that bound to the spheres with nickel as a cross-linker, respectively; **F** - SCOMT lysate in 10 mM Tris buffer pH 7.5 that did not bind to the magnetic spheres; **G, H and I** - Elution of SCOMT lysate with 10 mM MES buffer pH 5.2, with 100 mM NaCl and 750 mM NaCl in 10 mM MES buffer pH 5.2, that bound to the magnetic spheres.

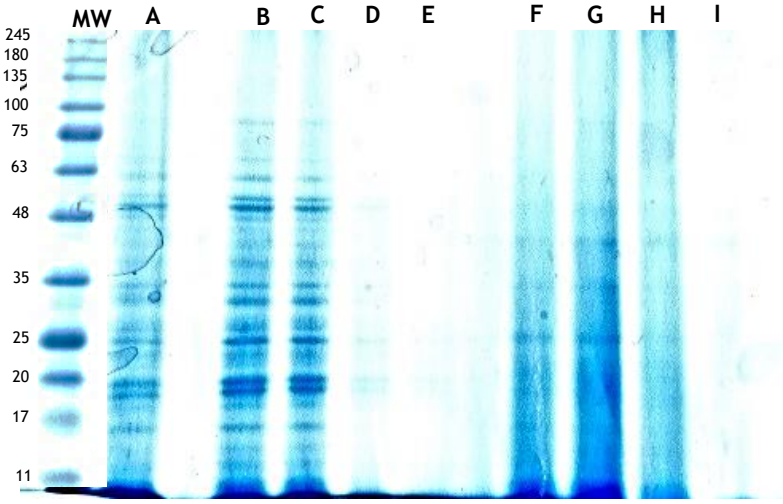

Figure 55 - SDS-PAGE electrophoretic analysis of the recovered supernatant from 10 mL of spheres with nickel as a cross-linker and from magnetic spheres, through batch method in SCOMT lysate. **MW** - Molecular weight standards **A** - SCOMT lysate; **B** - SCOMT lysate in 10 mM Tris buffer pH 7.5 that did not bind to the spheres with nickel as a cross-linker; **C, D and E** - Elution of SCOMT lysate with 10 mM MES buffer pH 5.2, with 100 mM NaCl and 750 mM NaCl in 10 mM MES buffer pH 5.2, that bound to the spheres with nickel as a cross-linker, respectively; **F** - SCOMT lysate in 10 mM Tris buffer pH 7.5 that did not bind to the magnetic spheres; **G, H and I** - Elution of SCOMT lysate with 10 mM MES buffer pH 5.2, with 100 mM NaCl and 750 mM NaCl in 10 mM MES buffer pH 5.2, that bound to the magnetic spheres.

Analysing the absorbance from the measured supernatant (table 26), it is observable that SCOMT protein binds to the beads, at pH 7.5, like occurs in the previous strategy tested. Curiously, a significant content of the sample was eluted by changing only the pH to 5.2 (8.80 and 14.76 for beads with nickel as a cross-linker and for magnetic beads, respectively) indicating that some negatively charged proteins, which were retained by ionic interactions with positive ligands, were eluted in this step. In addition, part of sample was also eluted with 100 mM NaCl (2.69 and 13.22 for beads with nickel as a cross-linker and for magnetic beads, respectively), suggesting that other interactions can be present. The steps of elution presented in figure 54 by lane C, D and E, corresponds to the elution of SCOMT lysate without

salt addition, with 100 mM NaCl and with 750 mM NaCl, in beads with nickel as a cross-linker and the lanes G, H and I, corresponds to the elution of SCOMT lysate without salt addition, with 100 mM NaCl and with 750 mM NaCl, in magnetic beads, demonstrate the progressive elution of the protein for the different salt concentrations. By observing the DOT-BLOT results, it seems that the elution step by changing the pH to 5.2 in the magnetic beads allowed the preferential elution of SCOMT due to the higher marker intensity and by electrophoresis analysis it seems that fraction G presents less contaminants beyond of SCOMT band at 24 kDa. On contrary, the results obtained for the beads with nickel as a cross-linker indicate that the selectivity cannot be achieved, once that some contaminants appears in all fractions of the SDS-PAGE.

Thus, the last assay consisted in the test of acidic pH (4.0), in order to turn the protein positively charged due to isoelectric point of SCOMT is 5.2, promoting the binding of the protein to the beads but probably promoting preferential interactions with the gellan polymer. Being the gellan beads negatively charged, the use of the protein positively charged can allow satisfactory results in the binding of SCOMT to the beads. The elution steps were performed with conditions similar to the previous assay but in at this time the pH was changed to 6.5 in order to neutralise the positive charge of SCOMT. Briefly, 4 mL of SCOMT lysate solution (with the same concentration described before), containing urea, in 10 mM citrate buffer, pH 4.0, were added to 10 mL of beads (previously equilibrated with 10 mM citrate buffer, pH 4.0). Then, the elution steps were performed with 10 mM MES buffer, pH 6.2, and with addition of salt (100 mM NaCl and 750 mM NaCl in 10 mM MES buffer, pH 6.2), consecutively
The absorbances measured of the supernatants recovered from the binding solution, the SCOMT that not bind to the spheres, the diverse steps of elution and the washing with distilled water, are listed in table 27. Also, DOT-BLOT and electrophoresis are illustrated in figures 56 and 57, respectively.

Table 27 - Absorbance obtained from the recovered supernatant, at 280 nm, with 4 mL of SCOMT lysate solution, containing urea, in 10 mM citrate buffer, pH 4.0, added to 10 mL of spheres.

	Spheres with nickel as a cross-linker	**Magnetic spheres**
Binding solution	85.6	
SCOMT lysate that did not bind to the spheres, pH 4.0	11.92	16.32
Elution of SCOMT lysate without salt addition, pH 6.2	33.15	36.6
Elution of SCOMT lysate with 100 mM NaCl, pH 6.2	15	11
Elution of SCOMT lysate with 750 mM NaCl, pH 6.2	4.75	0.387
Washing with distilled water	0.012	0.009

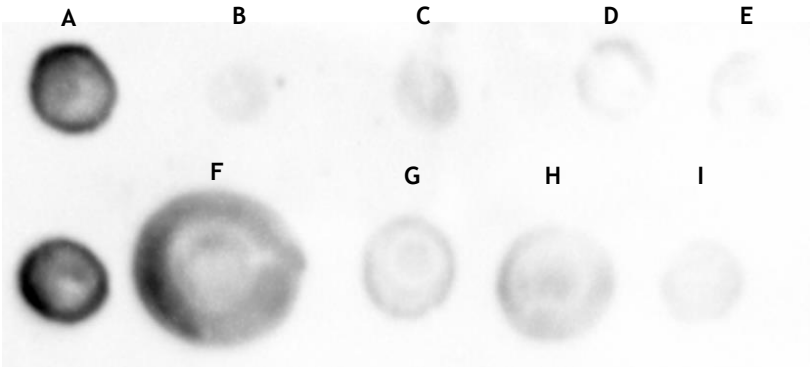

Figure 56 - DOT-BLOT analysis of the recovered supernatant from 10 mL of spheres with nickel as a cross-linker and from magnetic spheres, through the batch method. **A** - SCOMT lysate; **B** - SCOMT lysate in 10 mM citrate buffer pH 4.0 that did not bind to the spheres with nickel as a cross-linker; **C, D and E** - Elution of SCOMT lysate with 10 mM MES buffer pH 6.2, with 100 mM NaCl and 750 mM NaCl in 10 mM MES buffer pH 6.2, that bound to the spheres with nickel as a cross-linker, respectively; **F** - SCOMT lysate in 10 mM citrate buffer pH 4.0 that did not bind to the magnetic spheres; **G, H and I** - Elution of SCOMT lysate with 10 mM MES buffer pH 6.2, with 100 mM NaCl and 750 mM NaCl in 10 mM MES buffer pH 6.2, that bound to the magnetic spheres.

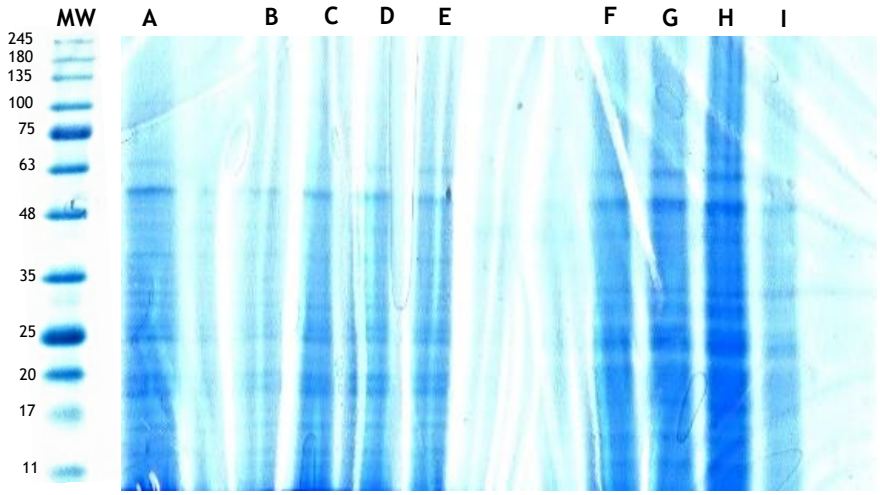

Figure 57 - SDS-PAGE electrophoretic analysis of the recovered supernatant from 10 mL of spheres with nickel as a cross-linker and from magnetic spheres, through batch method in SCOMT lysate. **MW** – Molecular weight standards; **A** – SCOMT lysate; **B** – SCOMT lysate in 10 mM citrate buffer pH 4.0 that did not bind to the spheres with nickel as a cross-linker; **C, D and E** – Elution of SCOMT lysate with 10 mM MES buffer pH 6.2, with 100 mM NaCl and 750 mM NaCl in 10 mM MES buffer pH 6.2, that bound to the spheres with nickel as a cross-linker, respectively; **F** – SCOMT lysate in 10 mM citrate buffer pH 4.0 that did not bind to the magnetic spheres; **G, H and I** – Elution of SCOMT lysate with 10 mM MES buffer pH 6.2, with 100 mM NaCl and 750 mM NaCl in 10 mM MES buffer pH 6.2, that bound to the magnetic spheres.

By analysis of the absorbance (table 27), the results demonstrate that at pH 4.0, the capture of the protein was very efficient for the spheres with nickel as a cross-linker (11.92) and for the magnetic beads (16.32). Also, observing the DOT-BLOT (figure 56), the results match with the absorbance and in lanes B and G it is presented the small content of SCOMT lysate solution that did not bind to the spheres with nickel as a cross-linker and to the magnetic spheres, respectively. As it occurred in the previous assay, the elution of sample by changing the pH (from 4 to 6.2) was very efficient (33.15 and 36.6 for spheres with nickel as a cross-linker and for magnetic spheres, respectively). However, the selectivity of the protein has not been achieved, as can be seen in the electrophoresis, presented in figure 57.

Thus, comparing all the assays tested to capture the SCOMT protein it is evident that diverse factors influence the binding and the interactions promoted between the protein and the spheres, such as the pH, the presence of urea in the lysate sample and the amount of spheres. Also, to elute the protein, the pH and the concentration of salt present in the elution buffers affect the elution and the isolation of SCOMT. Therefore, the best conditions for the capture of the total protein from the complex lysate, containing impurities such as host constituents and cell debris, are the equilibrium of 10 mL of spheres (with or without magnetization) with 10 mM citrate buffer, at pH 4.0, the binding step with 4 mL of a SCOMT lysate solution, containing urea, in 10 mM citrate buffer, at pH 4.0 and the elution step with change of pH to 6.2 and then with the increase of NaCl concentration at the same pH. However, to isolate the SCOMT, the strategy of binding at pH 7.5 and elution by decreasing the pH to the protein isoelectric point with magnetic spheres would be used to explore the selectivity of these spheres.

Chapter V – Conclusions

Gellan gum is one of the most widely studied polysaccharide of natural origin with many attractive properties, due to it advantageous properties, like biocompatibility, non-toxicity or rapid gelation in the presence of cations. Therefore, the proposed aim of this work was to produce gellan gum through *Sphingomonas paucimobilis* ATCC 31461 fermentation, formulate biosynthetic gellan spheres by using the water-in-oil emulsion and finally magnetize these spheres through the chemical co-precipitation method. Then, the spheres were used to capture model proteins, BSA and lysozyme, and a more complex protein, soluble catechol-*O*-methyltransferase (SCOMT).

The production of gellan gum has been very studied and different conditions have been tested in order to obtain a higher production of this biopolymer. In this work, two different media were tested, the N medium and the S medium, and it was observed that the best procedure to increase the gellan gum production was using the S medium.

Also, different methods for recover the gellan gum produced by fermentation were studied. Thus, techniques of dialysis, filtration, washing with acetone and ether and dissolution with distilled water were applied. After the FTIR and NMR analysis of the samples obtained from these methods, it was perceptible that the best procedure to recover the biopolymer was the filtration technique with washing with acetone and ether and, finally, with dissolution with distilled water. This method is, also, the best method to obtain gellan gum with a high purity degree.

After to recover the gellan gum with high purity, this biopolymer was used to formulate microspheres through the water-in-oil method. This method was chosen due to its advantages for industrial purposes, once that it can be easily scaled-up, does not require expensive and complex instruments and the procedure parameters are easily controlled. Thus, microspheres of commercial and biosynthetic gellan gum were performed, using different cross-linkers, such as barium, calcium, cobalt, copper and nickel. The mean diameter of spheres was determined by using a semi-optical microscope and to compare and evaluate the surface topography, morphology and porosity of gellan spheres, the scanning electron microscope was used. Also, the chemical elements present in the spheres were determined through energy-dispersive X-ray spectroscopy. Therefore, by analysing the mean diameter of spheres, the SEM and EDX results, the spheres with nickel as a cross-linker were chosen to be magnetized, due to their minimum mean diameter and to the surface form and the uniform spherical structure of the spheres. The magnetized spheres were, also, analysed by SEM and EDX and it was possible to conclude that biosynthetic

spheres present higher concentrations of manganese and iron ions, suggesting that these spheres can promote more cationic interactions with negatively charged molecules.

In order to capture the SCOMT protein, the batch method was tested, being optimized different conditions to improve the amount of bound and eluted proteins, such as the amount of beads, the presence of urea in the SCOMT solution and the buffer pH of the equilibrium and binding solutions. So, the best conditions for the capture of the total protein from the complex lysate are the equilibrium of 10 mL of spheres (with or without magnetization) at acidic pH, binding step with urea in the SCOMT lysate and elution step with the increase of pH and then the ionic strength. However, to selectively isolate the SCOMT, it could be more adequate to explore the equilibrium and binding conditions with a pH around 7.5 and the elution condition by decreasing the pH to the protein isoelectric point with magnetic spheres.

In addition, the use of magnetic beads facilitates the removal of the supernatant avoiding the centrifugation and demonstrate to be quick and easily used in protein capture. Thus, this work represents an innovative approach to capture the protein, using magnetic gellan gum beads, through the batch method that is more economic and rapid than the traditional chromatography.

Chapter VI – Future perspectives

Since this work is a new approach for the capture and isolation of SCOMT, it is necessary to improve the strategy of binding with pH of 7.5 and elution with pH of 5.2 with magnetic spheres or to test new conditions in order to explore the best selectivity of these spheres to properly isolate the SCOMT. For instance, it can be studied the effect of different concentrations of imidazole in the elution step. Also, should be tested an assay with and without the addition of urea, to compare the effect of this compound on the binding of the protein to the beads. In addition, the western bolt should be performed with the sample resultant from the capture of SCOMT with magnetic spheres through the elution by decreasing the pH to 5.2 in order to confirm the presence and increased content of SCOMT.

Also, the activity of the protein needs to be determine in order to study the effect of the pH in the activity of the enzyme, which can be affected with pH variations.

In the future, it will be also interesting to test the batch method, using magnetic gellan beads and gellan beads with different counter ions to capture other proteins positively charged from a complex mixture, contrary to SCOMT at a normal pH.

Chapter VII – References

1. Mende, S., Rohm, H., Jaros, D.: Influence of exopolysaccharides on the structure, texture, stability and sensory properties of yoghurt and related products. Int. Dairy J. 52, 57–71 (2016).
2. Ruas-madiedo, P., Hugenholtz, J., Zoon, P.: An overview of the functionality of exopolysaccharides produced by lactic acid bacteria. 12, 163–171 (2002).
3. Cerning, J.: Production of exopolysaccharides by lactic acid bacteria and dairy propionibacteria J Cerning To cite this version : (1995).
4. Rehm, B.H.A.: Bacterial polymers : biosynthesis , modifications and applications. Nat. Publ. Gr. 8, 578–592 (2010).
5. Mcswain, B.S., Irvine, R.L., Hausner, M., Wilderer, P.A.: Composition and Distribution of Extracellular Polymeric Substances in Aerobic Flocs and Granular Sludge. 71, 1051–1057 (2005).
6. Acta, A., Ogaji, I.J., Nep, E.I., Audu-peter, J.D.: Pharmaceutica Advances in Natural Polymers as Pharmaceutical Excipients. 3, 1–16 (2012).
7. Sutherland, I.W.: Novel and established applications of microbial polysaccharides. 16, 41–46 (1998).
8. Vu, B., Chen, M., Crawford, R.J., Ivanova, E.P.: Bacterial extracellular polysaccharides involved in biofilm formation. Molecules. 14, 2535–2554 (2009).
9. Kang, K.S., Veeder, G.T., Mirrasoul, P.J., Kaneko, T., Cottrell, W.: Agar-Like Polysaccharide Produced by a Pseudomonas Species : Production and Basic Properties. 43, 1086–1091 (1982).
10. Proposals of *Sphingomonas* paucimobilis gen . nov . and comb . nov ., *Sphingomonas* parapaucimobilis sp . nov ., *Sphingomonas* yanoikuyae sp . nov ., *Sphingomonas* adhaesiva sp . nov ., *Sphingomonas* capsulata comb . nov ., and Two Genospecies of the Genus Sph. 34, 99–119 (1990).
11. Coppotelli, B.M, Ibarrolaza, A., Del Panno, M.T., Berthe-Corti, L., Morelli, I.S.: Study of the degradation activity and the strategies to promote the bioavailability of phenanthrene by *Sphingomonas* paucimobilis strain 20006FA. Microb. Ecol. 59, 76–266 (2010).
12. Pszczola, D.E.: Gellan gum wins 1FT´s Food Technology Industrial Achievement Award. Food. 47, 94–96 (1993).
13. Lin, C.C., Casida, L.E.: GELRITE as a gelling agent in media for the growth of thermophilic microorganisms. Appl. Environ. Microbiol. 47, 427–429 (1984).
14. MESEGUER, G., BURI, P., PLAZONNET, B., ROZIER, A., GURNY, R.: Gamma Scintigraphic Comparison of Eyedrops Containing Pilocarpine in Healthy Volunteers. J. Ocul. Pharmacol. Ther. 12, 481–488 (1996).

15. LI, J., KAMATH, K., DWIVEDI, C.: Gellan Film as an Implant for Insulin Delivery. J. Biomater. Appl. 15, 321–343 (2001).
16. S, Karthika J, Vishalakshi, B.: Synthesis, swelling behaviour, salt-and pH-sensitivity of crosslinked gellan gum-graft-poly (acrylamide-co-itaconic acid) hydrogels. Pharma Chem. 5, 185–192 (2013).
17. Crescenzi, V., Dentini, M., Segatori, M., Tiblandi, C., Callegaro, L., Benedetti, L.: Synthesis and preliminary characterisation of new esters of the bacterial polysaccharide gellan. Carbohydr. Res. 231, 73–81 (1992).
18. Correia, S.I., Pereira, H., Silva-Correia, J., Van Dijk, C.N., Espregueira-Mendes, J., Oliveira, J.M., Reis, R.L.: Current concepts: tissue engineering and regenerative medicine applications in the ankle joint. J. R. Soc. Interface. 11, 20130784–20130784 (2013).
19. Jana, S., Das, A., Nayak, A.K., Sen, K.K., Basu, S.K.: Aceclofenac-loaded unsaturated esterified alginate/gellan gum microspheres: In vitro and in vivo assessment. Int. J. Biol. Macromol. 57, 129–137 (2013).
20. Jansson, P.-E., Lindberg, B., Sandford, P.A.: Structural studies of gellan gum, an extracellular polysaccharide elaborated by Pseudomonas elodea. Carbohydr. Res. 124, 135–139 (1983).
21. O'Neill, M.A., Selvendran, R.R., Morris, V.J.: Structure of the acidic extracellular gelling polysaccharide produced by Pseudomonas elodea. Carbohydr. Res. 124, 123–133 (1983).
22. Yuguchi, Y., Mimura, M., Kitamura, S., Urakawa, H., Kajiwara, K.: Structural characteristics of gellan in aqueous solution. Food Hydrocoll. 7, 373–385 (1993).
23. H. Gulrez, S.K., Al-Assaf, S., O, G.: Hydrogels: Methods of Preparation, Characterisation and Applications. Prog. Mol. Environ. Bioeng. - From Anal. Model. to Technol. Appl. (2011).
24. Crescenzi, V.: Microbial Polysaccharide of applied interest: Ongoing research activities in Europe. Biotechnol. progress. 11, 251–259 (1995).
25. Harvey, L. M. and Mc Neil, B.: Thickeners of Microbial Origin. Microbiol. fermented foods. 2nd ed. 1, 150–171 (1998).
26. Kanombirira, S. and Kailasapathy, K.: Effects of interactions of carrageenans and gellan gum on yields, textural and sensory attributes of Cheddar cheese. Milchwissenschaft. 50, 452–458 (1995).
27. Sanderson, G. R. and Clark, R.C.: Laboratory-produced microbial polysaccharide has many potential food applications as a gelling, stabilizing and texturizing agent. Food Techonol. 37, 63–70 (1983).
28. Osmałek, T., Froelich, A., Tasarek, S.: Application of gellan gum in pharmacy and medicine. Int. J. Pharm. 466, 328–340 (2014).
29. Vartak, N.B., Lin, C., Cleary, J.M., Fagan, M.J., Saier, M.H.: of a Glucose-6-Phosphate Dehydrogenase Insertion Mutant. Microbiology. 141, 2339–2350 (1995).
30. Fialho, A.M., Moreira, L.M., Granja, A.T., Popescu, A.O., Hoffmann, K., Sá-Correia, I.:

Occurrence, production, and applications of gellan: Current state and perspectives. Appl. Microbiol. Biotechnol. 79, 889–900 (2008).

31. Sá-Correia, I., Fialho, a M., Videira, P., Moreira, L.M., Marques, a R., Albano, H.: Gellan gum biosynthesis in *Sphingomonas* paucimobilis ATCC 31461: genes, enzymes and exopolysaccharide production engineering. J. Ind. Microbiol. Biotechnol. 29, 170–176 (2002).
32. Sutherland I. W: Biotechnology of microbial exopolysaccharides. Cambridge Univ. Press. Cambridge, New York, Port Chester; Melbourne, Sydney. (1990).
33. Martins, L. O., Sá-Correia, I.: Temperature profiles of gellan synthesis and activities of biosynthetic enzymes. Biotechnol. Appl. Biochem. 20, 385–395 (1993).
34. Videira, P.A., Cortes, L.L., Fialho, A.M., Sá-Correia, I.: Identification of the *pgmG* gene, encoding a bifunctional protein with phosphoglucomutase and phosphomannomutase activities, in the gellan gum-producing strain *Sphingomonas paucimobilis* ATCC 31461. Appl. Environ. Microbiol. 66, 2252–8 (2000).
35. Marques, A.R., Ferreira, P.B., Sá-Correia, I., Fialho, A.M.: Characterization of the ugpG gene encoding a UDP-glucose pyrophosphorylase from the gellan gum producer *Sphingomonas* paucimobilis ATCC 31461. Mol. Genet. Genomics. 268, 816–824 (2003).
36. Granja, A.T., Popescu, A., Marques, A.R., Sá-Correia, I., Fialho, A..: Biochemical characterization and phylogenetic analysis of UDP-glucose dehydrogenase from the gellan gum producer *Sphingomonas* elodea ATCC 31461. Appl.Microbiol. Biotechnol. 76, 1319–1327 (2007).
37. Silva, E., Marques, A.R., Fialho, A.M., Granja, A.T., Sá-Correia, I.: Proteins encoded by *Sphingomonas* elodea ATCC 31461 rmlA and ugpG genes, involved in gellan gum biosynthesis, exhibit both dTDP- and UDP-glucose pyrophosphorylase activities. Appl. Environ. Microbiol. 71, 4703–4712 (2005).
38. Kang, K.S., Veeder, G.T.: Fermentation process for preparation of polysaccharide S-60, (1981).
39. Martins, L.Q., and Sá-Correia, I.: Temperature profiles of gellan gum synthesis and activities of biosynthetic enzymes. Biotechonol Appl. Biochem. 20, 385–395 (1994).
40. Fialho, A.M., Martins, L.O., Donval, M.L., Leitão, J.H., Ridout, M.J., Jay, A.J., Morris, V.J., Sá-Correia, I.: Structures and properties of gellan polymers produced by Sphingomonas paucimobilis ATCC 31461 from lactose compared with those produced from glucose and from cheese whey. Appl. Environ. Microbiol. 65, 2485–2491 (1999).
41. West, T.P.: Effect of complex nitrogen sources upon gellan production by *Sphingomonas* paucimobilis ATCC 31461. (2016).
42. Jay, A.J., Colquhoun, I.J., Ridout, M.J., Brownsey, G.J., Morris, V.J., Fialho, A.M., Leitão, J.H., Sá-Correia', I.: Analysis of structure and function of gellans with different substitution patterns. Carbohydr. Polym. 35, 179–188 (1998).
43. Dreveton, É., Monot, F., Ballerini, D., Lecourtier, J., Choplin, L.: Effect of mixing and mass transfer conditions on gellan production by Auromonas elodea. J. Ferment. Bioeng.

77, 642–649 (1994).
44. Lobas, D., Schumpe, S., Deckwer, W.D.: The production of gellan exopolysaccharide with *Sphingomonas* paucimobilis E2 (DSM 6314). Appl. Microbiol. Biotechnol. 37, 411–415 (1992).
45. Manna, B., Gambhir, a., Ghosh, P.: Production and rheological characteristics of the microbial polysaccharide gellan. Lett. Appl. Microbiol. 23, 141–145 (2008).
46. Paul, F., Morin, A., Monsan, P.: Microbial polysaccharides with actual potential industrial applications. Biotechnol. Adv. 4, 245–259 (1986).
47. Papageorgiou, M., Kasapis, S.: The effect of added sucrose and corn syrup on the physical properties of gellan—gelatin mixed gels. Food Hydrocoll. 9, 211–220 (1995).
48. Durán, E., Costell, E., Izquierdo, L., Durán, L.: Low sugar bakery jams with gellan gum—guar gum mixtures. Influence of composition on texture. Food Hydrocoll. 8, 373–381 (1994).
49. Kelco Division of Merck & Co. Inc.: Gellan gum: multifunctional polysaccharide for texturizing. Tech. Monogr. San Diego, Calif. 92123 (1995).
50. Shiyani, B.G., Dholakiya, R.B., Akbari, B. V, Lodhiya, D.J., Ramani, G.K.: Development and evaluation of novel immediate release tablets of Metoclopramide HCl by direct compression using treated gellan gum as a disintegration-accelerating agent. J. Pharm. Res. 2, 1460–1464 (2009).
51. Vijan, V., Kaity, S., Biswas, S., Isaac, J., Ghosh, A.: Microwave assisted synthesis and characterization of acrylamide grafted gellan, application in drug delivery. Carbohydr. Polym. 90, 496–506 (2012).
52. Singh, S.R., Carreiro, S.T., Chu, J., Prasanna, G., Niesman, M.R., Collette III, W.W., Younis, H.S., Sartnurak, S., Gukasyan, H.J.: L-Carnosine: multifunctional dipeptide buffer for sustained-duration topical ophthalmic formulations. J. Pharm. Pharmacol. 61, 733–742 (2009).
53. Illum, L.: Nasal drug delivery - Recent developments and future prospects. J. Control. Release. 161, 254–263 (2012).
54. Shin, H., Olsen, B.D., Khademhosseini, A.: The mechanical properties and cytotoxicity of cell-laden double-network hydrogels based on photocrosslinkable gelatin and gellan gum biomacromolecules. Biomaterials. 33, 3143–3152 (2012).
55. Chang, S.J., Huang, Y.-T., Yang, S.-C., Kuo, S.-M., Lee, M.-W.: In vitro properties of gellan gum sponge as the dental filling to maintain alveolar space. Carbohydr. Polym. 88, 684–689 (2012).
56. Chang, S.J., Kuo, S.M., Liu, W.T., Niu, C.C.G., Lee, M.W., Wu, C.S.: Gellan gum films for effective guided bone regeneration. J. Med. Biol. Eng. 30, 99–103 (2010).
57. Wen, Y., Yang, X., Hu, G., Chen, S., Jia, N.: Direct electrochemistry and biocatalytic activity of hemoglobin entrapped into gellan gum and room temperature ionic liquid composite system. Electrochim. Acta. 54, 744–748 (2008).
58. Murano, E.: Use of natural polysaccharides in the microencapsulation techniques. J.

Appl. Ichthyol. 14, 245–249 (1998).

59. Prajapati, V.D., Jani, G.K., Zala, B.S., Khutliwala, T.A.: An insight into the emerging exopolysaccharide gellan gum as a novel polymer. Carbohydr. Polym. 93, 670–678 (2013).
60. Morris, E.R., Nishinari, K., Rinaudo, M.: Gelation of gellan – A review. Food Hydrocoll. 28, 373–411 (2012).
61. Kubo, W., Miyazaki, S., Attwood, D.: Oral sustained delivery of paracetamol from in situ-gelling gellan and sodium alginate formulations. Int. J. Pharm. 258, 55–64 (2003).
62. Brownsey, G.J., Chilvers, G.R., Anson, K.I., Morris, V.J.: Some observations (or problems) on the characterization of gellan gum solutions. Int. J. Biol. Macromol. 6, 211–214 (1984).
63. Kronick, P., Gilpin, R.W.: Use of superparamagnetic particles for isolation of cells. J. Biochem. Biophys. Methods. 12, 73–80 (1986).
64. Li, X., Sun, Z.: Synthesis of magnetic polymer microspheres and application for immobilization of proteinase of balillus sublitis. J. Appl. Polym. Sci. 58, 1991–1997 (1995).
65. Abudiab, T., Beitle, R.R.: Preparation of magnetic immobilized metal affinity separation media and its use in the isolation of proteins J. Chromatogr.A. 795, 211-217 (1998).
66. Gupta, P.K., Hung, C.T.: Minireview magnetically controlled targeted micro-carrier systems. Life Sci. 44, 175-186 (1989).
67. Liu, J.W., Zhang, Y., Chen, D., Yang, T., Chen, Z.P., Pan, S.Y., Gu, N.: Facile synthesis of high-magnetization γ-Fe2O3/alginate/silica microspheres for isolation of plasma DNA. Colloids Surfaces A Physicochem. Eng. Asp. 341, 33–39 (2009).
68. Horak, D., Bohacek, J., Subrt, M.: Magnetic poly(2-hydroxyethyl methacrylate-co-ethylene dimethacrylate) microspheres by dispersion polymerization. Polym. Sci. A. Polym. Chem. 38, 1161-1171 (2000).
69. Ding, X.B., Sun, Z.H., Wan, G.X., Jiang, Y. Y.: Preparation of thermosensitive magnetic particles by dispersion polymerization. React. Funct. Polym. 38, 11–15 (1998).
70. Moeser, G.D., Roach, K.A., Green, W.H., Alan Hatton, T., Laibinis, P.E.: High-gradient magnetic separation of coated magnetic nanoparticles. AIChE J. 50, 2835–2848 (2004).
71. Bucak, S., Jones, D.A., Laibinis, P.E., Hatton, T.A.: Protein Separations Using Colloidal Magnetic Nanoparticles. Biotechnol. Prog. 19, 477–484 (2003).
72. Arnold, F.H.: Metal-affinity separations: a new dimension in protein processing. Biotechnology. (N. Y). 9, 151–6 (1991).
73. Felinto, M.C.F.C., Parra, D.F., Lugão, A.B., Batista, M.P., Higa, O.Z., Yamaura, M., Camilo, R.L., Ribela, M.T.C.P., Sampaio, L.C.: Magnetic polymeric microspheres for protein adsorption. Nucl. Instruments Methods Phys. Res. Sect. B Beam Interact. with Mater. Atoms. 236, 495–500 (2005).
74. Cuatrecasas, P., Wilchek, M., Anfinsen, C.B.: Selective enzyme purification by affinity chromatography. Proc. Natl. Acad. Sci. 61, 636–643 (1968).

75. Porath, J.: From gel filtration to adsorptive size exclusion. J. Protein Chem. 16, 463–468 (1997).
76. Schulenberg-Schell, H., Tei, A.: Principles and Practical Aspects of Preparative Liquid Chromatography.
77. Jungbauer, A.: Chromatographic media for bioseparation. J. Chromatogr. A. 1065, 3–12 (2005).
78. Hatti-Kaul, R., Mattiasson, B.: Isolation and purification of proteins. Marcel Dekker (2003).
79. Sheehan, D.: Ion Exchange Chromatography & Chromatofocusing. Mol. Biomethods Handbook, 2nd Ed. G.E. Healthc. 711–718 (2009).
80. Costa, S.R., Bonifácio, M.J., Queiroz, J.A., Passarinha, L.A.: Analysis of hSCOMT adsorption in bioaffinity chromatography with immobilized amino acids: The influence of pH and ionic strength. J. Chromatogr. B Anal. Technol. Biomed. Life Sci. 879, 1704–1706 (2011).
81. Myöhänen, T.T., Schendzielorz, N., Männistö, P.T.: Distribution of catechol-O-methyltransferase (COMT) proteins and enzymatic activities in wild-type and soluble COMT deficient mice. J. Neurochem. 113, 1632–1643 (2010).
82. Karlsson, E., Ryden, L., Brewer, J.: Protein purification. Principles, high resolution methods and applications. In: Ion exchange chromatography. , Wiley-VCH, New York (1998).
83. Amercham Biosciences: Ion exchange chromatography. Principles and methods. In: Amercham Pharmacia. Biotech, SE 751 (2002).
84. Coskun, O.: Separation Tecniques: CHROMATOGRAPHY. North. Clin. Istanbul. 3, 156–160 (2016).
85. Walls, D., Sinéal, T.: Protein chromatography: methods and protocols. Methods Mol. Biol. 681, (2011).
86. Helmur, D.: Gel chromatography, gel filtration, gel permeation,molecular sieves. In: A laboratory Hand book, Springer-Verlag (1969).
87. Hutta, M., Góra, R., Halko, R., Chalányová, M.: Some theoretical and practical aspects in the separation of humic substances by combined liquid chromatography methods. J. Chromatogr. A. 1218, 8946–8957 (2011).
88. Nunes, V.S., Bonifácio, M.J., Queiroz, J.A., Passarinha, L.A.: Assessment of COMT isolation by HIC using a dual salt system and low temperature. Biomed. Chromatogr. 24, 858–862 (2010).
89. Liu, H.F., Ma, J., Winter, C., Bayer, R.: Recovery and purification process development for monoclonal antibody production. MAbs. 2, 480–99 (2010).
90. Melander, W.R., Corradini, D., Horv?th, C.: Salt-mediated retention of proteins in hydrophobic-interaction chromatography. J. Chromatogr. A. 317, 67–85 (1984).
91. Queiroz, J.A., Tomaz, C.T., Cabral, J.M.S.: Hydrophobic interaction chromatography of proteins. J. Biotechnol. 87, 143–159 (2001).

92. Hage, D.S., Ruhn, P.F.: An introduction to affinity chromatography. (2006).
93. Wilcheck, M., Chaiken, I.: An overview of affinity chromatography - methods and protocols. Humana Press. 1–6 (2000).
94. Magdeldin, S., Moser, A.: Affinity Chromatography: Principles and Applications. (2012).
95. Firer, M..: Efficient elution of functional proteins in affinity chromatography. J Biochem Biophys Methods. 49, 42–433 (2001).
96. Porath, J., Carlsson, J., Olsson, I., Belfrage, G.: Metal chelate affinity chromatography, a new approach to protein fractionation. Nature. 258, 598–9 (1975).
97. Yip, T.-T., Hutchens, T.W.: Immobilized Metal-Ion Affinity Chromatography. In: Protein Purification Protocols. pp. 179–190. Humana Press, New Jersey (2004).
98. Li, R., Wang, Y., Chen, G.L., Shi, M., Wang, X.G., Chen, B., Zheng, J. Bin: A Novel Silica-Based Metal Chelate Stationary Phase—L-Glutamic Acid–Copper(II). Sep. Sci. Technol. 46, 309–314 (2010).
99. Dong, X.-Y., Chen, L.-J., Sun, Y.: Refolding and purification of histidine-tagged protein by artificial chaperone-assisted metal affinity chromatography. J. Chromatogr. A. 1216, 5207–5213 (2009).
100. Hlady, V., Buijs, J., Jennissen, H.: Methods for Studying Protein Adsorption. Methods Enzymol. 309, 402–429 (1999).
101. Tüzmen, N., Akdoğan, F., Kalburcu, T., Akgöl, S., Denizli, A.: Development of the magnetic beads for dye ligand affinity chromatography and application to magnetically stabilized fluidized bed system. Process Biochem. 45, 556–562 (2010).
102. Axelrod, Julius, Senoh, Siro, Wrrkop, B.: O-Methylation of Catechol Amines in Viva *. (1958).
103. Bertocci, B., Miggiano, V., Da Prada, M., Dembic, Z., Lahm, H.W., Malherbe, P.: Human catechol-O-methyltransferase: cloning and expression of the membrane-associated form. Proc Natl Acad Sci U S A. 88, 1416–1420 (1991).
104. Salminen, M., Lundström, K., Tilgmann, C., Savolainen, R., Kalkkinen, N., Ulmanen, I.: Molecular cloning and characterization of rat liver catechol-O-methyltransferase. Gene. 93, 241–247 (1990).
105. Guldberg, H.C., Marsden, C..: Catechol-O-methyltransferase. Pharmacological aspects and physiological role. Pharmacol Rev. 27, 135–206.
106. Zhu, B.A.O.T., Patel, U.K., Cai, M.A.Y.X., Conney, A.H.: O -Methylation of Tea Polyphenols Catalyzed By Human Placental Cytosolic Catechol- O -Methyltransferase Abstract : Drug Metab. Dispos. 28, 1024–1030 (2000).
107. Sharpless, N.S., Mccann, D.S.: Dopa and 3-O-methyldopa in cerebrospinal fluid of parkinsonism patients during treatment with oral l-dopa. Clin. Chim. Acta. 31, 155–169 (1971).
108. Männistö, P.T., Kaakkola, S.: Rationale for Selective COMT Inhibitors as Adjuncts in the Drug Treatment of Parkinson's Disease. Pharmacol. Toxicol. 66, 317–323 (1990).
109. Schluckebier, G., O'Gara, M., Saenger, W., Cheng, X.: Universal Catalytic Domain

Structure of AdoMet-dependent Methyltransferases. J. Mol. Biol. 247, 16–20 (1995).
110. O'Gara, M., McCloy, K., Malone, T., Cheng, X.: Structure-based sequence alignment of three AdoMet-dependent DNA methyltransferases. Gene. 157, 135–138 (1995).
111. Lotta, T., Vidgren, J., Tilgmann, C., Ulmanen, I., Melén, K., Julkunen, I., Taskinen, J.: Kinetics of human soluble and membrane-bound catechol O-methyltransferase: a revised mechanism and description of the thermolabile variant of the enzyme. Biochemistry. 34, 4202–10 (1995).
112. Bonifácio, M.J., Palma, P.N., Almeida, L., Soares-da-Silva, P.: Catechol-*O*-methyltransferase and Its Inhibitors in Parkinson's Disease. CNS Drug Rev. 13, 352–379 (2007).
113. Lundström, K., Tenhunen, J., Tilgmann, C., Karhunen, T., Panula, P., Ulmanen, I.: Biochimica et biophysica acta. Protein structure and molecular enzymology.
114. Correia, F.F., Santos, F.M., Pedro, A.Q., Bonifácio, M.J., Queiroz, J.A., Passarinha, L.A.: Recovery of biological active catechol- *O* -methyltransferase isoforms from Q-sepharose. J. Sep. Sci. 37, 20–29 (2014).
115. Nunes, V.S., Bonifácio, M.J., Queiroz, J.A., Passarinha, L.A.: Assessment of COMT isolation by HIC using a dual salt system and low temperature. Biomed. Chromatogr. 24, 858–862 (2009).
116. Jatana, N., Sharma, A., Latha, N.: Pharmacophore modeling and virtual screening studies to design potential COMT inhibitors as new leads. J. Mol. Graph. Model. 39, 145–164 (2013).
117. Espírito Santo, G.M., Pedro, A.Q., Oppolzer, D., Bonifácio, M.J., Queiroz, J.A., Silva, F., Passarinha, L.A.: Development of fed-batch profiles for efficient biosynthesis of catechol-O-methyltransferase. Biotechnol. Reports. 3, 34–41 (2014).
118. Zhang, J., Dong, Y.C., Fan, L.L., Jiao, Z.H., Chen, Q.H.: Optimization of culture medium compositions for gellan gum production by a halobacterium *Sphingomonas* paucimobilis. Carbohydr. Polym. 115, 694–700 (2015).
119. Jin, H., Lee, N.K., Shin, M.K., Kim, S.K., Kaplan, D.L., Lee, J.W.: Production of gellan gum by *Sphingomonas* paucimobilis NK2000 with soybean pomace. Biochem. Eng. J. 16, 357–360 (2003).
120. Narkar, M., Sher, P., Pawar, A.: Stomach-Specific Controlled Release Gellan Beads of Acid-Soluble Drug Prepared by Ionotropic Gelation Method.
121. Frias, F., Passarinha, L., Sousa, A.: Optimization of a gellan gum support by experimental design for recombinant proteins partition, (2015).
122. Pedro, A.Q., Oppolzer, D., Bonifácio, M.J., Maia, C.J., Queiroz, J.A., Passarinha, L.A.: Evaluation of MutS and Mut+ Pichia pastoris Strains for Membrane-Bound Catechol-O-Methyltransferase Biosynthesis. Appl. Biochem. Biotechnol. 175, 3840–3855 (2015).
123. Bornhorst, J.A., Falke, J.J.: Purification of Proteins Using Polyhistidine Affinity Tags. Methods Enzym. 326, 245–254 (2000).
124. Laemmli, U.K.: Cleavage of structural proteins during the assembly of the head of

bacteriophage T4. Nature. 227, 680–5 (1970).
125. Rast, J.I.M., Johnston, J.M., Allen, J.E., Drum, C.: Modified gellan gum hydrogels with tunable physical and mechanical properties. J. Exp. Anal. Behav. 2, 195–206 (1985).
126. Prakash, S.J., Santhiagu, A., Jasemine, S.: Preparation, Characterization and In Vitro Evaluation of Novel Gellan Gum-Raloxifene HCl Nanoparticles. J. Pharm. Biosci. 2, 63–71 (2014).
127. Sabadini, R.C., Martins, V.C.A., Pawlicka, A.: Synthesis and characterization of gellan gum: chitosan biohydrogels for soil humidity control and fertilizer release. Cellulose. 22, 2045–2054 (2015).
128. Lee, M.W., Tsai, H.F., Wen, S.M., Huang, C.H.: Photocrosslinkable gellan gum film as an anti-adhesion barrier. Carbohydr. Polym. 90, 1132–1138 (2012).
129. Hamcerencu, M., Desbrieres, J., Khoukh, A., Popa, M., Riess, G.: Synthesis and characterization of new unsaturated esters of Gellan Gum. Carbohydr. Polym. 71, 92–100 (2008).
130. Costa, D., Sousa, A., Passarinha, L.: Development of a new microcarrier culture based in matrix of natural polymer. (2014).
131. Bajpai, S.K., Saxena, S.K., Sharma, S.: Swelling behavior of barium ions-crosslinked bipolymeric sodium alginate–carboxymethyl guar gum blend beads. React. Funct. Polym. 66, 659–666 (2006).
132. Picone, C.S.F., Cunha, R.L.: Influence of pH on formation and properties of gellan gels. Carbohydr. Polym. 84, 662–668 (2011).
133. Gonçalves, A.I.C., Rocha, L.A., Dias, J.M.L., Passarinha, L.A., Sousa, A.: Optimization of a chromatographic stationary phase based on gellan gum using central composite design. J. Chromatogr. B. 957, 46–52 (2014).

Chapter VIII - Annex

Annex I - FTIR spectrum of casein

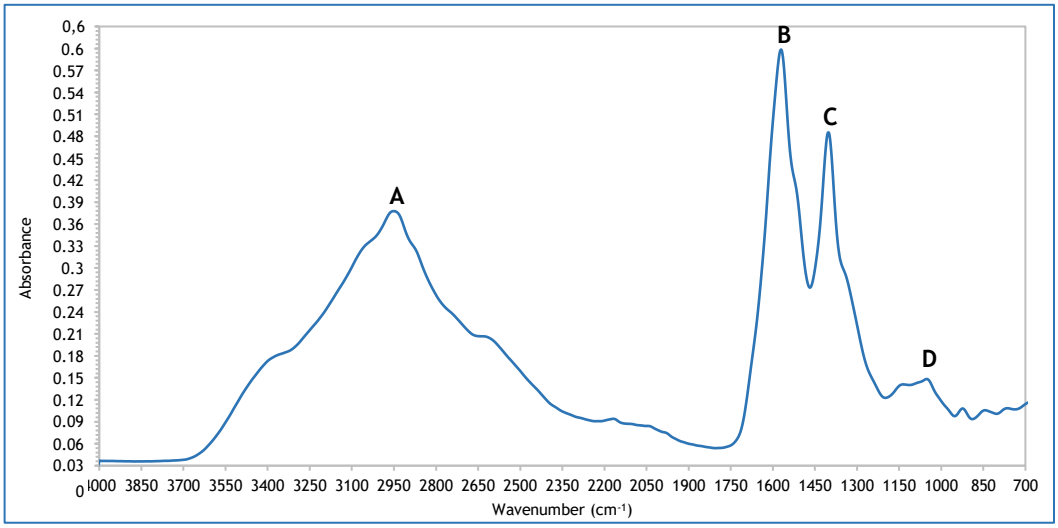

Figure 68 - FTIR spectrum of casein. **A** - 2950.95 cm^{-1}; **B** - 1570.65 cm^{-1}; **C** - 1402.06 cm^{-1}; **D** - 1051.61 cm^{-1} .

Annex II - FTIR spectrum of glucose

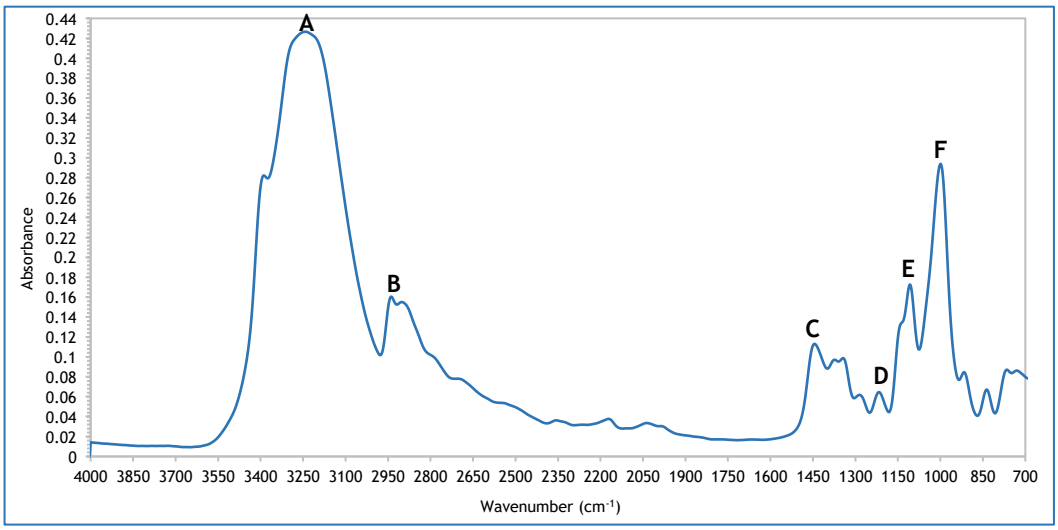

Figure 59 - FTIR spectrum of glucose. **A** - 3242.22 cm^{-1}; **B** - 2936.47 cm^{-1}; **C** - 1444.05 cm^{-1}; **D** - 1216.64 cm^{-1}; **E** - 1107.43 cm^{-1}; **F** - 999.52 cm^{-1}.

Annex III – NMR spectrum of casein

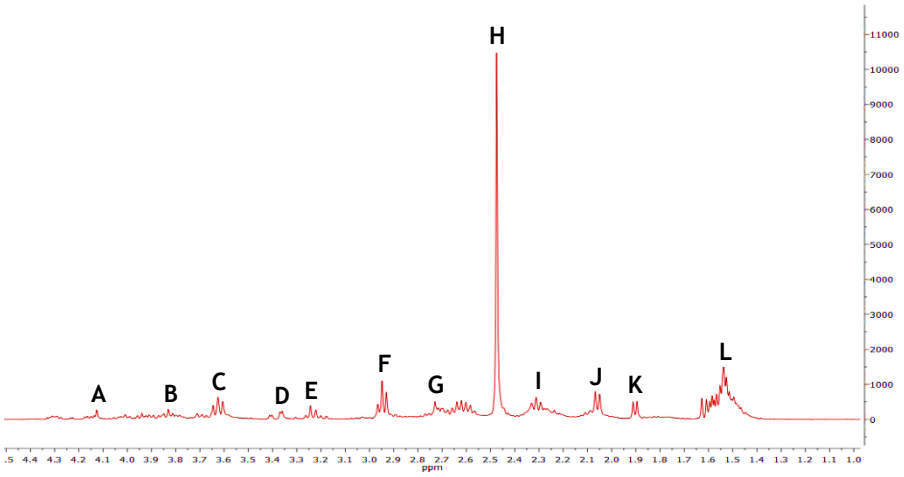

Figure 60 - ^{1}H-NMR spectrum of casein. **A** - 4.1257 ppm; **B** - 3.8301 ppm; **C** - 3.6252 ppm; **D** - 3.2621 ppm; **E** - 3.2432 ppm; **F** - 2.9651 ppm; **G** - 2.7288 ppm; **H** - 2.4747 ppm; **I** - 2.3114 ppm; **J** -2.0677 ppm; **K** - 1.9115 ppm; **L** - 1.5142 ppm.

Annex IV – NMR spectrum of yeast extract

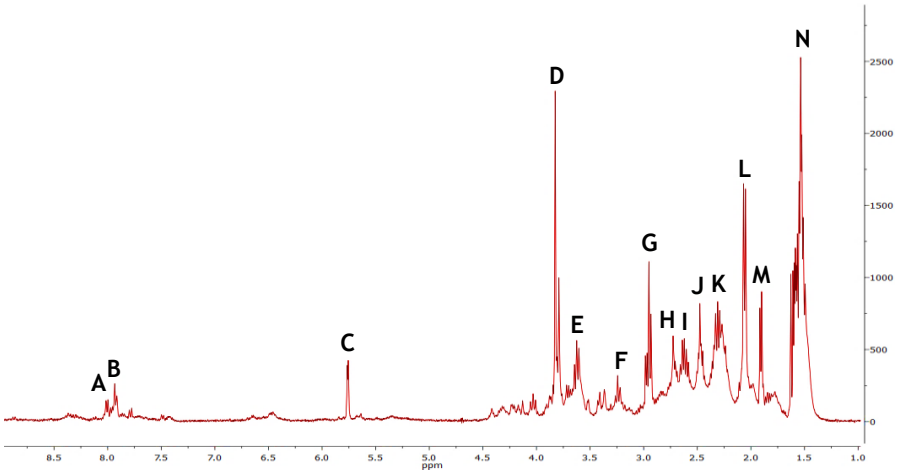

Figure 61 - ^{1}H-NMR spectrum of yeast extract. **A** - 7.9973 ppm; **B** - 7.9337 ppm; **C** - 5.7558 ppm; **D** - 3.6483 ppm; **E** - 3.6044 ppm; **F** - 3.2199 ppm; **G** - 2.9844 ppm; **H** - 2.7259 ppm; **I** - 2.6393 ppm; **J** - 2.4760 ppm; **K** - 2.2910 ppm; **L** - 2.2910 ppm; **M** - 1.900 ppm; **N** - 1.5360 ppm.